POLITECNICO DI MILANO

School of Industrial Engineering

Department of Energy

STUDY OF THE IMPACT OF COGENERATION PRESSURE AND TEMPERATURE ON THE EFFICIENCY OF A SUGAR PLANT AND ANALYSIS OF THE POSSIBLE REPOWERING

Advisors: Professor Fabio Rinaldi
Professor William Andrés Ocampo Duque
(Pontificia Univesidad Javeriana de Cali)

Master of Science Thesis of:

Guido Colombo - 783366

Academic Year 2012 – 2013

This work, and my whole academic career, is dedicated to my parents, to whom I owe simply everything.

Acknowledgements

I'd like to thank Manuelita S.A. for the great professional opportunity it offered me; especially John Jairo Ortiz and Alvaro Rodriguez for the time they spent with me and for teaching me how to face "real world" problems of engineering.

A special mention goes to Dr. William Andrés Ocampo Duque, my tutor at Pontificia Universidad Javeriana: first of all for accepting me for the exchange, then for the invaluable help and suggestions he provided me and for being a wise point of reference.

I am grateful to Dr. Fabio Rinaldi, my tutor at Politecnico di Milano, for supporting this project since the very beginning and for giving his help even from very far away; without his approval this amazing experience in Colombia would have never been possible.

I want to give thanks to all the friends of mine: the ones that even from thousands of kilometers were constantly at my side and that represent a wonderful reality of my life and the ones I met in Cali and in Colombia for sharing awesome adventures and incredible moments together: I wont forget you.

The last thought goes to Henry and Jorge for being like brothers during these months: I will miss Sunday family's breakfasts.

Index

Index of figures

Index of tables

Index of annexes

Abstract

All over the world, energy policies of the countries are moving to a reduction of fossil fuel share of the energy mix and to invest on renewable green energy sources. Biomass is one of these and it represents, in the form of sugar cane, a strategic source in Colombia, especially in the region of Valle del Cauca, where sugar industry is able to convert the energy content of the cane into different energy products: ethanol, which is obtained through fermentation, electric energy and steam which are cogenerated by combustion of the bagasse. In this work the case of sugar plant "Ingenio Manuelita" is considered. After performing the energy and material balance of the process, the study of the effect of different pressures and temperatures of cogeneration boilers is carried on in order to optimize the efficiency. Moreover, new innovative solutions and layout of the process are proposed in order to increase its energy performances. An economic analysis is managed considering the common investment indexes.

Keywords: Cogeneration, bio-refinery, optimization, bioenergy, repowering.

Sommario

In tutto il mondo, le politiche energetiche dei paesi si stanno muovendo verso una riduzione della partecipazione dei combustibili fossili nell'"energy mix" e verso investimenti in risorse rinnovabili. Le biomasse sono una di queste e svolgono un ruolo strategico in Colombia, specialmente nella regione della Valle del Cauca, dove l'industria zuccheriera è in grado di convertire il contenuto energetico della canna in diversi prodotti: etanolo che è ottenuto tramite la fermentazione e, energia elettrica e vapore che sono cogenerati attraverso la combustione del bagassa. In questa tesi si considera il caso dell'"Ingenio Manuelita". Dopo aver svolto il bilancio materiale ed energetico dell'impianto, si studia l'effetto di diverse pressioni e temperature delle caldaie per ottimizzarne l'efficienza. Si propongono nuove innovative soluzioni e configurazioni del processo per migliorarne le prestazioni energetiche. Si illustra infine la relativa analisi economica, considerando i tipici indici di investimento.

Parole chiave: cogenerazione, bioraffineria, ottimizzazione, energia rinnovabile, repowering.

Estratto in italiano

Introduzione

I combustibili fossili hanno ricoperto un ruolo decisivo nella crescita dell'economia sin dai tempi dell'industrializzazione [1], hanno dominato il settore energetico e continueranno a guidarlo per i prossimi anni [2], ma nell'ultimo secolo, l'aumento di problemi ambientali legati alla combustione di enormi quantitativi di queste risorse, preoccupazioni politiche legate all'instabilità dei paesi dove sono principalmente locate, problemi economici dovuti alla crescita del costo del petrolio e la crescente consapevolezza dell'impossibilità di mantenerne lo stesso tasso di consumo hanno portato nuovi campi di ricerca nell'ingegneria, per convertire l'economia e l'industria, ora completamente dipendenti dai combustibili fossili, verso uno sviluppo sostenibile legato all'uso di risorse rinnovabili.

Queste necessità, e il bisogno di diversificare le fonti di approvvigionamento energetico, hanno evidenziato l'importanza di poter sfruttare fonti energetiche come il sole, il vento, i fiumi, le biomasse, le onde e le maree. Inoltre occorre evolvere l'attuale produzione di beni e servizi basata sulla materia prima fossile in biologica. Lo sviluppo di sistemi in grado di convertire questa materia prima in una vasta gamma di prodotti saranno la "chiave per l'accesso alla produzione integrata di cibo, mangimi, prodotti chimici, materiali, beni, carburanti e per il futuro" [3]. Questo è il caso delle bioraffinerie: in Colombia, il più rappresentativo esempio di bioraffineria è dato dall'industria zuccheriera.

Obiettivi della tesi

La tesi si svolge su tre obiettivi principali, strettamente legati tra loro. Il primo obiettivo, che è fondamentale per i passi successivi, è la modellazione dei bilanci di massa ed energia del processo di produzione di zucchero e etanolo e del processo cogenerativo dell'impianto dell' "Ingenio Manuelita". Dal punto di vista industriale il modello rappresenta uno strumento molto importante e funzionale perché l'impianto non è provvisto di sufficienti strumenti per la misurazione dei flussi e delle potenze; di conseguenza può rappresentare una maniera efficace di comprendere i processi termodinamici che si stanno svolgendo secondo diverse condizioni di funzionamento. L'ottimizzazione delle pressioni e temperature delle caldaie ha lo scopo di verificare che l'impianto stia lavorando nelle migliori condizioni di funzionamento dal punto di vista di efficienza energetica: in questo caso l'obiettivo è la ricerca del massimo profitto

economico (una migliore efficienza si traduce in un risparmio di combustibile) e dell'uso razionale delle risorse.

La proposta di migliorie e di una nuova configurazione della cogenerazione ha lo scopo di aggiornare il layout dell'impianto, ormai superato, e permettere di raggiungere un'efficienza tale da garantire all'impresa di rimanere competitiva rispetto al costo di produzione di concorrenti dotati di processi produttivi più moderni. La possibilità di vendere energia elettrica alla rete inoltre, oltre a rappresentare una nuova fonte d'ingressi per la compagnia, rappresenta un potenziale benefit per l'intera regione e paese Colombia, perché permette di aumentare la frazione di energia prodotta da risorse rinnovabili e di aumentare la concorrenza nel settore di generazione di energia.

Metodi

Il processo di produzione dello zucchero è ben conosciuto e perfettamente descritto dalla letteratura tecnica del settore: le equazioni per i bilanci sono ricavate e adattate dai più importanti libri sull'industria zuccheriera [4-5]. Per quanto riguarda la produzione di bioetanolo, nella tesi sarà dimostrato che il fabbisogno energetico (energia elettrica e termica) del processo non è direttamente legato alla quantità di canna da zucchero che l'impianto sta processando, e che è il principale parametro d'input del modello. La ragione di ciò è che l'impianto di produzione dell'alcool è fisicamente separato dal resto della struttura industriale, dotato di proprie cisterne di accumulazione e quindi è manovrato in modo indipendente rispetto alla produzione dello zucchero.

Le equazioni dell'acqua, necessarie per lo studio della cogenerazione, sono quelle della "International Association for Properties of Water and Steam Industrial Formulation", (IAPWS IF-97) [6].

Le ottimizzazioni sono condotte con il "Global Optimization Toolbox" di Matlab, in particolare si fa uso dell'algoritmo "Pattern Search" che permette di trovare gli ottimi globali di funzioni multi-variabili, con punti di non derivabilità e condizionate da vincoli lineari e non, grazie al vantaggio di essere un metodo diretto e quindi non relazionato al calcolo delle derivate [7].

Conclusioni

Il modello per i bilanci di massa ed energia del processo produttivo presentato nella tesi risulta essere sufficientemente accurato nel tipico range di operazione dell'impianto. L'analisi della configurazione attuale evidenzia la presenza di alcuni punti critici dal punto di vista dell'efficienza energetica, corrispondenti

all'attemperazione del vapore prodotto dal Boiler 7 e alle laminazioni per la riduzione della pressione del vapore stesso. In particolare, ha un effetto particolarmente negativo sull'efficienza la riduzione di pressione da 300 a 25 PSIG, necessaria quando il flusso di vapore che attraversa le turbine non è sufficiente a coprire i fabbisogni di vapore saturo a 25 PSIG del processo produttivo di zucchero ed etanolo. Il modello conferma l'arretratezza dell'impianto rispetto allo stato dell'arte. Mentre molte imprese sono in grado di estrarre surplus energetici dalla combustione della bagassa, l'Ingenio Manuelita è in grado di coprire solo il 97.6% del proprio fabbisogno e per soddisfare la propria domanda energetica deve comprare carbone. L'analisi di sensibilità effettuata sulle principali variabili e l'ottimizzazione numerica confermano però che, per come è stato progettato l'impianto, le caldaie stanno già lavorando in una condizione prossima alla ottimale.

Considerando le future evoluzioni del processo, che comporteranno una riduzione del consumo di vapore, il modello presentato conferma la possibilità di aumentare l'efficienza di secondo principio dell'impianto dal 19.6% attuale fino al 21.2% grazie al passaggio da macchine mosse da turbine a macchine elettriche. Tuttavia l'elettrificazione può essere solo parziale perché si incontra una limitazione nella capacità generativa disponibile dei turbogeneratori. In aggiunta, emerge la necessità di uno sviluppo parallelo da parte del processo produttivo e della cogenerazione per evitare la necessità di laminazione di parte del vapore o lo scarico in atmosfera.

Alla luce dei risultati e dell'analisi sulla prima fase di riduzione del vapore, appare chiara la necessità di riprogettare la parte cogenerativa per affiancare la seconda e radicale riduzione di vapore del processo produttivo. Sostituendo i vecchi Boiler 5 e 6 con un nuovo che affianchi il Boiler 7, due differenti cicli Rankine sono presentati, per permettere di coprire il fabbisogno di energia elettrica e termica dell'Ingenio Manuelita e per produrre un surplus di energia elettrica. La prima proposta prevede un normale ciclo Rankine con estrazione e condensazione, mentre la seconda prevede un ciclo dotato di risurriscaldamento. Le ottimizzazioni di entrambi i cicli permettono all'impianto di raggiungere efficienze di secondo principio del 25.8% e 27.0% rispettivamente. Tali nuove configurazioni potrebbero essere installate con un investimento il cui Tasso Interno di Rendimento sarebbe dell'11.0% e 12.7%.

Bibliografia

[1] A. O'Sullivan, S. Shefferin, *Economics: Principles and Tools*, 2nd edition, Prentice Hall, 2003.
[2] International Energy Agency, *World Energy Outlook 2011*, 2011.
[3] Committee on Biobased Industrial Products, National Research Council, *Biobased industrial products: research and commercialization priorities*, National Academic Press, Washington, (2000), pp. 74.
[4] E. Hugot, *Handbook of cane sugar engineering*, 3rd edition, Elsevier, New York, 1986.
[5] P. Rein, *Cane sugar engineering*, 1st edition, Verlag Dr. Albert Bartens KG, Berlin, 2007.
[6] International Association for the Properties of Water and Steam, *IAPWS Industrial Formulation 1997,* 1997.
[7] R. Hooke, T.A. Jeeves, *"Direct search" solution of numerical and statistical problems,* Journal of the Association for Computing Machinery (ACM), vol.8 (1961), pp 212-229.

1. Introduction and State of the Art

Fossil fuels have played a determinant role in the growth of economies since industrialization [1]. They have led the primary energy mix of the world and will continue to lead it for the next years [2]. But in the last century, the rise of environmental issues due to the combustion of huge quantities of them, political concerns given by the instability of the countries where these sources are principally located, economic matters related to the increasing cost of oil and the increasing awareness of their not supportable consumption rate have driven engineering to new fields of research, in order to move from a fossil dependent economy and industry to a more bearable form of development by the use of renewable sources. These needs and the necessity to diversify the energy mix, have pointed out the importance of being able to exploit energy sources like sun, wind, rivers, biomasses, waves and tides.

In addition, some change from current production of goods and services from fossil to biological raw materials is necessary and the development of substance-converting basic product systems and poly-product systems will be the "key for the access to an integrated production of food, feed, chemicals, materials, goods and fuels for the future" [3]. This is the case of bio-refineries.

The present work, which is the result of a cooperation of between Politecnico di Milano, Pontificia Universidad Javeriana de Cali and the sugar and ethanol company Manuelita S.A., has three main different objectives. The first objective is to build the energy and material balance of the processes of sugar and ethanol production and of the cogeneration of the plant. This model should supply the lack of measurement of the flows in different parts of the process and may represent a strong instrument to understand how the system is behaving under different operating conditions. The model is also the base for the following objectives. Pressure and temperature of the boilers are analysed in order to optimize the efficiency of the plant. The optimization and consequent reduction of fuel consumption has a double meaning. From economic point of view it represents a possible additional source of incomes, because bagasse may be sold to paper industry. From an environmental point of view it represents a sustainable choice because it allows reducing the consumption of fossil fuel, increasing the biomass share of energy input. The last objective is the analysis of some innovation to be implemented on the existing layout, and the study of a new cogeneration configuration. This is a necessary innovation that the company has to afford because the existing layout is now far from the actual state of art. More recent plants are able to produce with fewer costs, so the upgrade has to be done in order not to be cut out of the market in the next years.

Moreover the new configuration will allow Manuelita S.A. to produce a surplus of electric energy that could be sold to the grid. This energy surplus has for the company an economic value because it is an income while, for the region and the country, represents a benefit because it allows increasing the renewable fraction of the energy mix and increasing the competition in the market of electric energy production.

1.1 Biomass and Biorefineries

1.1.1 Biomass characterization

Biomass is defined as organic matter that is available on a renewable or recurring base (excluding old-growth timber), including dedicated energy crops and trees, agricultural food and feed crop residues, aquatic plants, wood and wood residues, animal wastes and other waste materials [4]. Beyond these major groups, it has to be underlined that biomasses are characterized by very different moisture content, amount of cellulose, hemicellulose and lignin. Cellulose is a glucose polymer; hemicellulose a mixture of polysaccharides (composed by sugars like glucose, xylose and arabinose, and some acids) and lignin is a term in which a group of amorphous high molecular weight compounds is included.

The most important properties that determine the suitability of plant species for processing as energy crops or for other converting processes are the moisture content, the calorific value, the proportions of fixed carbons and volatiles, the ash and residue content, the alkali metal content and the cellulose and lignin ratio. Usually cellulose fraction represents the 40-50% in weight of the biomass [5]). The photosynthesis allows plants to convert light energy into chemical energy that is stored into the chemical bonds, according to Equation 1.1.

$$nCO_2 + H_2A + light\ energy = (CH_2O)_n + A_2 \quad (1.1)$$

This is a generalized, unbalanced formula of photosynthesis, which occurs because of the presence of chlorophyll, where the symbol *A* stands for Oxygen in case of the majority of photosynthetic organisms and for S in case of some bacteria. The term (CH_2O) represents the general carbohydrates incorporated by the growing organism, used by the organism itself to synthetize more complex materials.

Even though through photosynthesis, plants store just a small amount of the available sunlight energy, biomasses have always been a major source of energy because of their large availability [5]. They used to be considered as a source of energy for third world countries but since 20 years ago, they started to attract a

worldwide renewed interest, because development in conversion technologies and crop production nowadays allow for higher efficiency and cheaper transformations, because of the possibility to reduce Greenhouse gases emissions and because of, in the case of the EU and the US, the agricultural food production surplus [5].

What makes biomasses particularly attractive is also the possibility to convert them (through different processes) into different output products, which are energy products (electric energy, heat and fuels for transportation), or material products (industrial products). Figure 1.1 shows the different uses of biomass.

Figure 1.1 Scheme of possible uses for biomasses

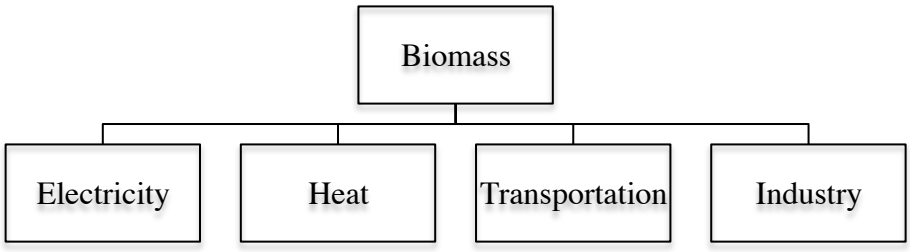

1.1.2 Concept of Biorefinery

Petrochemistry is based on the principle of generating a wide range of simple and complex, well-defined, chemically-pure products from petrol hydrocarbons. The same idea is being transferred to bio-refineries. Green biorefineries are complex systems of sustainable, environmentally and resource-friendly technologies for the comprehensive material and energetic utilization as well as exploitation of biological raw materials in form of green and residue biomass from a targeted sustainable land utilization [6]. The term “bio-refinery” includes, indeed, a broad range of technologies and processes, whose aim is to separate biomass resources, which have a complex composition, into their building blocks (carbohydrates, proteins, triglycerides), in order to convert them, through de-polymerization and de-oxygenation, into higher value products like fuels and chemicals.

Bio-refineries can accept different carbon raw materials as feedstock. They can come from dedicated crops or from residues. Their origin can be agriculture, forestry, industries, households or aquacultures. The composition of biomass is clearly not homogeneous (grass, wood, grains, biological waste…), and it can

also experience seasonal changes: these and the different. They have different C to H to O ratios.

The biorefinery feedstock can be divided into three main groups:

- Carbohydrates and lignin;
- Triglycerides;
- Mixed organic residues.

Carbohydrates are the most common biomasses. They are complex molecules of polysaccharides like starch, cellulose and hemicellulose, while lignocellulosic materials are principally made of cellulose, hemicellulose and lignin. Starches $(C_6H_{10}O_5)_n$ and cellulose $(C_6H_{10}O_5)_n$ are polymers made by glucose molecules $(C_6H_{12}O_6)$. Hemicellulose $(C_5H_8O_5)_n$ is an amorphous component made of C6 and C5 sugars. Lignin $(C_9H_{10}O_2(OCH_3)_n)$ is made of phenolic polymers and it is the element that supply rigidity to the structure of the plants [4,7]. The most relevant carbohydrates available are sugar cane, sugar beet (sugar crops) and corn (starch crop). Lignocellulose is provided by both crops and residues (straw from agriculture, wood waste from pulp and paper industry, forestry residues). Triglycerides feedstock is made of oils and fats that are composed of glycerine, saturated and unsaturated acids and is provided by vegetables (soybean, palm, rapeseed and sunflower oil), wastes of food industry and animal fats. The term "mixed organic residues" includes municipal solid waste, manure, wild fruits and crops, proteins and residues from fresh fruit and vegetable industries.

The feedstock has to undergo different processes in order to be converted into desired products. These processes are classified by their nature. Thermochemical processes include gasification and pyrolysis. Biochemical processes involve fermentation and anaerobic digestion. Mechanical processes are usually the preliminary steps for the following treatments. Chemical processes are hydrolysis and transesterification.

The final products of biorefineries are divided into material products, whose value is given by their chemical and physical properties, and energy products, these are energy or products whose value is related to their energy content.
The most important energy products of a bio-refinery are [7]:

- Heat and electric energy;
- Gaseous biofuels (biogas, syngas, hydrogen, bio-methane);
- Solid biofuels (pellets, lignin, charcoal, bagasse);
- Liquid biofuels for transportation (bioethanol, biodiesel, FT-fuels, bio-oil).

The most important material products are [7]:

- Chemicals (fine chemicals, building blocks, bulk chemicals);
- Organic acids (succinic, lactic, itaconic and other sugar-derivatives);
- Polymers and resins (starch-based plastics, phenol resins, furan resins);
- Biomaterials (wood panels, pulp, paper, cellulose);
- Food and animal feed;
- Fertilizers.

1.2 Biofuels

1.2.1 Biofuels Outlook and Classification

Biofuels are fuels derived from biological renewable sources as plant or animal materials. They contain energy from geologically recent carbon fixation. Biofuels can be liquid like biodiesel, corn ethanol, sugar alcohol, hydro-treating oil, lignocellulosic ethanol, butanol, bio-oil and Fischer-Tropsch oils, gaseous like biogases or hydrogen or solid like wood, grass, agricultural waste, domestic refuse and sawdust. In a context where fossil fuels cover around 80% of the world's primary energy demand [8,9], and where transportation represents more than 50% of this part [10], it is necessary to recognize the importance of biofuels as a major output of bio-refineries. In 2012, biofuels composed 3% of the whole road transport fuel consumption [11]. Many developed and developing countries in the last years have started to invest in biofuels to reduce their dependence on foreign oil, to reduce GHG emissions and to meet rural development goals [12-14]. As shown in Figure 1.2, biofuels world production is led by North America, that in 2011 produced 49.6% of the total production (58,868 thousands of TEP), Central and South America represented 27.4% of the share, Europe and Eurasia 16.7%, Asia Pacific 6.2%, while Middle East and Africa did not supply any significant contribution (<0.05%) [10].

The current technological paths for biofuels production are classified into generations, which differ in feedstock and processes [15]. *First generation biofuels* were the first response to the huge oil price increase. The main three types of first generation biofuels available on commercial scale are biodiesel, bioethanol and biogas [16]. The term Biodiesel refers to methyl esters made (mostly) by transesterification, a chemical process that reacts a feedstock oil or fat with methanol or ethanol and with an acid or enzymatic catalyzer [15, 16]. The feedstock can be vegetable oil like the ones derived from oilseed crops (soy, sunflower, rapeseed), or animal fat, like beef tallow, poultry fat, pork lard [17]. Biodiesel can be, with minor engine modifications, a substitute of diesel [16].

Bioethanol is the most well-known first generation fuel. It is produced by fermenting sugars extracted from crop plants and starch contained in maize

kernel or other starchy crops [18]. Theoretically, it may be produced by any biological feedstock containing an appreciable amount of sugar (sugar cane and sugar beet are the most typical) or containing materials that can be converted into sugar (for example starch). Bioethanol is usually blended with gasoline, but can represent (for flex fuel vehicles) a complete substitute of it [16]. Biogas (biomethane) is a fuel that can be used in gasoline vehicles (through some adaptations) and is produced by anaerobic digestion of liquid manure and other digestible feedstock.

Figure 1.2 World biofuels production, data from BP [9]

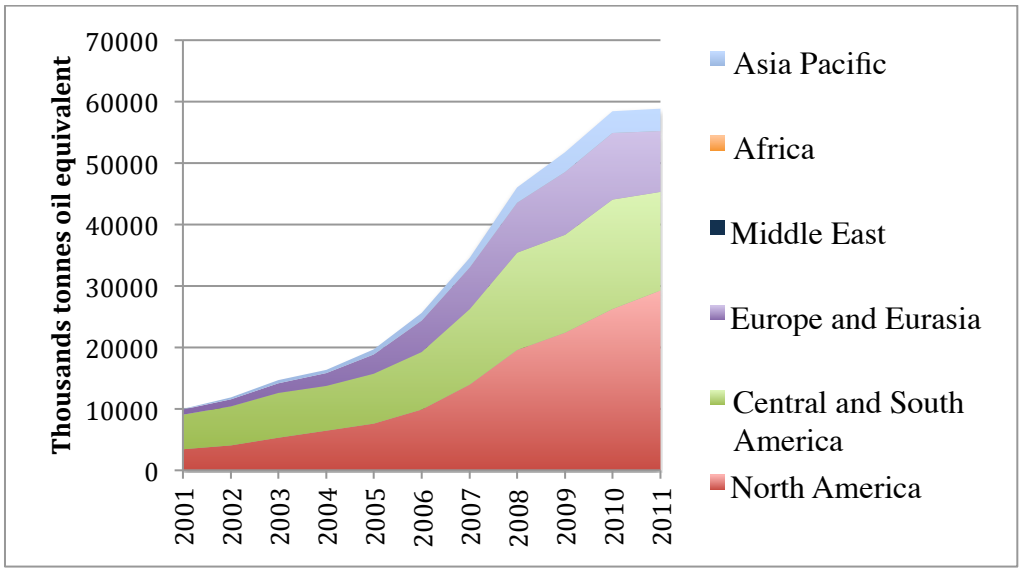

First generation technologies allow, through many different processes, the production of a wide range of valued products, but they also have limits. The "food versus fuel" debate has to be taken into account because first generation fuels are in conflict with food supply. Plants that are usually used for food are feedstock of these kinds of processes. The problems of land occupation and water consumption have to be strongly evaluated also.

Second generation biofuels, also known as advanced biofuels, differ from first generation ones in being produced from non-food feedstock. Their advantage is indeed to limit the direct "food VS fuel" competition. Raw materials for these kinds of fuels are non-food crops, waste vegetable oil and lignocellulosic biomass. Typical examples of second-generation feedstock are short rotation energy crops like poplar, willow and eucalyptus, perennial grasses like miscanthus, switch grass and reed canary grass, residues from forestry, agriculture, and wood industry, as well as waste vegetable oils [19]. There are

several different technological processes that allow for the production of second generation biofuels. From lignocellulosic material, hydrolysis allows for the extraction sugars, that ferment and produce advanced bioethanol. Gasification of the lignocellulosic biomass produce syngas that can be transformed into liquid biofuel (Fischer-Tropsch diesel) or into gaseous fuels (bio-Synthetic Natural Gas, which can be used in gasoline cars with some adaptations, or bio-dimethyl ether, that, with adaptations can be used in diesel engines). Figure 1.3 depicts the production path of second generation biofuels.

Figure 1.3 Scheme of second generation biofuels production

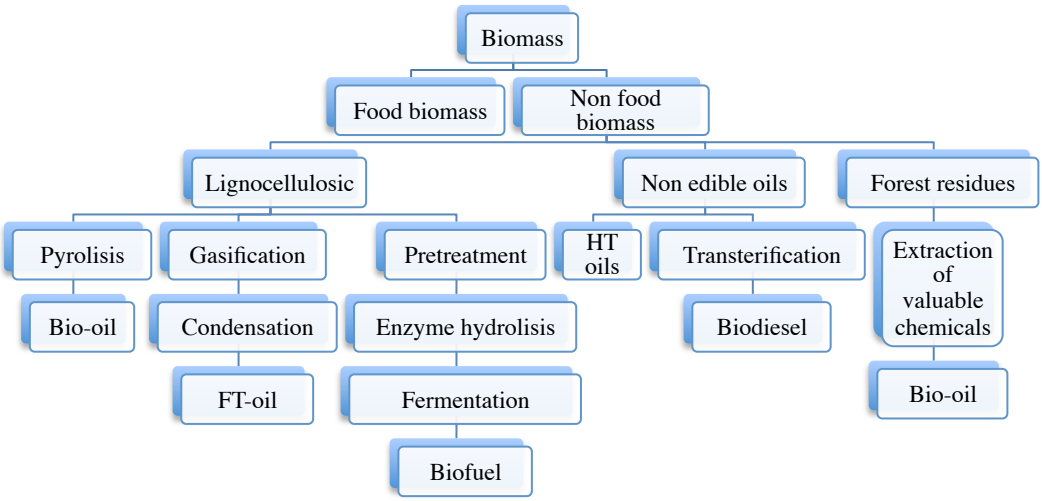

Second generation biofuels still are not able to solve all the issues related to land use, water consumption and deforestation, so the attention of researchers is now focusing on the possibility to get biofuels from microbes and microalgae, which would potentially be able to avoid all the drawback of the previous generations [15]. These biofuels are named *third generation biofuels*.

1.2.2 Bioethanol

Since this Thesis is related to the study of a sugar and ethanol production plant, it is thus important to go deeper into some bioethanol aspects. Ethanol is an alcohol, whose formula is CH_3CH_2OH. It is a flammable liquid. In its pure form it is colorless. It is miscible in all proportions with polar substances like water

and partially miscible with gasoline, acetone, benzene and other organic polar solvents. Figure 1.4 depicts a ternary diagram ethanol-gasoline-water. A ternary diagram is a plot of three variables whose sum is constant. The variables are represented on the sides of an equilateral triangle. When ethanol is obtained using renewable biomass, it is called bioethanol. The use of bioethanol as a fuel for spark ignition engines, presents some advantages and some drawbacks compared to the use of gasoline, and this is due to their characteristics. They are similar but have slight differences. Table 1.1 displays ethanol physical properties.

Figure 1.4 Ethanol-gasoline-water ternary phase diagram. Point 1- E85 (85% ethanol and 15% gasoline). Point 2- E85 contaminated with water. Point 3- contaminated E85 blended with pure gasoline (phase separated)

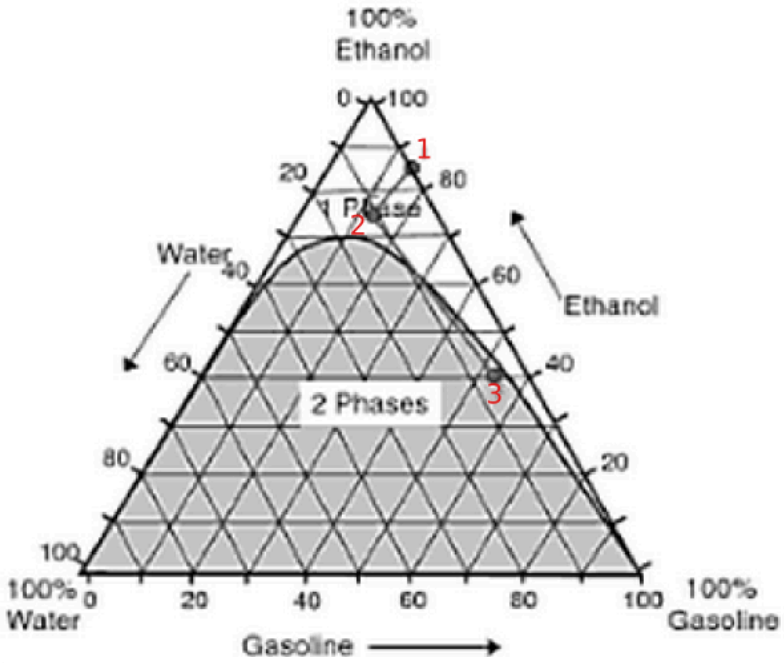

Source [20]

Table 1.1 Properties of ethanol compared to gasoline

Fuel property	*Ethanol*	*Gasoline*
Formula	C_2H_5OH	C_4 to C_{12}
Density at 15 °C [kg/l]	0.69	0.69-0.79
Freezing point [°C]	-114	-40
Normal boiling point [°C]	78.4	27-225
Vapor pressure at 38 °C [kPa]	15.9	48-103
Specific heat [kJ/kgK]	2.4	2

Lower Heating Value 10^3 kJ/l	21.1	30-33
Auto-ignition temperature [°C]	423	257
Lower flammability limit [%Vol]	4.3	1.4
Higher flammability limit [%Vol]	19	7.6
Stoichiometric air-fuel ratio [weight]	9.0	14.7
Flash point [°C]	13	-43
Motor Octane Number (MON)	89.7	80-90

Source [21]

The main advantages of bioethanol, if compared to gasoline are: better anti-knock characteristic (higher MON) and lower CO and unburned hydrocarbons emissions; higher auto-ignition and flash point temperature, which make its use safer for transportation; much lower vapor pressure (and higher latent heat of evaporation), which allows a better filling coefficient of the combustion chamber (due to lower temperature in the intake manifold). The drawbacks are given by the miscibility of the alcohol with water that may cause corrosion problems in the engine and by the lower LHV, which implies that we need a higher volume of fuel to get the same energy output.

Flexi-fuel vehicles can run with pure ethanol. In common spark ignition engines ethanol is mixed with gasoline to get a mixture with a adequate boiling point. These mixtures are named with the percentage of ethanol they contain. For instance, E85 contains 85% ethanol and 15% gasoline and it is one of the richest mixtures. Fuel ethanol production and consumption have experienced a huge increase in the last two decades, following the same increasing trend of transportation energy consumption [22,23]. But in the last two years there has been a small decrease in the global production. In 2012 the total production was 83.1 billion liters, down 1.3% by volume from 2011 [11]. This trend was primarily caused by the USA, whose ethanol production reduced because of a corn price increase (due to a drought). In the rest of the world the total production increased by 4% [11]. Figure 1.5 shows the ethanol fuel production in the last decades.

Figure 1.5 World fuel ethanol production [11, 22-25]

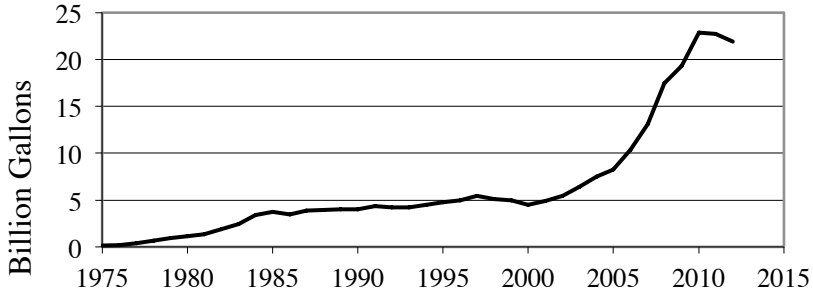

The USA and Brazil are the countries that lead global ethanol production. In 2012 the USA shared 61% of total production (63% in 2011), while Brazil accounted for 26% (25% in 2011) [11]. In these and other countries, some policies have been adopted in order to stimulate and ensure the consumption and production of bioethanol. In Brazil, for example, state policies were directly responsible for the success of the ethanol program. They forced minimum blending requirements, and supported industries and research [26]. In Brazil, for example, cars are required to run with ethanol mixture between 20 and 25% (v/v) (E25), but are built in order to be able to use a higher percentage of ethanol. In the USA, cars are also built able to run on high percentage mixtures, but the effective use of the ethanol depends on the state. In some states the use of E85 is taking place, while in others the use of higher percentage than E10, is prohibited. However, 10% of the 2011 transport fuel demand of the USA was covered by ethanol [27].

In the world there are 650 plants producing bioethanol, whose complete production capacity is around 100 billion liters/year, but some facilities are working under their nominal capacity, others had to close because of fluctuating demand and concerns about the environmental sustainability of the product and others are under construction [11]. Figure 1.6 represents evolution world ethanol producing countries from 1993 to 2013.

Figure 1.6 Ethanol producing countries in 1993, 2003 and 2013. The countries in yellow produce mostly from grains, green ones from sugars

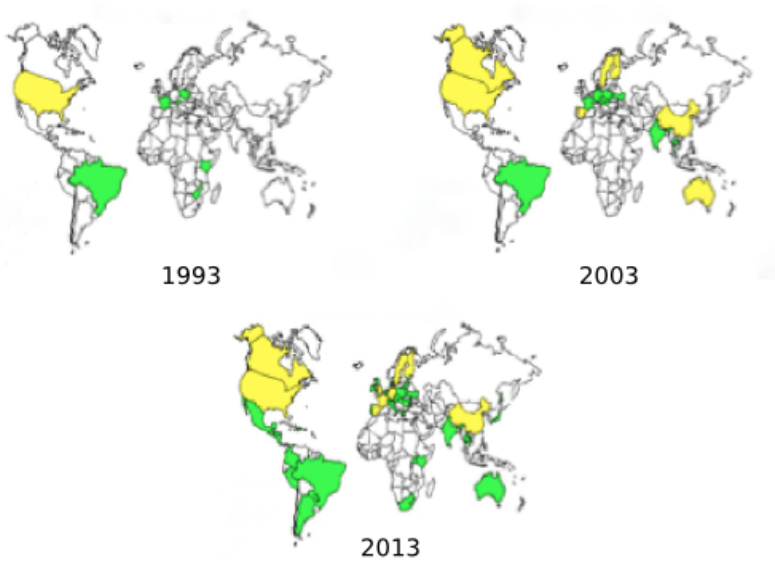

Source: *World Fuel Ethanol Analysis and Outlook* [28]

1.2.3 Waste to energy

Waste to energy is the process to produce electric energy and heat from the incineration of waste. The incineration occurs with direct combustion of the wastes or with the combustion of Refuse Derived Fuels produced from the waste. Waste to energy technologies obtain two other important objectives, which are the hygienization of the waste and the volume reduction, which can be of the order of 90% [29]. The waste generated by households and commercial establishments takes the name of Municipal Solid Waste (MSW). Such waste is considered a heterogeneous fuel mainly composed by organic matter, paper and cardboard, plastic, fines, metals, inert matter, textile and woods [29]. An important fraction of waste is then composed by biomass. Such waste a high potential of energy generation. In industrialized countries the yearly production pro capita of solid waste is 400-900 kg [29]. Considering a 35% level of separation in the source (typical value for a country as Italy), the remaining solid waste is 250-600 kg/inhabitant-year [29]. Being the LHV of MSW 10MJ/kg, it results that, supposing 25% as reasonable net electric efficiency of incinerators, MSW would be able to cover 3-5% of primary energy demand of such countries [29]. Taking the example of Italy, by incinerating the 20 million Tons of MSW yearly disposed in landfills, 14 TWh of electric energy would be yearly produced, which correspond to the 4% of Italian electric consumption [29]. Unluckily, in many countries, incineration is not well accepted by people, which oppose to the construction of new plants, which would be required to exploit in an efficient way the MSW. Energy from bagasse wastes belongs to this category.

1.3 Sugarcane Biorefineries

Sugarcane is a tall perennial grass, native of warm temperate climate and common in tropical regions, as Brazil, India, Africa and Asia pacific. It is composed by a stem, which is the part that is milled to obtain the juice that is used to produce sugar (sucrose) or alcohol (ethanol) and by straw (trash), which is composed by fresh leaves, dry leaves and tops available before harvesting. Figure 1.7 shows the morphology of a sugarcane plant.

The plant is physically made by four principal components: fiber (organic solid fraction, mainly in the stem, very heterogeneous), non-soluble solids (inorganic substances, like soil or rocks, component depending on the cane processing, cutting, harvesting), soluble solids (sucrose, waxes…) and water [30]. The residue of the process of grinding to obtain juice is called bagasse. Bagasse and straw are a trash part of the simple cane processing devoted to extract juice.

They can be used as a direct fuel to be burnt or as a source for second generation bioethanol.

Straw is mainly composed by cellulose (33.3-36.1%, w/w, dry basis, Brazilian case), hemicellulose (18.4-28.9%) and lignin (25.8-40.7%). To obtain ethanol from these components of the plant, the cellulose has to be firstly converted into glucose by enzymatic hydrolysis and then fermented. Hemicellulose has to be separated by lignin with some pretreatment, to liberate the sugars and then to be fermented, while lignin is mainly used as fuel [30]. Minor components of straw are ashes (2.1-11.7%) and extractives (non-fiber compounds) (5.3-11.5%) [30]. Figure 1.8 depicts the composition of sugarcane plant.

Figure 1.7 Sugarcane plant morphology [30]

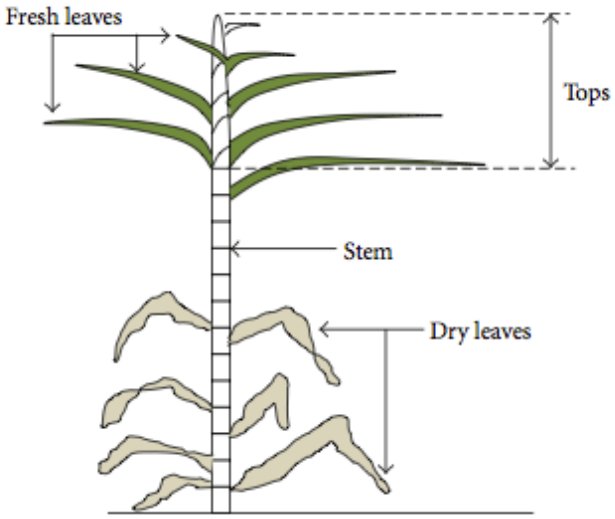

Typically, bagasse is composed by 38.4-45.5% of cellulose (w/w, dry basis), by 22.7-27% of hemicellulose, 19.1-32.4% of lignin, 1-2.8% of ashes and 4.6-9.1% of extractives [30]. Sugarcane bagasse has a lower content of ashes than other crop residues (like rice straw and wheat straw, that have around 17.5% and 10% respectively of ashes [30]). So it is a rich component of the process and it may also be considered not just like a sub-product but like a co-product. Beyond ethanol production, bagasse could be used as a raw material for cultivation of microorganisms, for the production of industrial enzymes, and xylitol. Bagasse can be used to produce energy. Brazil is the world most important producer of sugarcane. In 2012 Brazil shared the 37.8% of the global amount (1,773,814 Thousand Metric Tons), followed by India (19.6%) and People's Republic of China (7%) [31].

Indian people were the first to discover the possibility to produce sugar from the sugarcane, then they exported this plant firstly to China and to nearby regions around the 4500 B.C. Only in the IV century B.C. the sugar came to Europe, thanks to the expansion of Alexander the Great in the far east, and finally it was imported to South America by Cristoforo Colombo, who introduced the cultivation of the cane in a zone corresponding to actual Dominican Republic, from which it moved towards Puerto Rico and Jamaica and later until Peru. It came to Brazil through the Portugueses [33]. Nowadays sugar is a fundamental product of human life, and this is reflected by the fact that sugarcane is now the first agriculture product by volume of the world (in 2010 1,685 Million Tons of sugar were produced) [32]. The production of sugar is very concentrated. The 75% of the overall production is located in just 10 countries lead by Brazil, as shown in Table 1.2.

Figure 1.8 General simplified scheme of sugarcane composition [30]

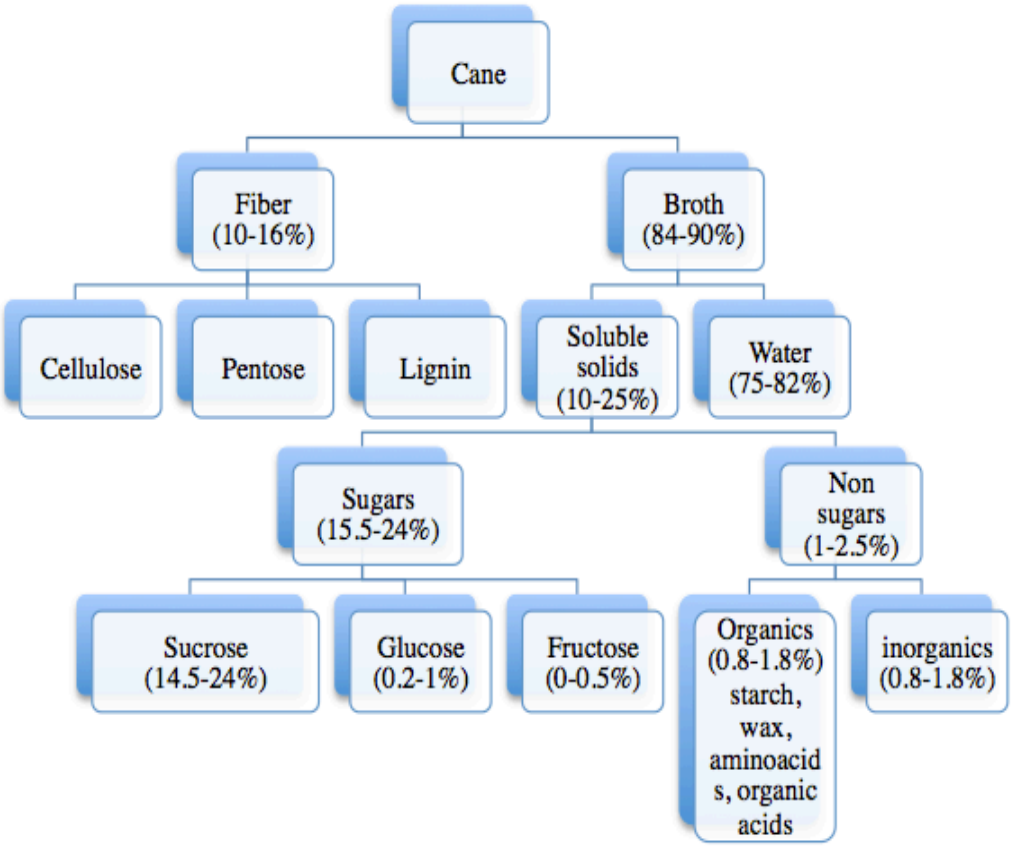

Table 1.2 World sugar main producers [32]

Country	*Production [ton/year]*	*Share of world production %*
Brazil	39,450,539	25.18
India	21,150,846	13.50
UE	16,760,296	10.70
China	11,600,000	7.40
USA	7,635,221	4.87
Thailand	6,769,978	4.32
Mexico	5,075,000	3.24
Australia	3,634,218	2.32
Pakistan	3,860,000	2.46
Russia	2,973,380	1.90
Others	3,776,1489	24.10
Total	156,670,967	100

1.3.1 First generation Biorefineries

The process of biorefining for the production of first generation bioethanol is able to obtain the fuel using sugarcane juice as a feedstock. The process produces a large amount of a lignocellulosic material, bagasse, which has a typical LHV of 8MJ/kg and a moisture content of 48% [33]. Bagasse is used as a fuel in the boilers for cogeneration of vapor and electric energy while the trash is partially burnt in the fields and partially used for the cogeneration also [34]. Figure 1.9 shows the scheme of the ethanol production process of a first generation biorefinery.

In an autonomous first generation biorefinery, ethanol production can be divided into five main steps: raw material pretreatment, hydrolysis, fermentation, separation and dehydration, and waste water treatment. The process begins with washing of the feedstock, crushing and milling, in order to obtain the juice and to separate the bagasse, which is sent to the cogeneration section. Cane juice undergoes a clarification stage, whose aim is to fit the Ph and eliminate impurities. These impurities are the filter cake obtained by filtering the suspended solids in the juice, and have a commercial value, because they are sold as a component for animal feed or for composting [35]. Clarified juice is concentrated into multiple effect evaporators, sterilized (to avoid contamination in fermentation), cooled and then is ready for fermentation, which is performed by the yeast *Saccharomyces Cerevisiae*. It converts sugar into ethanol and CO_2. During fermentation the yeast is continuously separated by centrifugation and recycled to the fermenter. Fermentation gases, mostly composed by CO_2, are

sent to an absorption column, where they are washed and where more than 98% of the volatized ethanol they contain is recovered [35]. The outlet of the fermentation process is a broth, containing 8-11% (weight basis) of ethanol, which has to be separated. The separation occurs in two distillation columns. In the first one, aqueous solution of ethanol is concentrated up to 63%. In the second one the concentration of ethanol reaches a composition of 95.6%, near to its azeotrope [35].

Figure 1.9 Diagram of an autonomous distillery producing anhydrous bioethanol from sugarcane juice [35]

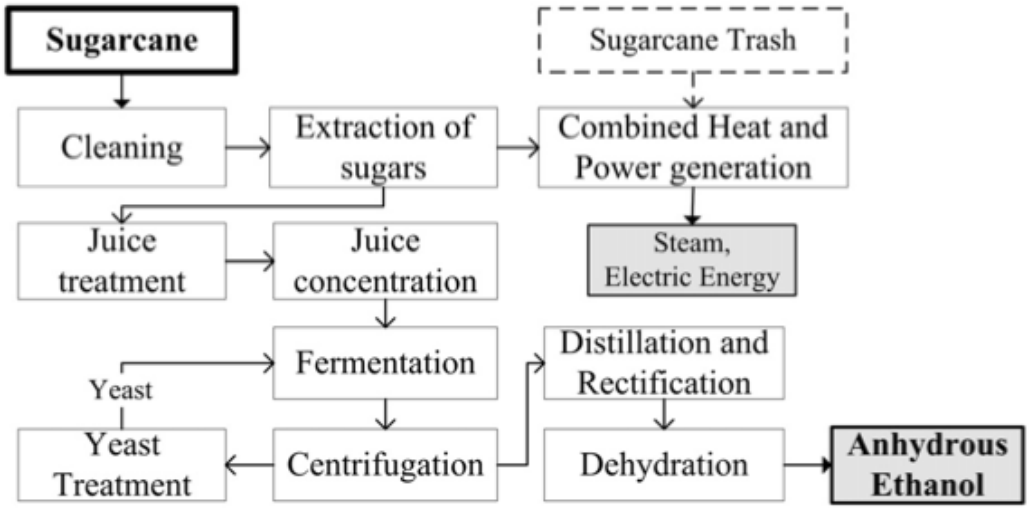

Finally, the dehydration is performed with adsorption in steam phase with molecular sieves (with special zeolities). The stream obtained during the regeneration of molecular sieves is still containing ethanol (70%) and it is then recycled to the rectification column [35]. The main liquid residue of distillation, called vinasse, can be treated, obtaining a valued outcome. Through an evaporation step, a product used as a fertilizer can be achieved. If the stillage is not too concentrated, it can also be used for irrigation. Condensed water from evaporators and bottoms from the rectification column are collected and sent to the wastewater treatment step. Part of this water can be used as feed water for the cogeneration system [35].

1.3.2 Cogeneration

Cogeneration is the production of more than one form of useful power (typically heat and electric power) from the same energy source. In sugar industries, cogeneration boilers are fed with bagasse and trash. They are usually coupled to

a backpressure turbine or to a condensing-extraction turbine [36-37] whose aim is to supply steam and electric energy. Backpressure turbine is the cheapest option in terms of initial investment. Only the steam required by the industrial process is generated at high pressure, then it is expanded in the turbine until the value of pressure of the demand. This solution presents anyway some disadvantages. Electric energy surplus is fluctuating in relation with cane supply and process demand steam. It is also possible to produce surplus energy during the crushing season only.

Condensing and extraction steam turbine allows processing all the possible feedstock, because only a part of the generated steam is extracted (at a selected point of the expansion) and sent to the industrial process, while the remaining is further expanded and condensed. The electric output is maximized because it permits to expand steam till the minimum pressure obtained in the condenser. Following this route, a more constant electric energy surplus can be produced. Actual boilers and turbines are operating with pressures varying from 15 to 105 bar, corresponding to a temperature range of 300-525 °C. Higher values of surplus energy output per ton of cane can be obtained with the high pressure condensing extraction steam cycles (CEST) than with backpressure steam turbines (BPST), as shown in Table 1.3, where some Brazilian and Indian units are compared [36,38]. The reduction of process heat and power consumption can further increase these values. Typically, plants require 400-550 kg of steam per each ton of sugarcane but, by using the state of the art technology, sugar manufacturing and ethanol distillation would require just 280-300 kg-steam/tc (ton of sugarcane). This would imply a significant increase in the electric power production [39].

Figure 1.10 Configuration of Backpressure turbine in a steam cycle [37]

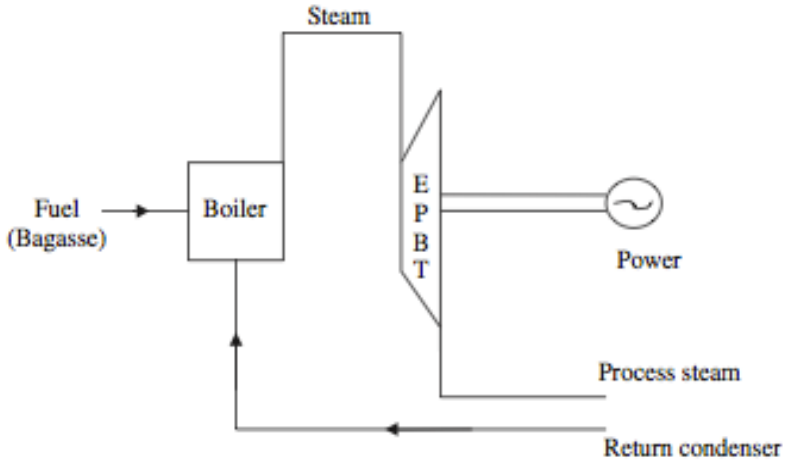

Figure 1.11 Configuration of Condensing with extraction turbine in a steam cycle [37]

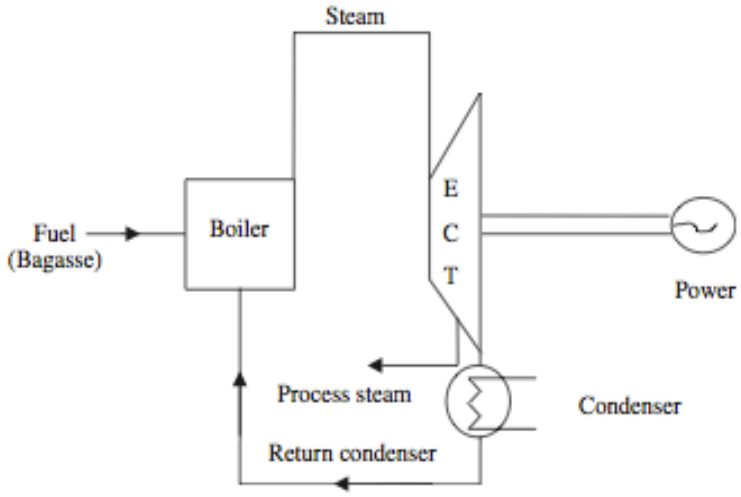

Other possible layout configurations are based on gasification of the biomass. These options require a bagasse dryer, a gasifier and gas cleaning system. The gas is burnt in a gas turbine whose exhaust gases feed an HRSG (Heat Recovery Steam Generator) for the generation of steam, which can be used for the process or in a combined cycle BIGCC (Biomass Integrated Gasification Combined Cycle). It is studied that the application of supercritical steam cycles could provide a surplus energy of nearby 140 kWh/tc while a plant with biomass integrated gasification combined cycle could provide 200-250 kWh/tc of surplus [36,40]. Figures 1.10 and 1.11 provide BPST and CEST schemes.

Table 1.3 Sugar plants electricity surplus

Country	*Power mode*	*Configuration*	*Use of trash*	*Surplus electricity [kWh/tc]*
Brazil	BPST	22 bar, 300 °C	No	0-10
Brazil	BPST	42 bar, 440 °C	No	20
Brazil	BPST	67 bar, 480 °C	No	40-60
Brazil	CEST	65 bar, 480 °C	Yes (50%)	139.7
Brazil	CEST	105 bar, 525 °C	Yes (50%)	158
India	CEST	67 bar, 495 °C	No	90-120
India	CEST	87 bar, 515 °C	No	130-140

Source [36,38]

The theme of the optimization of the energy process of a sugar mill has been considered by several authors. Traditional Rankine steam cycles are still studied [41] but now the attention of the researchers is mainly focused on advanced cogeneration systems as BIGCC and supercritical steam cycles [40], which may guarantee higher results in terms of electric energy surplus. Although the BIGCC seems the best solution, their technology is not ready for commercial scale and supercritical Rankine steam cycles seem to be the following step for the evolution of sugar mills.

1.3.3 Second Generation Biorefineries

Sugarcane bio-refineries that produce second-generation bioethanol, receive bagasse and straw as inputs. It has been demonstrated that, by integrating the lignocellolosic process in the same biorefinery where first generation bioethanol is produced, better results in terms of amount of production and reduction of costs can be obtained, if compared to a bio-refinery where just the lignocellolisic material is fermented [41-42]. Bagasse is also the input for the cogenerative part of the plant. So a trade off between these two different needs has to be found, in order to obtain the configuration that guarantee the best energy and economic performances. In integrated first and second generation bio-refineries, after obtaining the juice, the bagasse, instead of being directly sent to be burnt, follows two possible paths: electricity or fuel production. A bio-refinery is called flexible if it is able to divert the lignocellulose to different path, answering to price signals and market conditions.

The production of ethanol from bagasse and straw, which are lignocellulosic biomasses, pursues similar main steps to that one of first generation but it is more complex. A crucial step here is the pretreatment whose aim is to render cellulose more amenable for hydrolysis by firstly increasing the accessible surface, and then to loosen the structure of the lignocellulosic biomass, by decrystallizing and partially depolymerizing the cellulose, solubilizing hemicellulose and lignin. Lignin has to be removed. This target has to be reached by minimizing the loss of sugars and the costs and it is chased with a huge number of possible technical solutions [43]. Different pretreatments have been studied and are still the focus of the research: pretreatment with different acids, steam explosion, alkaline and ultrasound assisted alkaline treatment, biological treatment, wet oxidation, organosolv pretreatment, liquid hot water pretreatment, pretreatment with peracetic acid and ionic liquids, and ozonolysis [43-51].

The pentoses coming from the pretreatment can follow different paths. In the example of Figure 1.12 [34], they can either be bio-digested and burnt as a

biogas in the cogeneration part, or can continue the process to be transformed into ethanol, but they could also be used for the production of butanol [52]. There are different possible configurations of the process to handle saccharification and fermentation. The process can be conducted on the whole slurry coming from pretreatment, or (more commonly) a filtration followed by hydrolysis and fermentation can be performed [53]. If this second configuration is chosen, then three paths can be pursued: separate hydrolysis and fermentation (SHF), simultaneous saccharification and fermentation (SSF) or presaccharification followed by simultaneous saccharification and fermentation (PSSF).

In the enzymatic hydrolysis (saccharification), cellulosic and hemicellulosic fractions are converted into fermentable sugars by cellulases (cellulolytic enzymes) that attack the cellulose and by xylanase, b-xylosidase, glucuronidase, acetylesterase, galactomannanase, and glucomannanase that act on the hemicellulose. The out stream of the hydrolysis is then joined to the juice coming from the juice treatment and follow the same conversion path of the previous extracted and treated cane juice.

In case of integrated first and second generation ethanol production, the electric energy surplus is, of course, lower than the optimized first generation one and the use of high pressure boilers (65-82 bar) for the cogeneration can give better results than low pressure ones. This configuration, compared with low pressure ones, is characterized by lower ethanol production, higher investment costs but much larger electric energy surplus, so it is economically favorable [41].

1.3.4 Energy balance, sustainability and economics

Second generation bioethanol plants are still not commercially available, but first generation ones are already able to guarantee interesting results in terms of energy balances and GHG emissions. Many analysis on the energy balances of different processes to produce bioethanol have been performed. The result was that Brazilian sugarcane is able to guarantee a higher energy output than any other first generation raw material for the same input. Because of this, Brazil has been selected by the literature as a reference point [54]. The calculated output/input energy ratios have, according to different researchers, different values varying from 2.29 to 9.4 (units), but it is important to remark that their values are always bigger than 1, which means that the process is favorable from energy point of view [54-55].

Macedo and Seabra [55] forecasted the ethanol energy ratio for two possible 2020 scenarios: the *electricity scenario* and *bioethanol scenario*. In the

electricity scenario it is supposed to keep producing ethanol by first generation process, and using the surplus bagasse and trash to produce electricity while in the *ethanol scenario* second generation bioethanol is supposed to be produced. Being 9.4 the result of the current situation (2006), both scenarios are forecasted to reach values of 12.1 (including co-products). This improvement is more optimistic than the one provided by Sun and Minowa who calculated the ratio of the single bagasse process in the range 1.33-1.55 [56]. Figure 1.13 shows the output/input energy ratios for different feedstock, according to different authors.

Figure 1.12 Diagram of an integrated first and second generation ethanol production process from sugarcane. Dashed lines stand for possible alternative paths of pentoses [41]

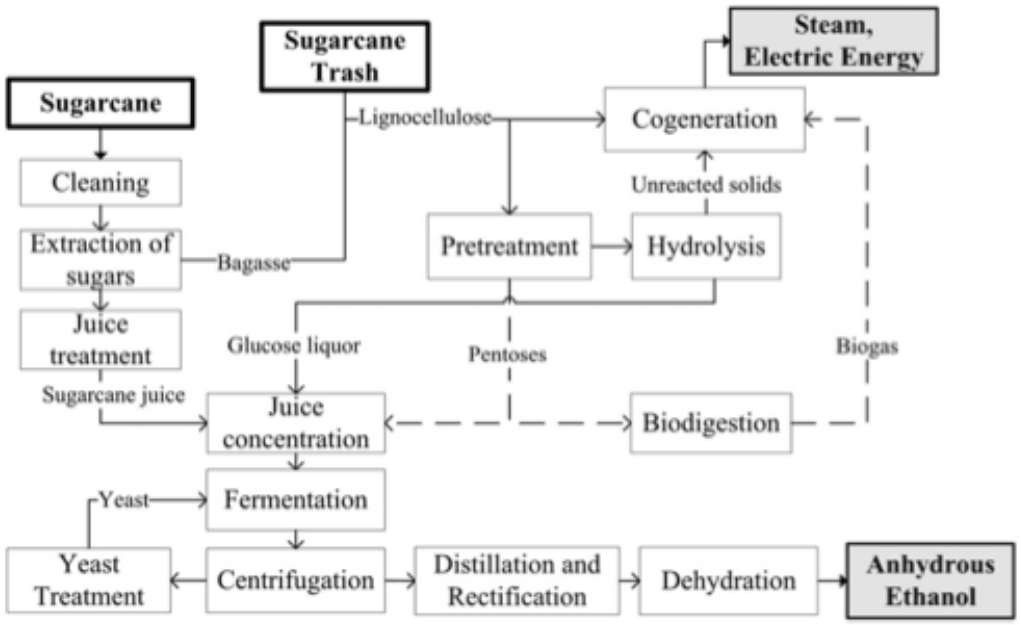

GHG emissions of the processes are a crucial aspect to be taken into account when studying the biorefining. GHG emissions for gasoline are of the order of 3,100 kg equivalent of CO_2 per m^3. Recent researchers affirm that GHG emissions of Brazilian sugarcane are between 436 and 610 kg of CO_2 per m^3. US corn ethanol is estimated between 800 and 2,500 kg of CO_2 per m^3 [58]. If we consider a net energy equivalent basis, corn ethanol decreases emissions by 44% compared to gasoline, while sugarcane ethanol reduces emissions by 65-79% [55, 58-59]. Macedo and Seabra [55] forecasted that, in 2020, this value could increase to 86% (if only ethanol is considered), and to 95% (*ethanol scenario*) or 120% (*electricity scenario*) if all co-products credits and emissions are

considered. Sugarcane is the raw material that allows the cheapest bioethanol production cost between the first generation feedstock. Table 1.4 shows the production cost for ethanol from different feedstock.

Table 1.4 Ethanol production costs [60, adapted from 61]

Feedstock	*Production cost €/ GJ_{HHV}*
Corn	25
Wheat	21-38
Sugar beet	26-40
Sugarcane (Brazil)	7-9
Sugarcane (Colombia)	10-13

Figure 1.13 Overview of output/input athanol energy ratio. The highest value is the only one taking into account the co-products. Data about beet and corn have been elaborated as an average value from the review of the literature of Gnansounou and Dauriat [57].

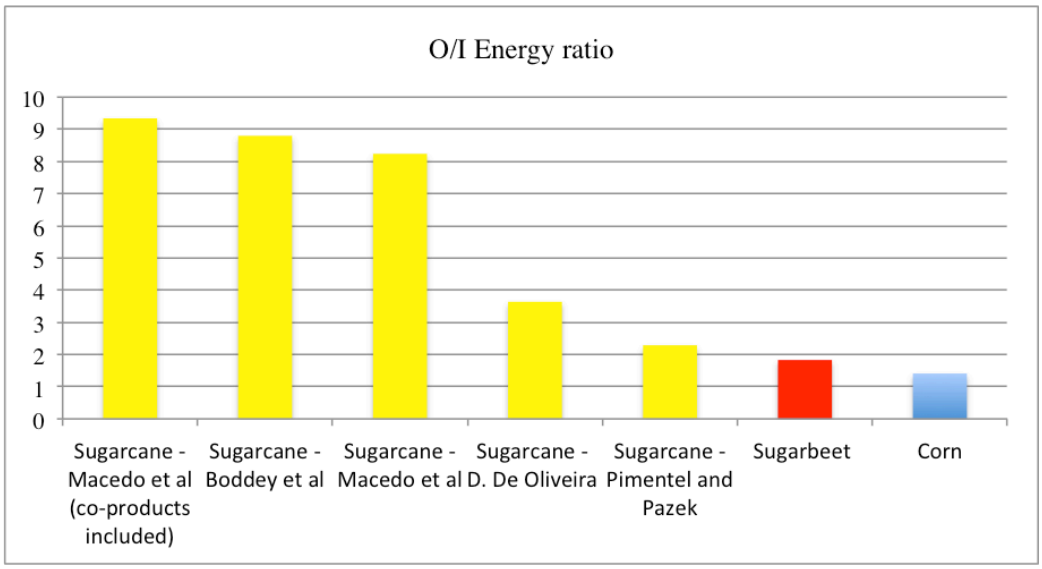

Brazilian ethanol stands out also for the land use. More liters of ethanol are obtained from the unit area than the rest of the world. The Table 1.5 shows the ethanol yield of 2005 and a forecasted scenario for 2030, where second generation technology will hypothetically be developed [62]. This forecast is not according to the one provided by Macedo and Seabra, who are expecting a larger improvement in land use. In their study, they predicted that a 29% smaller area than first generation process is required to get the same amount of ethanol [55].

Table 1.5 Ethanol present and future yields. Present (2008) Colombian yield is 10,200 l/ha. Adapted from [61], [62].

Producer region	*Feedstock*	*2005 yield (L ha^{-1})*	*2030 yield (L ha^{-1})*
EU	Wheat	2500	2980
EU	Sugar beet	5000	5950
US	Corn	3000	3570
Brazil	Sugarcane	6800	8100
Rest of World	Sugarcane	5500	7050
Rest of World	Grain	2000	2560
World	Lignocellulose	4300	5940

It is well known that the mix of ethanol to gasoline causes an oxygenation of the mixture. Because of this the combustion reaches better efficiencies and less CO is released to the atmosphere [63]. The oxygenation causes an increase of CO_2 emission during the combustion but, as previously mentioned, considering the whole life cycle assessment, overall CO_2 emissions are reduced. Unluckily, the mix of ethanol with gasoline presents some disadvantages. It is characterized by a higher value of Reid Vapor Pressure (RVP), which means that the volatility of the liquid increases. As a consequence, there is a higher emission of toxic substances as hydrocarbons, which rise the formation of tropospheric ozone. The ethanol represents a stronger contamination source to the groundwater than gasoline because it filters more easily through the ground and can mix with the water [63]. Moreover, it has been demonstrated that the oxygenation of gasoline with ethanol is not the cheapest option for the GHG emission reduction [63]. The bioethanol production is not economically sustainable by itself and has to be sustained by government policies. As an instance, during the 90s, Brazil government paid 2 billion USD yearly to finance the ethanol program [63]. These costs are reflected on final users and paid by population.

1.3.5 Sugarcane industry in Colombia

Sugarcane came to Colombia imported by Pedro de Herediaa who set the first cultivation in 1538 in Cartagena, and then was brought by Sebastián de Belalcázar in 1540 to Cali, from which it expanded through all the Cauca Valley. [32]. Nowadays sugarcane industry in Colombia is mostly located in the Cauca Valley region, where weather condition and the soil allow for year-round production and harvesting. In Colombia 224,000 cultivated hectares are able to produce 21-23 millions of tons of sugarcane every year, whose 60% sugar is sold in internal market, with the remaining 40% destined to export [59].

Although Colombian sugarcane production does not have a very relevant role in the world context (1.6%) [59], it has to be remarked that its industry is the most efficient in the world in terms of sucrose yield tons/area/year. Moreover, it is ranked sixth in the cost of production, with 146 US$ per ton. Brazil is the leading country with 100 US$ per ton [31]. In the Colombian context sugarcane industry employs 188,000 people. It covers 1% of the country GDP, and the 6% of the GDP of Cauca Valley [59].

The ethanol program in Colombia started in 2005, following the Act 693 of 2001 of the Congress which issued the addition of 10% (v/v) ethanol to gasoline in cities with more than 500,000 inhabitants (this Act was later extended to most of the country). Five distilleries have been built and their capacity is 1,250,000 liters per day. This production is able to cover the 8% of the whole gasoline consumption and leads Colombia to be the second Southamerican ethanol producing country. Because of the increasing forecasted gasoline consumption, the ethanol-gasoline mixture has been reduced to E8, compulsory for the whole county with the only exception of the areas close to Venezuela. Two plants are now under construction ("Bioenergy" plant in Puerto López and distillery of Ingenio Riopaila-Castilla, likely active in 2015), with a total predicted capacity of 880,000 liters per day, which will be able to bring the mixture even to a higher value than E10 [59].

Sugarcane biorefineries in Colombia are producing first generation ethanol, where the bagasse is used for cogeneration, to fully (or partially when they burn coal also) cover the plants' needs and to produce surplus electric energy. The overall capacity of the plants is 185 MW, whose exceeding 55 MW are sold to the electric grid: it represents the 0.4% of the whole Colombian installed capacity. It is planned to reach an overall sugarcane cogeneration capacity of 333 MW, with a surplus of 145 MW before 2015 [59].

Colombian biorefineries are using Indian technology, which may even be superior to the Brazilian one, because it is able to reduce the vinasse production (a byproduct generated after the distillation of fermented molasses) from 15 liters per each liter of ethanol produced to an amount of just 2 liters [61]. In Colombian plants, the vinasse can be further processed to obtain a fertilizer, due to its high content of potassium, phosphorus and magnesium. According to a study provided by EMPA [64] Colombian Bioethanol is most eco-friendly since it reduces GHG emissions in a 74% respect to gasoline, while Brazilian ethanol was in estimated at 65%, UE sugar beet ethanol at 53%, and USA maize ethanol at 10%. Figure 1.14 shows the location of Cauca Valley, where Colombian sugarcane industry is concentrated.

Figure 1.14 Location of Cauca Valley [61].

1.4 References

[1] A. O'Sullivan, S. Shefferin, *Economics: Principles and Tools* (Second ed.) Prentice Hall, 2003.
[2] International Energy Agency, *World Energy Outlook 2011*, 2011.
[3] Committee on Biobased Industrial Products, National Research Council, *Biobased industrial products: research and commercialization priorities*, National Academic Press, Washington D.C. (2000), 74, ISBN 0-309-05392-7.
[4] F. Ullmann, *Ullmann's Encyclopedia of Industrial Chemistry*, 6th ed., electronic release. Weinheim. Wiley-Vch, 1999.
[5] P. McKendry, *Energy Production from Biomass (part 1): Overview of Biomass*, Bioresource Technology 83 (2002), pp 37–46.
[6] K. Soyez, B. Kamm, M. Kamm (eds.), *The Green Biorefinery*, Proceedings of 1st International Green Biorefinery Conference, Neuruppin, Germany, 1997, GO˙T, Berlin (1998), ISBN 3-929672-06-5.
[7] F. Cherubini, *The Biorefinery Concept: Using Biomass instead of oil for producing energy and chemicals*, Energy Conversion and Management 51 (2010), pp 1410-1421.
[8] A. K. Agrawa, *Biofuels (alcohols and biodiesel) applications as fuels for internal combustion engines*, Progress in Energy and Combustion Science 33 (2007), pp 233-271.
[9] British Petroleum, *BP statistical Review of World Energy June 2012*, http://www.bp.com/statisticalreview, 2012.
[10] J.C. Escobar, E. S. Lora, O. J. Venturini, E. E. Yanez, E. F. Castillo, O. Almazan, *Biofuels: environment, technology and food security*, Renewable Sustainable Energy Reviews 13 (2009) pp 1275-87.
[11] Ren 21, Renewable Energy Policy Network for the 21st century, *Renewables 2013, Global status report*, http://www.ren21.net, 2013.
[12] L. Fulton, T. Howes, J. Hardy, *Biofuels for transport: an international perspective*, Paris: International Energy Agency (IEA); 2004.
[13] W. J. Armbruster, W. T. Coyle, *Pacific food system outlook 2006 and 2007: the future role of biofuels*, Singapore: Pacific Economic Cooperation Council, http:// www.pecc.org/food/pfso-singapore2006/PECC_Annual_06_07.pdf, 2006.
[14] J. Pickett, D. Anderson, D. Bowles, T. Bridgwater, P. Jarvis, N. Mortimer, M. Poliakoff, J. Woods, *Sustainable biofuels: prospects and challenges*, London, UK: The Royal Society, http://royalsociety.org/document.asp?id, 2008.
[15] P. S. Nigam, A. Singh, *Production of biofuels from renewable sources*, Progress in Energy and Combustion Science 37 (2011) pp 52-68.
[16] S.N. Naik, V. V. Goud, P. K. Rout, A. K. Dalai, *Production of first and second generation biofuels: a comprehensive review*, Renewable and Sustainable Energy Reviews 14 (2010) pp 578–597.
[17] International Energy Agency, *Biofuels for transport, an internal*

prospective, 2004.
[18] E. D. Larson, *Biofuel production technologies: status, prospects and implications for trade and development*, Report No. UNCTAD/DITC/TED/2007/10, United Nations Conference on Trade and Development, New York and Geneva, 2008.
[19] S.N. Naik, V. V. Goud, P. K. Rout, A. K. Dalai, *Production of first and second generation biofuels: A comprehensive review*, Renewable and Sustainable Energy Reviews 14 (2010), pp 578–597.
[20] M. Kutz, *Environmentally Conscious Transportation,* John Wiley & Sons, 2008, pag 220.
[21] F. Yüksel, B. Yüksel, *The use of ethanol–gasoline blend as a fuel in an SI engine*, Renewable Energy 29 (2004), pp 1181–1191.
[22] A. Walter, F. Rosillo-Calle, P. Dolzan, E. Piacente, K. Borges da Cunha, *Perspectives on fuel ethanol consumption and trade*, Biomass and Bioenergy, 32 (2008), pp 730–748.
[23] F.O. Licht, *World ethanol and biofuels report*, vol.6, no 4 (2007), pag 63.
[24] F.O. Licht, *World ethanol and biofuels report*, vol.7, no 18 (2009), pag 365.
[25] F.O. Licht, *World ethanol and biofuels report*, vol.10, no 16 (2010), pag 323.
[26] A. Hira, L. Guilherme de Oliveira, *No substitute for oil? How Brazil developed its ethanol industry*, Energy Policy 37 (2009), pp 2450–2456.
[27] Renewable Fuel Association, *Accelerating Indusry Innovation -2012-ethanol industry outlook*, 2012.
[28] C. Berg, F.O. Licht, *World Fuel Ethanol Analysis and Outlook*, 2013.
[29] F. Viganò, M. Grosso, *Bioenergy and Waste-to-Energy Techonologies,* Lectures of the course, Politecnico di Milano, 2013.
[30] L. Canilha, A. K. Chandel, T. S. dos Santos Milessi, F. A. Fernandes Antunes, W. L. da Costa Freitas, M. das Gracias Almeida Felipe, S. Silverio da Silva, *Bioconversion of Sugarcane Biomass into Ethanol: An Overview about Composition, Pretreatment Methods, Detoxification of Hydrolysates, Enzymatic Saccharification, and Ethanol Fermentation*, Journal of Biomedicine and Biotechnology, Volume 2012, 2012.
[31] Food and Agriculture Organization of United Nations, *Crop production*, www.faostat.fao.org, 2013.
[32] Asocaña Sector Azucarero Colombiano, *Informe annual de Asocaña 2011-2012*, http://www.asocana.org/modules/documentos/2/234.aspx, 2012.
[33] C.A. Cardona, J.A. Quintero, I.C. Paz, *Production of bioethanol from sugarcane bagasse: Status and perspectives*, Bioresource Technology 101 pp 4754–4766, 2010.
[34] M. O.S. Dias, T. L. Junqueira, C. E.V. Rossell, R. M. Filho, A. Bonomi, *Evaluation of process configurations for second generation integrated with first*

generation bioethanol production from sugarcane, Fuel Processing Technology 109, pp 84–89, 2013.
[35] J.A. Quintero, M. I. Montoya, O.J. Sanchez, O.H. Giraldo, C.A. Cardona, *Fuel ethanol production from sugarcane and corn: Comparative analysis for a Colombian case*, Energy 33, pp 385–399, 2008.
[36] D. Khatiwada, J. Seabra, S. Silveira, A. Walter, *Power generation from sugarcane biomass - A complementary option to hydroelectricity in Nepal and Brazil*, Energy 48, pp 241-254, 2012.
[37] P. Purohit, , A. Michaelowa, *CDM potential of bagasse cogeneration in India*, Energy Policy 35, pp 4779–4798, 2007.
[38] Coordination BNDES and CGEE, *Sugarcane-based bioethanol, Energy for sustainable development,* Rio de Janeiro, http://www.sugarcanebioethanol.org/en/download/ bioetanol.pdf; 2008.
[39] R. Deshmukh, A. Jacobson, C. Chamberlin, D. Kammen, *Thermal gasification or direct combustion? Comparison of advanced cogeneration systems in the sugarcane industry*, Biomass and Bioenergy 55, pp 163-174, 2013.
[40] L. F. Pellegrini, S. de Oliveira Jùnior, J. C. Burbano, *Supercritical steam cycles and biomass integrated gasification combined cycles for sugarcane mills*, Energy 35, pp 1172–1180, 2010.
[41] M. O.S. Dias, T: L. Junqueira, O. Cavalett, M. P. Cunha, C. D.F. Jesus, P. E. Mantelatto, C. E.V. Rossell, R. M. Filho, A. Bonomi, *Cogeneration in integrated first and second generation ethanol from sugarcane*, Chemical Engineering Research and Design 91, pp 1411–1417, 2013.
[42] M.O.S. Dias, T. L. Junqueira, O. Cavalett, M. P. Cunha, C. D. F. Jesus, C. E.V. Rossell, R. M. Filho, A. Bonomi, *Integrated versus stand-alone second generation ethanol production from sugarcane bagasse and trash*, Bioresource Technology 103, pp 152–161, 2012.
[43] G. J. Moraes Rocha, C Martin, I. Barbosa Soares, A. M. Souto Maior, C. A. Moraes de Abreu, *Dilute mixed-acid pretreatment of sugarcane bagasse for ethanol production*, Biomass and Bioenergy 35, pp 663-670, 2011.
[44] G.J.M. Rocha, A.R. Gonc¸alves, B.R. Oliveira, E.G. Olivares, C.E.V. Rossell, *Steam explosion pretreatment reproduction and alkaline delignification reactions performed on a pilot scale with sugarcane bagasse for bioethanol production*, Industrial Crops and Products 35, pp 274–279, 2012.
[45] R. Velmurugan, K. Muthukumar, *Ultrasound-assisted alkaline pretreatment of sugarcane bagasse for fermentable sugar production: Optimization through response surface methodology*, Bioresource Technology 112, pp 293–299, 2012.
[46] M.Camassola, A. J.P. Dillon, *Biological pretreatment of sugar cane bagasse for the production of cellulases and xylanases by Penicillium echinulatum*, Industrial Crops and Products 29, pp 642–647, 2009.

[47] C. Martìn, H. B. Klinkea, A. B. Thomsen, *Wet oxidation as a pretreatment method for enhancing the enzymatic convertibility of sugarcane bagasse*, Enzyme and Microbial Technology 40, pp 426–432, 2007.
[48] L. Mesa, E. González, C. Cara, M. González, E. Castro, S.I. Mussatto, *The effect of organosolv pretreatment variables on enzymatic hydrolysis of sugarcane bagasse*, Chemical Engineering Journal 168, pp 1157–1162, 2011.
[49] Z. Hongdan, X. Shaohua, W. Shubin *Enhancement of enzymatic saccharification of sugarcane bagasse by liquid hot water pretreatment*, Bioresource Technology 143, pp 391–396, 2013.
[50] Ujua, K. Abe , N. Uemura, T. Oshima, M. Goto, N. Kamiya, *Peracetic acid–ionic liquid pretreatment to enhance enzymatic saccharification of lignocellulosic biomass*, Bioresource Technology 138 (2013), pp 87–94, 2013.
[51] R. Travaini, M. D. Morales Otero, M. Coca, R. Da-Silva, S. Bolado, *Sugarcane bagasse ozonolysis pretreatment: Effect on enzymatic digestibility and inhibitory compound formation*, Bioresource Technology 133, pp 332–339, 2013.
[52] A. P. Marianoa, M. O.S. Dias, T. L. Junqueira, M. P. Cunha, A. Bonomi, R. M. Filho, *Utilization of pentoses from sugarcane biomass: Techno-economics of biogas vs. butanol production*, Bioresource Technology 142, pp 390–399, 2013.
[53] L. Mesa, E. González, I. Romero, E. Ruiz, C. Cara, E. Castro, *Comparison of process configurations for ethanol production from two-step pretreated sugarcane bagasse*, Chemical Engineering Journal 175 , pp 185–191, 2011.
[54] C. A. Ramìrez Triana, *Energetics of Brazilian ethanol: Comparison between assessment approaches*, Energy Policy 39, pp 4605–4613, 2011.
[55] I. C. Macedo, J. E. A. Seabra, *Mitigation of GHG emissions using sugarcane bioethanol, Sugarcane ethanol Contributions to climate change mitigation and the environment*, ISBN 978-90-8686-090-6, Wageningen Academic Publishers, The Netherlands, 2008.
[56] X. Z. Sun, S. Fujimoto, T. Minowa, *A comparison of power generation and ethanol production using sugarcane bagasse from the perspective of mitigating GHG emissions*, Energy Policy 57, pp 624–629, 2013.
[57] E. Gnansounou, A. Dauriat, *Energy balance of ethanol: a synthesis*, European Biomass Conference, Paris, France, Oct. 2005.
[58] C. L. Crago, M. Khanna, J. Bartonc, E. Giuliani, W. Amaral, *Competitiveness of Brazilian sugarcane ethanol compared to US corn ethanol,* Energy Policy 38, pp 7404–7415, 2010.
[59] Asocaña Sector Azucarero Colombiano, *Informe annual de Asocaña 2012-2013*, http://www.asocana.org/modules/documentos/2/234.aspx, 2013.
[60] C. N. Hamelinck, A. P.C. Faaij, *Outlook for advanced biofuels*, Energy Policy 34 (2006), pp 3268–3283, 2006.
[61] J. Toasa, *Colombia: A New Ethanol Producer on the Rise?*, United States Department of Agriculture, WRS-0901, January 2009.

[62] M. R. L. V. Leal, L. A. Horta Nogueira, L. A.B. Cortez, *Land demand for ethanol production*, Applied Energy 102, pp 266–271, 2013.
[63] W.A. Ocampo Duque, *¿Es la biogasolina una alternativa ambiental en Colombia?,* Revista Facultad de Ingenieria Universidad de Antioquia 38, pp 7-19, 2006.
[64] Consorcio CUE (EMPA, CNPML y Universidad Pontificia Bolivariana), *Evaluación del ciclo de vida de la cadena de producción de biocombustibles en Colombia*, Jan 2012.

2. Materials and Methods

2.1 The process at Ingenio Manuelita

2.1.1 The company, history and location

Manuelita S.A. is a company part of "Grupo Manuelita", a multinational group working principally in the field of sugar and biofuels with plants and investments in Colombia, Brazil and Peru. Figure 2.1 shows an aerial view of the plant object of this Thesis, is located in the city of Palmira, in the region Cauca Valley. It was firstly built in 1864, being one of the oldest manufacture companies of Colombia. In 1901 became the first plant of Colombia equipped with steam machines. The current configuration of the plant was set in the 50s and, although some equipment has been renewed (like boilers, heat exchangers, etc) and others were added (scrubbers, precipitator, etc). However, any major changes of the layout have been made.

In 2006 the bioethanol plant was inaugurated, able to produce 250,000 l/day. The range of products includes nowadays different types of sugar, ethanol and byproducts like vinasse and sludge that can be used as fertilizers. Bagasse also can be considered a byproduct because it may be sold to paper industry. Manuelita S.A. has agreements in order to exchange a percentage of bagasse by coal, which is burnt in the boilers. Nowadays it employees around 3,000 people (directly and indirectly) and it produces 260,000 tons/year of sugar, 70% of which is sold to industry customers and the other 30% to mass consumption.

Figure 2.1 View of the plant of Ingenio Manuelita

2.1.2 The process

The process starts in the field, where the cane is firstly partially burnt -if it is planned to be manually cut-, in order to eliminate the leaves and to facilitate the job of the cutters. If mechanical cut is performed there is not need of burning. Figure 2.2 shows a simplified scheme of the production process of Ingenio Manuelita.

Figure 2.2 Scheme of the Process of Ingenio Manuelita [1]

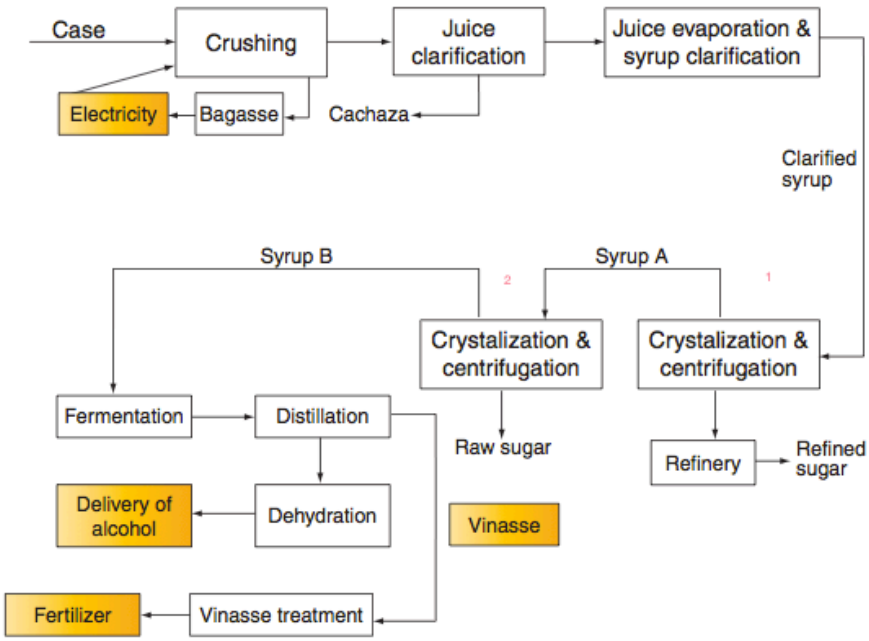

Once brought to the plant with trucks, the cane is ready to undergo at the preparation step, whose aim is to reduce the cane pieces into a suitable size for the operation of the mills, to break sugar bearing cells to facilitate the extraction of sugar. A material with the correct characteristics for the milling must be prepared. Preparation is a crucial step because a greater breakage of sugar-containing cells results in higher extraction of sugar and lower bagasse moisture [2]. After crossing two levelers knives, cane preparation is given by a shredder, which is a rotor provided by hammers.

After being defibered, cane is sent to the two mill tandems where it is squeezed under high pressure between successive pairs or rolls. Around 66% of cane is going to Tandem Two provided by six mills. Each mill is moved by a steam turbine and has the aim to continue cane preparation and to separate the fiber

and the sucrose-containing juice. The remaining cane is milled into Tandem One, provided with six mills and a crusher.

Through the mills the separated fiber forms the bagasse that has typical moisture of 50% and is sent to the boilers. Thanks to the addition of hot imbibition water, the sucrose extraction cane reaches a level of 96% [3]. 4% is lost with bagasse. The juice is collected into tanks and lime ($Ca(OH)_2$) is added to control pH. Then, the juice is heated through a series of heat exchangers, fed by the gases coming from the multi-effect evaporators. The next step is the clarification whose aim is to form flocs to trap the suspended matter: pH, temperature and ion concentration is required to optimize the precipitation of soluble impurities of the juice. Thus a clarified juice of high quality, with minimum turbidity and color, and with a pH that minimizes the inversion of sugars is produced. Also a settled mud is produced which undergoes a filtration process that allows the recovery of deposited sucrose. The final sludge, called "cachaza", trashed by clarification and filtration, is a byproduct of the process used as compost.

Clarified juice enters to a five-effect evaporator tandem, whose aim is to increase the brix of the solution (quantity of soluble matter in the solution, mostly sucrose). In multi-effect evaporators water is boiled in a sequence of vessels, each one held with a lower pressure than the previous. In this way the evaporated mass of one vessel, is able to evaporate part of the liquid of the next vessel, obtaining in this way an increase of efficiency. Moreover, the gases extracted by the first three effects, since the brix of the solution has to be controlled to avoid crystallization in the evaporator, are more than the required amount in evaporation itself. So they are used to cover an important percentage of heat demand of the plant.

After being concentrated, the juice is ready to produce sugar crystals. This happens through sugar boiling in a process very similar to the one of the evaporation: in vacuum pans, low pressure and heat supply to create the conditions of super-saturation. Thus, sucrose crystals separate from the solution. The output of the pan is called massecuite. It is then formed by crystals and by a syrup called molasses. Massecuite is sent to centrifuges where crystals and molasses are divided. Crystals go to refining process and molasses go to the pans B where the same procedure is done.

Molasses separated by B pans and B centrifuges are the sent to the distillery to produce ethanol, while B crystals are dissolved into water and recycled to the A pans. A crystals are melt and the solution undergoes the refining step, whose aim is to remove the remaining impurities and color of the sucrose. This is

reached by another clarification with the addition of phosphoric acid and calcium saccharide and by a filtration through activated charcoal.

The solution is then ready to release its sucrose content. Another passage through vacuum pans is performed and sugar is finally delivered. B molasses from B pans are firstly fermented by the action of yeasts, which transform sucrose into ethanol and carbon dioxide, then distillated till the azeotropic point (95.6% ethanol, at 78 °C and 1 atm of pressure). The azeotropic ethanol is then dehydrated through filtration in tanks of molecular sieves. Finally the ethanol is ready for the storage and delivery. A more detailed scheme than Figure 2.2, including sugar and ethanol process, is depicted in Annex 1, while Annex 2 provides some pictures taken at the plant.

2.1.3 The Equipment

The plant requires electric, mechanic and heat power to fulfill the process demand. It is equipped with a wide variety of machinery. Table 2.1 shows a list of the equipment involved in the production of sugar. The Rankine cycle for the cogeneration of electric, mechanic and heat power is a core part of the plant. It is structured with three different pressure heads: 400 PSIG (28.6 bar), 300 PSIG (21.7 bar) and 25 PSIG (2.7 bar). As shown in the scheme of steam of Annex 3, the steam is generated into 3 different boilers, named Boiler 5, Boiler 6 and Boiler 7. (See Figure 2.17). In Boiler 7 the steam is generated at 400 PSIG and 410 °C (before undergoing a tempering process that brings its temperature to 370 °C) and only bagasse is burnt. Bagasse has a LHV of 7,984 kJ/kg. Boilers 5 and 6 generate superheated steam at 300 PSIG and 330 °C and burn both bagasse and coal, which has an average LHV of 23,303 kJ/kg.

The plant is equipped with 23 Turbines, operating on the two available enthalpy drops and supplying energy to different equipment. The head of 400 PSIG feeds five turbines for electric power generation, the turbines that are running the turbo-pumps of Boiler 7 and the turbine of the fan of the same boiler. All the other turbines are connected to the head of 300 PSIG. There are the Turbines joined to the pumps and fans of Boilers 5 and 6, Turbines of the mills, of the shredder, and of the crusher. All the turbines discharge finally steam in the head of 25 PSIG, which is maintained, through the addition of tempering water, at vapor saturated condition. It provides most of the steam for the heat requirement of the sugar and ethanol processes. Part of the distillery of ethanol and some equipment of the sugar plant, like the drier, are fed with steam from the head of 300 PSIG. It is important to remark that, not having the plant the possibility to inject electric energy in the grid, only the electric energy that is internally consumed is produced.

Table 2.1 Equipment of the whole process of sugar production

PROCESS	*EQUIPMENT*	*AMOUNT*
Cane Preparation	Crane	3
	Shredder	1
	Cane carrier	4
	Cane handler	5
	Leveler	3
	Crusher	1
Milling	Mill	12
	Cane carrier	13
	Pump	13
	Tromel filter	1
	Juice strainer	1
Boiler	Boiler	3
	Pump	2
	Turbo-pump	2
	Forced air fan	3
	Bagasse blower fan	3
	Coal blower fan	3
	Bagasse carrier	14
Electric energy generation	Turbo-generator	5
	Diesel generator	1
Juice heating	Heater	6
Clarification	Clarifier	1
Filtration	Filter	7
	Sludge transporter	1
	Pump	1
Evaporation	Evaporator	17
	Pump	5
Crystallization	Vacuum Pan	9
Centrifuge	A centrifuge	13
	B centrifuge	3
	Pump	3
Drying	Dryer	4
	Separator	6
Packaging	Packer	7

The circuit of steam is provided of two stations of pressure reduction to laminate the steam from 400 to 300 PSIG, and from 300 to 25 PSIG. The head of the 300 has the possibility to discharge steam in excess to the atmosphere. Figure 2.3 and 2.4 provides the T-s diagrams of the two different cogenerative Rankine cycles of the plant.

Figure 2.3 T-s diagram of 400-25 PSIG Rankine cycle. Point 1-Boiler 7 internal superheated steam; Point 2-Boiler 7 steam after tempering; Point 3-Turbine outlet; Point 4-Process outlet.

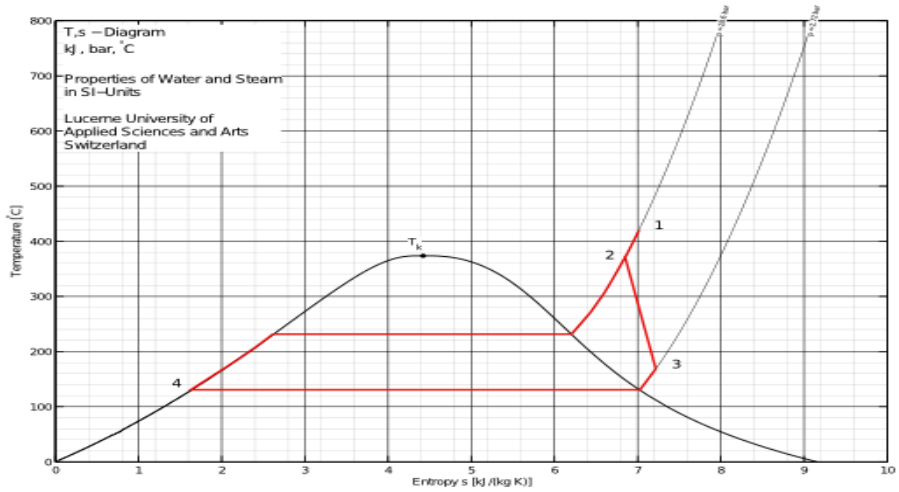

Figure 2.4 T-s diagram of 300-25 PSIG Rankine cycle. Point 1-Boiler 5-6 superheated steam; Point 2- Turbine outlet; Point 3-Process outlet.

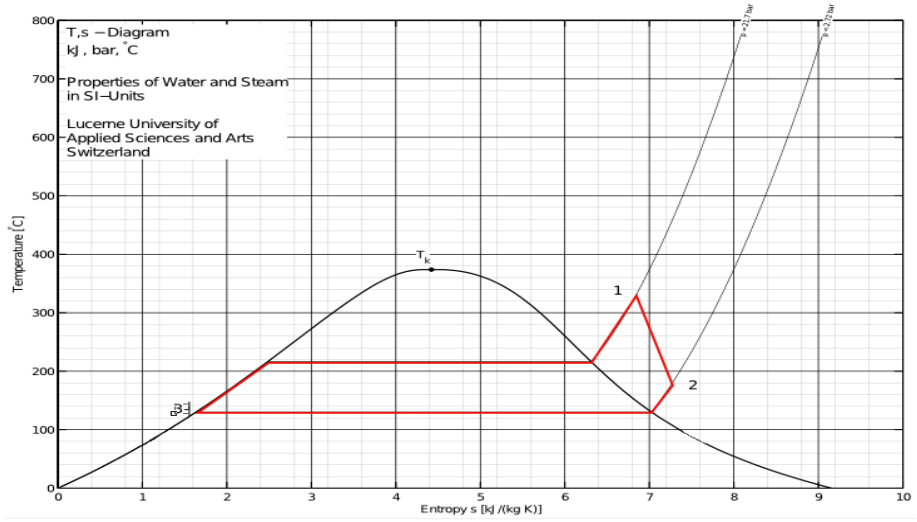

2.2. Current Model – Mass and Energy Balances

The properties of the main variables have been taken into account as an average of the data of the last three years at Ingenio Manuelita, and the parameters of the process have been chosen in order to fit these data. Matlab R2010b (with Global Optimization Toolbox), Excel 2011 and XLStat were the programs used to develop the model, run optimizations and the statistical analysis. Water equations, required to compute water and steam properties, are given by "International Association for Properties of Water and Steam Industrial Formulation", (IAPWS IF-97) [4].

2.2.1 Milling

Figure 2.5 shows a simplified mass balance of a mill tandem where m_C is the cane, m_W the water added, m_{DJ} the diluted juice, and m_{BAG} the bagasse. The cane input in the process has been modeled with the following properties [3]:

- Sucrose content: $x_{SC} = 0.1328$;
- Fiber and insoluble: $x_{INS} = 0.1586$;
- Sucrose purity: $\Phi = 85.79\%$;

It is important to remark the meaning of sucrose purity, which is the ratio between sucrose and total soluble matter content x_{SOL} (Equation 2.1):

$$\Phi = \frac{x_{SC}}{x_{SOL}} \tag{2.1}$$

Using the definition 2.1 and the above data it is then possible to calculate the "other soluble" content x_{SL}, the water by subtraction to the complement and then to describe completely the cane.

$$x_{SL} = \frac{x_{SC}}{\Phi} - x_{SC} \tag{2.2}$$

The imbibition water addition in the milling has been calculated in order to obtain a 1.061 ratio between the weight of the extracted juice and the input cane. Other parameters selected for the milling were [3]:

- Milling efficiency, which is the ratio between extracted sucrose and sucrose content of the cane: $\eta_{MILL} = 0.9591$;
- Extraction of other soluble: $e_{SL} = 0.840$;
- Humidity of the bagasse: $x_W = 0.4957$;
- Water loss by evaporation in milling [5]: 0.15%;
- Reducing sugars fraction in diluted juice: $x_{RS\text{-}DJ} = 0.0055$;

- Insoluble content in diluted juice: $x_{INS\text{-}DJ} = 0.011$;
- Mass flow of diluted juice m_{DJ} [kg/s];
- Mass flow of cane m_C [kg/s];
- Sucrose mass flow in diluted juice and in cane $m_{SC\text{-}DJ}$ and $m_{SC\text{-}C}$ [kg/s];
- Other soluble mass flow in diluted juice $m_{SL\text{-}DJ}$ [kg/s];
- Reducing sugars mass flow in diluted juice $m_{RS\text{-}DJ}$ [kg/s];
- Insoluble matter mass flow in diluted juice $m_{INS\text{-}DJ}$ [kg/s];
- Water mass flow in diluted juice $m_{W\text{-}DJ}$ [kg/s];

The composition of diluted juice is then calculated with the following equations (2.3-2.8):

$$m_{DJ} = 1.061 * m_C \ [\frac{kg}{s}] \quad (2.3)$$

$$m_{SC-DJ} = m_{SC-C} * \eta_{MILL} \ \left[\frac{kg}{s}\right] \quad (2.4)$$

$$m_{SL-DJ} = x_{SL} * m_C * e_{SL} \ \left[\frac{kg}{s}\right] \quad (2.5)$$

$$m_{RS-DJ} = m_{DJ} * x_{RS-DJ} \ \left[\frac{kg}{s}\right] \quad (2.6)$$

$$m_{INS-DJ} = m_{DJ} * x_{INS-DJ} \ \left[\frac{kg}{s}\right] \quad (2.7)$$

$$m_{W-DJ} = m_{DJ} - \left(m_{SC-DJ} + m_{SL-DJ} + m_{RS-DJ} + m_{INS-DJ}\right) \ \left[\frac{kg}{s}\right] \quad (2.8)$$

Figure 2.5 Simplified mass balance of a mill tandem

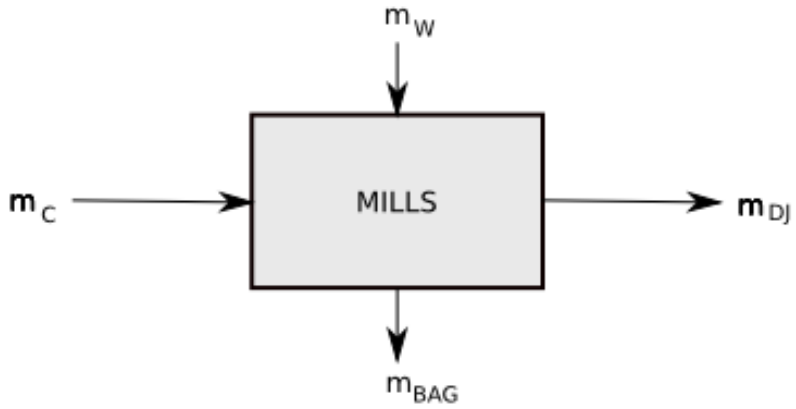

According to the average of the data provided by the manufacturer [6], the power demand of the shredder has been calculated as 34.98 kW/tfh. (tons of fiber per hour). After this preparation step, one third of the cane is sent to tandem 1, while the remaining is milled in Tandem 2.

It is quite difficult to express the energy requirement of the mills and crusher, because it depends on the fiber content of the cane, on the friction absorbed between journals and bearings, on the friction between bagasse and trash plate, on the friction between scrapers and rollers, on the power absorption of the intermediate carrier drive, on the gearing, among others. Anyway, it is known that the power absorption can be expressed with a simplified equation, whose result is approximates fairly well the actual values [2, 5]. According to Hugot [5] the power requirement (P in kW) to mill the cane is depending on the milling rate, on the diameter of the device, on the rotational speed, and on a constant that depends on the degree of preparation of the cane. The equation that represents this consumption is the following:

$$(2.9) \quad P = k * n * D * TF \quad [kW]$$

where k is an adimensional constant, the rotational speed n is expressed in rpm, the diameter D in meters and the total high pressure (TF) in ton. The following constants presented in Table 2.2, giving the result in kW, where selected from Hugot [5] for being the most similar to the case of Manuelita.

Moreover, Hugot [5] affirms that, for long tandems (17-25) rollers, it is possible to estimate an average tandem power requirement of 15-18 HP per mill, per teach on of fiber processed per hour (HP/tfh-mill). Figure 2.6 shows a typical mill tandem provided by four mills and a crusher. Considering that the tandems of Manuelita plant are made of 18 rollers, taking an indicative value of 17 HP/tfh-mill (due to the kind of preparation at which the cane comes at the tandems, which is different in the two tandems because of the presence of the crusher), the total power of each tandem is computed, and, by using the coefficients of the previous table, different power requirement is then associated to each mill.

Table 2.2 Parameters to estimate the mills power

Equipment	*Value of constant k*
Crusher	0.150
Mill position 1 in the tandem	0.199
Mill position 2 in the tandem	0.169
Mill position 3 in the tandem	0.151

Mill position 4 in the tandem	0.145
Mill position 5 in the tandem	0.145
Mill position 6 in the tandem	0.145

Figure 2.6 Scheme of a typical mill tandem provided by four mills and a crusher

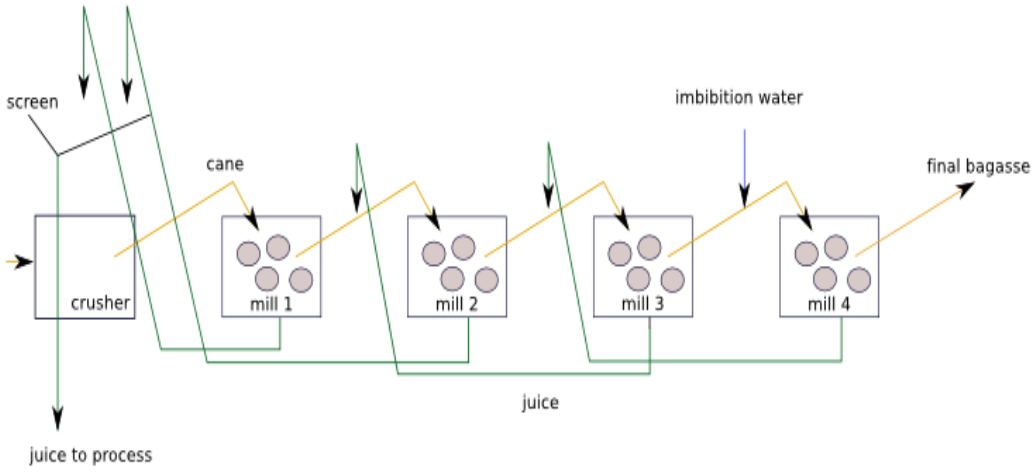

2.2.2 Heating and clarification

Figure 2.7 shows a part of the heating and clarification stage. Outputs from this stage are the clarified juice (m_{CJ}) and the sludge (m_S). Clarification requires a flocculant. For the clarification, in two different phases, 0.4 kg of lime are added per each ton of cane at 5 degree Baumé. It means that 21.6 kg of water are mixed per each kg of lime. Being the juice a mixture of sucrose, reducing sugars, and other soluble and insoluble matters, a parameter called Brix degrees has a fundamental role to determine the properties. The Brix degrees are defined as the percentage of soluble matter dissolved in a mixture. After being diluted and partially alkalized, the juice is heated into two series of heat exchangers. in the first series, parallel plate types, the juice is heated from 30 °C to 50 °C by "Gases 3", while in the following shell and tubes it is heated up to 75 °C by "Gases 2" (Figure 2.10).
The heat absorbed (Q) by the juice is given by the formula

$$Q = m_J * c_p * \Delta T \quad [kW] \tag{2.10}$$

where m_J is juice mass flow expressed in kg/s, C_p is specific heat at constant pressure of the juice (kJ/kg/K) and ΔT the temperature difference between juice inlet and outlet (°C). The C_p for the juice can be considered constant with

respect to temperature with a good precision [5], and is dependent of the Brix degrees of the solution, as follows:

$$c_{p_{juice}} = 4.186 * \left(1 - (0.006 * B)\right) \left[\frac{kJ}{kg}\right] \quad (2.11)$$

The steam required by these devices (m_{vap}), which is considered to be in saturated condition, is calculated with the following equation, and increased by 10% to take into account the heat losses to the environment:

$$m_{VAP} = \frac{Q}{\Delta h_{COND}} \left[\frac{Kg}{s}\right] \quad (2.12)$$

In the secondary tank (Figure 2.7), the juice coming from the mills (m_{DJ}) is mixed with juice coming from the filtering of the sludge of clarification (m_{FJ}) and with the foam coming from the clarification of the refining part of the process ($m_{J\text{-}CR}$).

The following parameters are assumed for the stream coming from the filters:

- Amount of juice coming from the filters x_{FJ}: 11% of juice coming from the mills;
- Brix of filtered juice: $B_{FJ} = 9.48$;
- Sucrose content of filtered juice: $x_{SC\text{-}FJ} = 0.0826\%$;
- Filtered juice is supposed to be completely cleaned from insoluble matter and from soluble matter different from reducing sugars;

With these parameters is possible to estimate the composition of the filtered juice stream, its Brix degrees and its water content. New variables are introduced to identify the different streams:

- Mass flow of filtered juice m_{FJ} [kg/s];
- Sucrose mass flow in filtered juice $m_{SC\text{-}FJ}$ [kg/s];
- Total soluble matter mass flow in filtered juice $m_{SOL\text{-}FJ}$ [kg/s];
- Water mass flow in filtered juice $m_{W\text{-}FJ}$ [kg/s];

The Equations 2.13 to 2.16 are the mass balances and expressions for the filtered juice stream. The indices mean *W*: water, *SOL*: other soluble, *SC*: sucrose, *FJ*: filtered juice.

$$m_{FJ} = x_{FJ} * m_{DJ} \left[\frac{kg}{s}\right] \quad (2.13)$$

$$m_{SC-FJ} = x_{SC-FJ} * m_{FJ} \left[\frac{kg}{s}\right] \quad (2.14)$$

$$m_{SOL\_FJ} = B_{FJ} * m_{FJ} - m_{SC\_FJ} \left[\frac{kg}{s}\right] \quad (2.15)$$

$$m_{W\_FJ} = m_{FJ} - m_{SC\_FJ} - m_{SOL\_FJ} \left[\frac{kg}{s}\right] \quad (2.16)$$

Figure 2.7 Scheme of part of heating and clarification stage

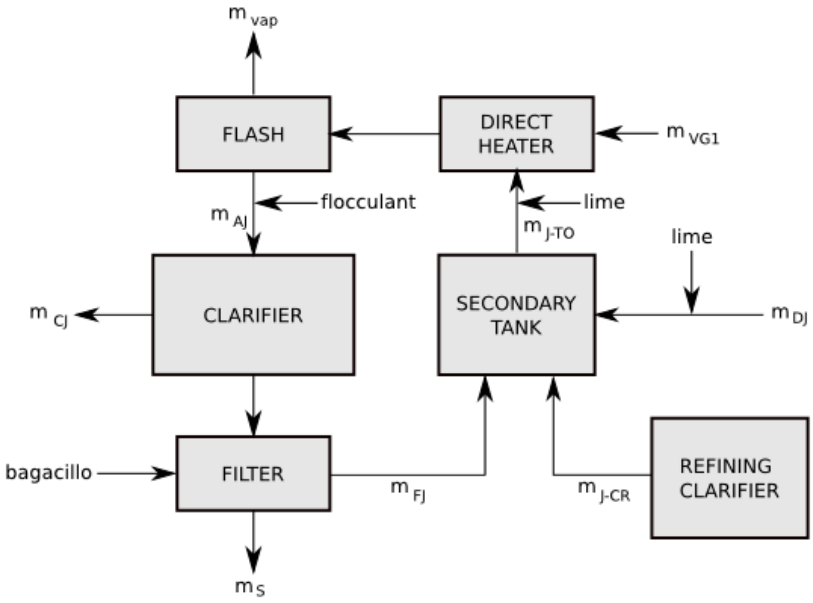

The same calculations are performed for the stream coming from the clarifier of the refining stage but with different parameters:

- Amount of foam $m_{J\text{-}CR}$: 3% of juice coming from mills m_{DJ};
- Sucrose content of the foam: $x_{SC\text{-}F} = 0.468$;
- Other soluble matter content of the foam: $x_{SL\text{-}F} = 0.227$;
- Insoluble fraction of the foam: $x_{INS\text{-}F} = 0.003$;

Once calculated the properties of all the input streams of the tank of secondary juice, the output stream ($m_{J\text{-}TO}$) is defined as follows:

$$m_{J-TO} = m_{DJ} + m_{FJ} + m_{J-CR} \left[\frac{kg}{s}\right] \quad (2.17)$$

$$B_{J-TO} = \frac{B_{J-TI}}{m_{J-TO}} \ [°B] \quad (2.18)$$

where:

- $B_{J\text{-}TI}$ stands for the inlet of dissolved matter in the tank, and is calculated as the sum of the dissolved matter of the three different streams
- $B_{J\text{-}TO}$ represents Brix degrees at secondary tank outlet [°B];
- $m_{J\text{-}TO}$ is the juice mass flow at tank outlet [kg/s];
- $m_{J\text{-}CR}$ is the juice (foam) mass flow coming from the refining clarifier [kg/s];

All the components of the output stream in the secondary tank (sucrose $m_{SC\text{-}TO}$, others soluble $m_{SL\text{-}TO}$ and insoluble matter $m_{INS\text{-}TO}$, water $m_{W\text{-}TO}$) can be calculated, in steady state condition, with the mass balance. Equation 2.19 explains the procedure to obtain sucrose mass flow of tank output stream. $m_{SC\text{-}CR}$ represent sucrose mass flow in foam mass flow of refinery clarifier, expressed in kg/s.

$$(2.19)\quad m_{SC\_TO} = m_{SC\_DJ} + m_{SC\_FJ} + m_{SC\_CR} \left[\frac{kg}{s}\right]$$

The juice is heated up to 98 °C in another shell and tubes heat exchanger fed by "Gases 1". The Figure 2.8 shows the next direct heater stage, where the heat is provided by "Gases 1" (m_{VG1}, coming from the first effect of the evaporator), where the heat losses to environment are supposed to be of 15% and, after that, in a direct heater, where the juice is directly mixed with the "gases 1" until reaching a temperature of 103 °C (pressure is higher than atmospheric, so juice is in liquid condition). The amount of required gases can be computed numerically, since the addition of water vapor in the juice affects also the Brix and its enthalpy, indeed. For the energy and material balance at the direct heater (Equations 2.20-2.22), the following variables are introduced:

- Mass flow of incoming juice in the heater $m_{J\text{-}in}$ [kg/s];
- Specific enthalpy of incoming juice in the heater $h_{J\text{-}in}$ [kJ/kg];
- Brix degrees of incoming juice in the heater B_{in} [°B];
- Mass flow of outgoing juice from the heater $m_{J\text{-}out}$ [kg/s];
- Specific enthalpy of outgoing juice from the heater $h_{J\text{-}out}$ [kJ/kg];
- Brix degrees of outgoing juice from the heater B_{out} [°B];
- Mass flow of incoming steam in the heater m_{VG1} [kg/s];
- Specific enthalpy of incoming steam in the heater $h_{SAT\text{-}VAP\ @pVG1}$ [kJ/kg];

$$(2.20)\quad m_{J\_in} * h_{J\_in} + m_{VG1} * h_{SAT\_VAP}@\,p\,VG1 = \left(m_{J\_in} + m_{VG1}\right) * h_{J\_out} \left[\frac{kg}{s}\right]$$

$$(2.21)\quad B_{out} = B_{in} * \frac{m_{J\_in}}{\left(m_{J\_in} + m_{VG1}\right)} \ [°B]$$

$$m_{J_{-out}} = m_{J_{-in}} + m_{VG1} \left[\frac{kg}{s}\right] \quad (2.22)$$

Figure 2.8 Scheme of direct Heater

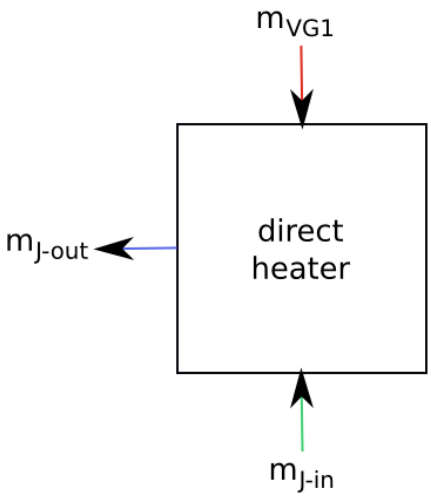

With the same procedure it is possible to perform the energy and mass balances of the flash tank, taking into account that the output is at atmospheric pressure. New variables are added, and the assumed parameters of the clarifier are the ones regarding the sludge output:

- Ratio between sludge and input sugar cane in the process: m_S/m_C = 0.0415;
- Ratio between flocculating addition (*FL*) and input sugar cane m_C in the process: m_{FL}/m_C = 0.001;
- Sucrose fraction of the sludge: $x_{SC\text{-}S}$ = 0.017;
- "Bagacillo" (*BL*) percentage of the sludge: $x_{bagacillo}$ = 5%;
- Mass flow rate of alkalized juice m_{AJ} [kg/s];
- Ratio between insoluble matter of the sludge and insoluble matter input in the clarifier: $m_{INS\text{-}S}/(m_{INS\text{-}AJ}+m_{FL})$ = 98%;
- Ratio between other soluble matter of the sludge and other soluble matter input in the clarifier: $m_{SL\text{-}S}/m_{SL\text{-}AJ}$ = 45%;
- Mass flow rate of clarified juice m_{CJ} [kg/s];

Equations 2.23 to 2.28 represent the mass balances and expressions for the sludge.

$$m_S = 0.0415 * m_C \left[\frac{kg}{s}\right] \quad (2.23)$$

$$m_{SC\_S} = 0.017 * m_S \left[\frac{kg}{s}\right] \quad (2.24)$$

$$m_{INS\_S} = 0.98 * \left(m_{INS\_AJ} + m_{FL}\right) \left[\frac{kg}{s}\right] \quad (2.25)$$

$$m_{SL\_S} = 0.45 * m_{SL\_AJ} \left[\frac{kg}{s}\right] \quad (2.26)$$

$$m_{W\_S} = m_S - m_{SC\_S} - m_{INS\_S} - m_{SL\_S} - m_{BL} \left[\frac{kg}{s}\right] \quad (2.27)$$

$$m_{CJ} = m_{AJ} - m_S - m_{FJ} \left[\frac{kg}{s}\right] \quad (2.28)$$

All other properties of the clarified juice output are calculated, through conservation of mass equations, by subtraction between the inlet stream and the outlet sludge and filtered juice streams. Equation 2.29 calculates the balance for sucrose flow streams and the terms represents in the order the sucrose mass flow rate of clarified juice ($m_{SC\text{-}CJ}$), alkalized juice ($m_{SC\text{-}AJ}$), filtered juice ($m_{SC\text{-}FJ}$) and sludge ($m_{SC\text{-}S}$).

$$m_{SC\_CJ} = m_{SC\_AJ} - m_{SC\_FJ} - m_{SC\_S} \left[\frac{kg}{s}\right] \quad (2.29)$$

Clarified juice is collected in a tank, where it is mixed with a 2.5% of water of its weight. Such water is supposed to contain the 1% of sucrose, since it is the water coming from the cleaning of other tanks. The mass stream, Brix and sucrose content are then updated and he juice undergoes another heating process before entering to the evaporators. It is firstly heated from a temperature of about 90 to 103 °C (the pressure I this point is 1.69 bar) from "gases 1" in a parallel plate heat exchanger, and then till 115 °C in another plate heat exchanger by exhaust steam of the turbines (VE), which is coming from the head of 25 PSIG (2.72 bar) which is always kept at saturated steam condition by tempering water (Figure 2.9).

Figure 2.9 Scheme of heaters

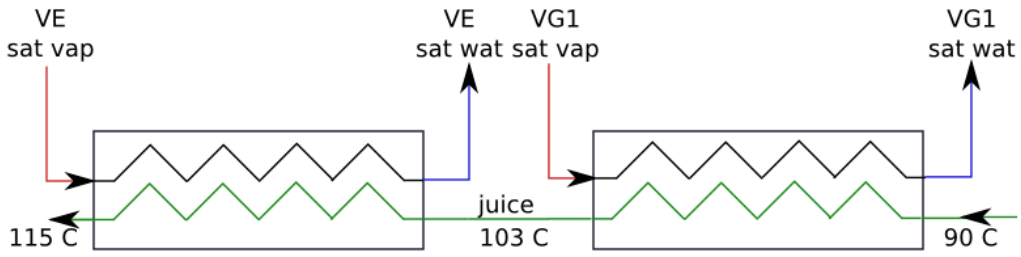

2.2.3 Evaporation section

The evaporation section has five different effects, as shown in Figure 2.10. The purpose is to eliminate water from the clarified juice (m_{CJ}) to concentrate the sucrose in the juice (m_{CNJ}). The operating conditions in evaporators are depicted in Table 2.3.

Figure 2.10 Scheme of juice material balance in the five effects of evaporation

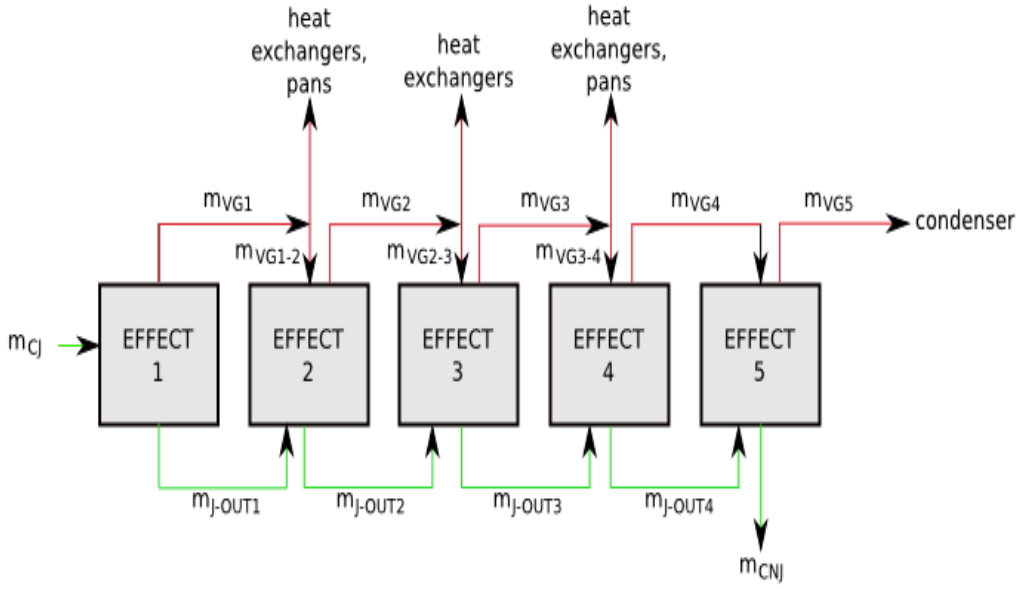

Table 2.3 Operating conditions of the evaporating tandem

Effect	*Pressure [bar]*	*Brix at Output [°Bx]*
1	1.69	21.09
2	1.34	27.63
3	1.07	36.01*
4	0.68	45.93
5	0.29	65.3*

*Model predicted

The first effect is fed with exhaust gases, while the heat of all the other effects is provided by the steam of the antecedent effects, which has higher enthalpy because of the difference in pressure. It is necessary to fix the Brix at output of some effects because, for example, the steam of Effect 1 is used in many devices. So, in order to perform the mass balance such parameter has to be assumed. Differently, in the case of Effect 3, the gases of Effect 2 are used in heaters

whose requirement have already been calculated, and it is then know the amount of "Gases 2" available for the third effect and the balance is closed. In the case of Effect 5, the "Gases 4" have just the aim to feed this effect, so once again the balance is closed.

Being the juice an impure solution of water and sucrose, saturation temperature undergoes a change, called "Boiling Point Rise". This BPR, at a given pressure, increases with the concentration of the solution, or with the Brix of the juice. For high purities, and in the range of pressures at which the evaporators operate, the BPR can be calculated with the following expression [5]:

$$BPR = \frac{2 * B}{100 - B} \quad [°C] \tag{2.30}$$

The temperatures in nth effect and of the relative steam flows are:

$$T_{nthEFF} = T_{SAT@p_{nt}hEFF} + BPR_{nthEFF} \quad [°C] \tag{2.31}$$

Moreover, in the nth effect, given inlet and outlet juice mass flow ($m_{J\text{-}IN}$ and $m_{J\text{-}OUT}$, [kg/s]), inlet and outlet Brix degrees (B_{IN} and B_{OUT} in [°B]), evaporated water (m_{VAP} [kg/s]), specific enthalpy of evaporation ($\Delta h_{EVAP\ @T\ nth\ effect}$ [kJ/kg]), and heat absorbed by evaporating water (Q_{EVAP} [kW]), mass and energy balances for the nth effect, where Brix output is fixed, are as follows:

$$m_{J-OUT} = B_{IN} * \frac{m_{J-IN}}{B_{OUT}} \quad \left[\frac{kg}{s}\right] \tag{2.32}$$

$$m_{VAP} = m_{J-IN} - m_{J-OUT} \left[\frac{kg}{s}\right] \tag{2.33}$$

$$Q_{EVAP} = m_{VAP} * \Delta h_{EVAP@T_{nthEFF}} [kW] \tag{2.34}$$

In Effects 3 and 5 the algorithm follows the opposite path. Knowing the available "gases" it is possible to compute the available heat and then the evaporated water, the juice mass flow and its Brix, as follows:

$$m_{VG2_{-3}} = m_{VG2} - m_{VG2_{-ST}} \left[\frac{kg}{s}\right] \tag{2.35}$$

$$m_{VG4_{-5}} = m_{VG4} \left[\frac{kg}{s}\right] \tag{2.36}$$

These steam flow rates refers to Figure 2.10: the general term $m_{VGi\text{-}i+1}$ stands for the amount of steam of effect i which provides heat power to $i+1$ effect while

the term $m_{VG2\text{-}ST}$ indicates the steam from Effect 2 which is sent to the heaters. The heat power available to the *nth+1* effect (Q_{nth+1}) is given by the availability of gases of the *nth* effect and by the enthalpy of condensation of steam at the temperature of the *nth* effect.

$$Q_{nth+1} = m_{VG(nth)} * \Delta h_{COND@T_{nthEFF}} \quad [kW] \tag{2.37}$$

Evaporated water has been computed iteratively, because its value influences the Brix, the BPR and thus the energy balance, which is strictly related to mass one.

2.2.4 Sugar Boiling

The juice, now called "concentrated", for having reached around 60 degrees Brix after the fifth effect of the evaporation, is collected in a tank where it is mixed with syrup coming from the refining, whose parameters are:

- Ratio between syrup addition (*SR*) and mass flow of concentrated juice: $m_{SR}/m_{CNJ} = 0.0168$;
- Sucrose content in concentrated juice: $x_{SC\text{-}CNJ} = 0.727$;
- Other soluble matter content in concentrated juice: $x_{SL\text{-}CNJ} = 0.009$;

This stream is injected into the A vacuum pans, operating at a pressure of 0.265 bar. In the pans, it is mixed with the stream of B magma, whose properties has to be calculated through an iterative process and, thanks to the action of low pressure, and of heating (heat provided by gases 1), more water evaporates and, a condition of super-saturation of the solution is reached. Because of this the sucrose contained in the juice starts to crystallize. The parameter that is assumed to perform calculations is the Brix of A massecuite (the mix of crystals and liquid "molasses" at output of the pans). Its value was taken as the average of the last three years and is 0.92. First of all the different components of the mass inside the pan are calculated, like sucrose in this example (it refers to Figure 2.11):

$$m_{SC-P} = m_{SC-CNJ} + m_{SC-SR} + m_{SC-B-M} \left[\frac{kg}{s}\right] \tag{2.38}$$

where the terms represent sucrose mass flow inside the pan ($m_{SC\text{-}P}$), in concentered juice($m_{SC\text{-}CNJ}$), in syrup ($m_{SC\text{-}SR}$) and in the B-magma ($m_{SC\text{-}B\text{-}M}$). In figure 2.11 $m_{W\text{-}EVAP}$ is the flow of evaporated water and $m_{A\text{-}MS}$ is the flow of the massecuite A.

Figure 2.11 Scheme of sugar boiling stage

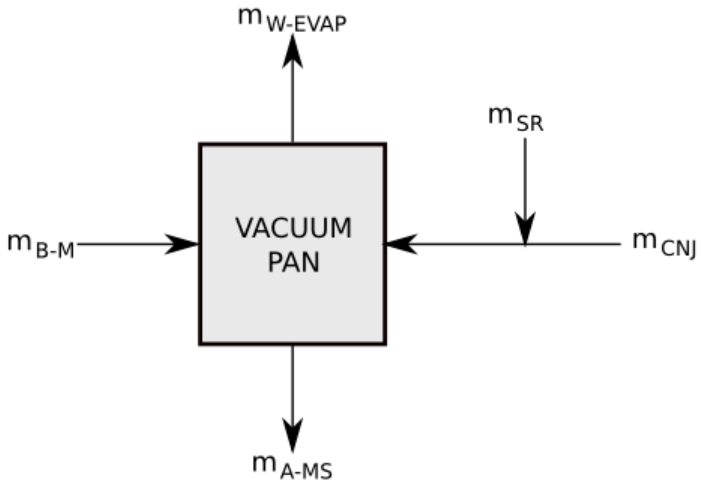

Then, the mass balance on the water allows computing evaporated water, heat requirement and solubility of the massecuite to evaluate the amount of crystals that are formed. The following streams and properties are defined:

- A-massecuite mass flow $m_{A\text{-}MS}$ [kg/s];
- Mass flow of sucrose $m_{SC\text{-}in}$, other soluble $m_{SL\text{-}in}$ and insoluble matter $m_{INS\text{-}in}$ incoming in the pan [kg/s];
- Mass flow of evaporated water in the pan $m_{W\text{-}EVAP}$ [kg/s];
- Mass flow of water ($m_{W\text{-}A\text{-}MS}$), sucrose ($m_{SC\text{-}A\text{-}MS}$), other soluble ($m_{SL\text{-}A\text{-}MS}$) and insoluble matter ($m_{INS\text{-}A\text{-}MS}$) in A-massecuite [kg/s];

$$m_{A-MS} = \frac{m_{SC-in} + m_{SL-in} + m_{INS-in}}{B_{out}} \left[\frac{kg}{s}\right] \quad (2.39)$$

$$m_{W-EVAP} = m_{CNJ} + m_{SR} + m_{B-M} - m_{A-MS} \left[\frac{kg}{s}\right] \quad (2.40)$$

$$m_{W-A-MS} = m_{A-MS} - (m_{SC} + m_{SL} + m_{INS})_{A-MS} \left[\frac{kg}{s}\right] \quad (2.41)$$

It has to be considered that the BPR is affected by the vacuum (in the equation expressed by the term v [cmHg], and that the specific heat of the massecuite ($C_{p\ A\text{-}MS}$) changes slightly from the one of juice because of the presence of crystals [5]. Equations 2.42-2.48 show how to calculate the BPR, the specific heat of massecuite and the energy and mass balances in the pans.

$$BPR = 0.025 * B * \left(\frac{30 + B}{103.6 - B}\right) * \left(1 - \frac{0.54 * v}{229 - v}\right) [°C] \quad (2.42)$$

$$C_{p_{A\_MS}} = 4.1686 * \left(1 - (0.007 * B)\right) \left[\frac{kJ}{kg}\right] \quad (2.43)$$

$$Q_{P\_in} = Q_{CNJ} + Q_{SR} + Q_{B\_M} [kW] \quad (2.44)$$

$$Q_{VAP\_out} = m_{W\_EVAP} * h_{SAT\ VAP\ @T} \quad [kW] \quad (2.45)$$

$$Q_{A\_MS\_out} = m_{A\_MS} * h_{A\_MS} [kW] \quad (2.46)$$

$$Q_{VG1\_in} = Q_{A\_MS} + Q_{VAP\_out} - Q_{P\_in} [kW] \quad (2.47)$$

$$m_{VG1} = \frac{Q}{\Delta h_{COND@p_{VG1}}} \left[\frac{kg}{s}\right] \quad (2.48)$$

The terms $Q_{P\text{-}in}$, Q_{CNJ} , Q_{SR}, $Q_{B\text{-}M}$, $Q_{VAP\text{-}out}$, $Q_{VG1\text{-}in}$, $Q_{A\text{-}MS}$ stand respectively for the heat related to the inlet mass flow in the pan, to the mass flow of concentrated juice, of syrup, of B-magma, of outlet steam, inlet saturated Gases 1 and of A-massecuite and are expressed in kW. The general term Q of Equation 2.48 represents the total heat exchanged by Gases 1 in the pan. The inlet temperature of juice is the same as output of the evaporator, while the output temperature of the massecuite is supposed as the same of boiling in the pans.

2.2.5 Crystallization and centrifuging

Solubility of an impure sucrose solution is given by many authors [2,5,7], even if much confusion is present, due to the opposite use of terminology between cane and beet sugar industry. In this work, although dealing with sugarcane, the terminology of beet industry will be used, because its bibliography is more intuitive.
The solubility ($KS_{\%\ pure}$ expressed in percentage or KS expressed in kg/kg) of a pure sucrose solution is temperature T depending [2]:

$$KS_{\%pure} = 64.397 + 0.07251 * T - 0.002057 * T^2 - (9.035 * 106) - T^3 \left[\%\frac{kg}{kg}\right] \quad (2.49)$$

$$KS = \frac{KS_{\%}}{100 - KS_{\%}} \left[\frac{kg}{kg}\right] \quad (2.50)$$

The "Non Sucrose to Water" (*NSW*) ratio is defined as [8] and allows introducing the saturation coefficient *st* [6]:

$$NSW = x_{SL} * \frac{100}{(100 - (x_{SL} + x_{SC}) * 100)} \left[\frac{kg}{kg}\right] \quad (2.51)$$

$$st = 0.178 * NSW + 0.82 + 0.18 * e^{-2.1 * NSW} \ [\%] \quad (2.52)$$

and, finally, the solubility coefficient of an impure solution (KS_{impure}) [8]:

$$KS_{impure} = KS_{pure} * st \left[\frac{kg}{kg}\right] \quad (2.53)$$

The amount of formed crystals m_{CRS} (kg/s) is then:

$$m_{CRS} = B_{A\_MS} * m_{A\_MS} - KS_{impure} * m_{W\_A\_MS} \left[\frac{kg}{s}\right] \quad (2.54)$$

It is supposed that the fraction between formed crystals and inlet liquid component is the same for both sucrose and other soluble matter, which is now mostly made of reducing sugars and also that crystals have 1% humidity. The amount of juice, now called molasses (m_{ML}), that stays liquid, is found by subtraction:

$$m_{ML} = m_{A\_MS} - m_{CRS} \left[\frac{kg}{s}\right] \quad (2.55)$$

A-massecuite enters in the centrifuges, where the aim is to separate molasses from crystals. Anyway it is supposed that 5% of inlet molasses adhere to crystals. The mass of crystals is then called "A-sugar" ($m_{A\text{-}SG}$) and is again dissolved in water, while A molasses are sent to the B vacuum pans. Introducing sucrose mass flows in crystals ($m_{SC\text{-}CRS}$) and in molasses ($m_{SC\text{-}ML}$), other soluble matter mass flow in crystals ($m_{SL\text{-}CRS}$) and molasses ($m_{SL\text{-}ML}$), and water mass flow in molasses ($m_{W\text{-}ML}$), A-massecuite ($m_{W\text{-}A\text{-}MS}$) and crystals ($m_{W\text{-}CRS}$) expressed in kg/s, the mass balances are the following:

$$m_{SC\_ML} = m_{SC\_P} - m_{SC\_CRS} \left[\frac{kg}{s}\right] \quad (2.56)$$

$$m_{SL\_ML} = m_{SL\_P} - m_{SL\_CRS} \left[\frac{kg}{s}\right] \quad (2.57)$$

$$m_{W\_ML} = m_{W\_A\_MS} - m_{W\_CRS} \left[\frac{kg}{s}\right] \quad (2.58)$$

All the insoluble matter is supposed to be centrifuged with the crystals, total centrifuged mass flow is the A-sugar ($m_{A\text{-}SG}$), and the components of this stream are sucrose ($m_{SC\text{-}CNT}$), other soluble ($m_{SL\text{-}CNT}$) and insoluble matter ($m_{INS\text{-}CNT}$), water

($m_{W\text{-}CNT}$) and molasses ($m_{ML\text{-}CNT}$).

(2.59) $$m_{A-SG} = m_{SC-CNT} + m_{SL-CNT} + m_{INS-CNT} + m_{W-CNT} + m_{ML-CNT} \quad \left[\frac{kg}{s}\right]$$

A molasses follows in B pans the same procedure, where the only differences are that the pans are fed with "Gases 3", and the adherence of B molasses in the centrifuges is supposed to be of 2%. B molasses are sent to the alcohol plant for the production of bioethanol, while crystals, B sugar, are melt in a solution that takes the name of B magma, till reaching a 88.1 Brix degrees. Figure 2.12-2.13 show the centrifuging stage and the connections among the A and B vacuum pans stages.

Figure 2.12 Scheme of centrifuging stage

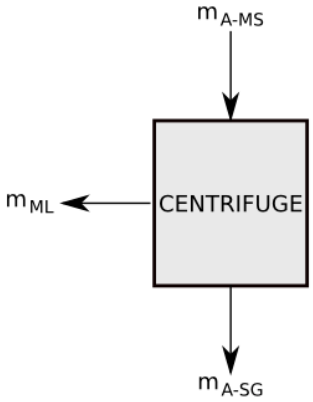

Figure 2.13 Connections among the A and B vacuum pans stages

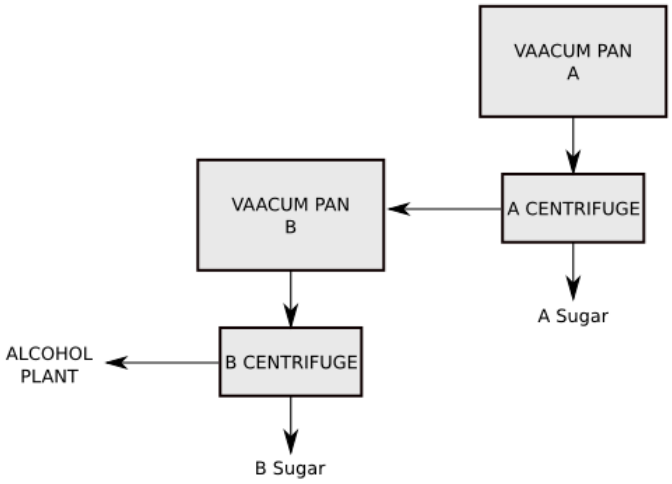

2.2.6 Refining

Refining step starts when A-sugar is melt in water. It reaches 66.1 Brix and takes the name of "liquor". The following Equations (2.60-2.63) describe the mass balance of the melting stage. New streams are introduced:

- Liquor mass flow m_L [kg/s];
- Sucrose mass flow in liquor $m_{SC\text{-}L}$ [kg/s];
- Other soluble and insoluble matter $m_{SL\text{-}L}$ and $m_{INS\text{-}L}$ in liquor [kg/s];
- Liquor Brix degrees B_L [°B];
- The terms with the subscript $_{-A\text{-}SG}$ (standing for A-sugar) are identical to the one with the subscript $_{-CNT}$ (standing for centrifuged) of Equation 2.59.

$$m_{SC\_L} = m_{SC\_A\_SG} \left[\frac{kg}{s}\right] \quad (2.60)$$

$$m_{SL\_L} = m_{SL\_A\_SG} \left[\frac{kg}{s}\right] \quad (2.61)$$

$$m_{INS\_L} = m_{INS\_A\_SG} \left[\frac{kg}{s}\right] \quad (2.62)$$

$$m_L = \frac{(m_{SC} + m_{SL} + m_{INS})_L}{B_L} \left[\frac{kg}{s}\right] \quad (2.63)$$

Liquor is firstly heated from around 70 to 85 °C by "Gases 1" (10% of heat losses to environment are considered), then undergoes another clarification, and filtration, characterized by following parameters:

- Ratio between removed insoluble matter and incoming in the clarifier: $r_{INS} = 0.7$;
- Ratio between removed sucrose and inlet sucrose $r_{SC} = 0.13$;
- Humidity of the foam $x_{W\text{-}J\text{-}CR} = 30\%$;
- Others soluble matter removal $r_{SL} = 90\%$;
- Humidity of sludge removed by the filter $x_{W\text{-}S\text{-}CR}$ 50%;
- Insoluble matter removal in the filter $r_{INS\text{-}FILTER} = 100\%$;

The filtered foam is sent back to the juice secondary tank and follows all the process once again (Figure 2.14). Clarified liquor enters in another crystallizer, which has the same characteristics as the previous ones, and is centrifuged with a supposed 1% of molasses adherence. The extracted syrup (molasses) has the characteristics already described. The 10% of it is supposed to be recycled to the tank before A pans, while the other 90% undergoes to the last crystallization, where Brix at output is, once again, supposed to be of 92 degrees. Molasses of last centrifuge are recycled to the last pans, while crystals are ready to be dried.

Figure 2.14 Scheme of refining stage

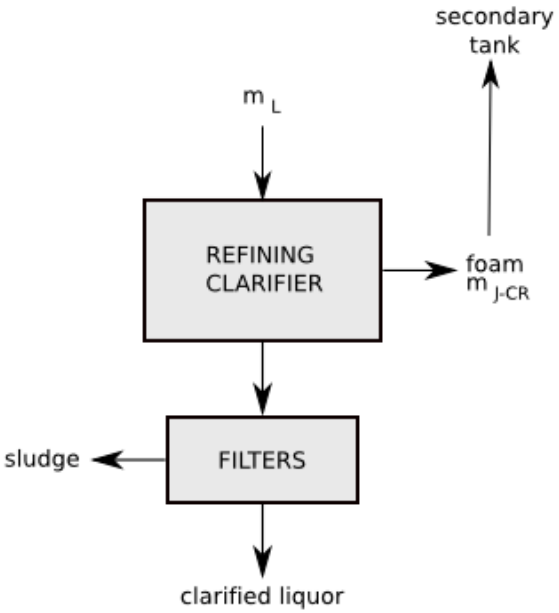

2.2.7 Drying

Driers are equipment where there is a double heat transfer. Firstly air is heated by steam at 125 PSIG (9.6 bar). Then hot air is blown through sugar crystals to evaporate their humidity content. The heat to be provided is given by three components [5]: heat necessary to heat the weight of dry air, heat necessary to evaporate the water content of sugar and heat necessary to warm the humidity content of air. The following parameters were used:

- Inlet temperature of air: $T_1 = 30$ °C;
- Outlet temperature of air: $T_2 = 62$ °C;
- Humidity of inlet air: $H_0 = 26$ [kg H_2O/1000 kg air] (the worst possible condition is considered: saturated air);
- Humidity of outlet air: $H_1 = 150$ [kg H_2O/1000 kg air];
- Final humidity of crystals: $x_{W\text{-}CRS} = 0.001$;

Given final crystals mass flow rate (m_{CRS}) and their evaporator inlet and outlet humidity ($x_{W\text{-}in\text{-}D}$, $x_{W\text{-}out\text{-}D}$) the amount of water to be evaporated ($m_{EVAP\ W\text{-}CRS}$) is:

$$m_{EVAP_{W-CRS}} = m_{CRS} * \left(x_{W-in} - x_{W-out}\right)_D \left[\frac{kg}{s}\right] \quad (2.64)$$

and the required air m_{AIR} is [4]:

$$m_{AIR} = \frac{\left(1500 * m_{EVAP_{W-CRS}}\right)}{\left(H_1 - H_0\right)} \quad \left[\frac{kg}{s}\right] \tag{2.65}$$

The heat to be provided (Q_D) is then:

$$Q_1 = m_{AIR} * \left(\frac{1000 - H_0}{1000}\right) * c_{p_{air}} * \left(T_1 - T_0\right) \quad [kW] \tag{2.66}$$

$$Q_2 = m_{AIR} * \left(\frac{H_0}{1000}\right) * c_{p_{vap}} * \left(T_1 - T_0\right) \quad [kW] \tag{2.67}$$

$$Q_3 = m_{EVAP_{W-CRS}} * \Delta h_{EVAP_{@p_{atm}}} \quad [kW] \tag{2.68}$$

$$Q_D = Q_1 + Q_2 + Q_3 \quad [kW] \tag{2.69}$$

The steam demand of the drier $m_{VAP\text{-}D}$ is:

$$m_{VAP-D} = \frac{Q_D}{\Delta h_{COND_{@p=125PSIG}}} \left[\frac{kg}{s}\right] \tag{2.70}$$

where the term $\Delta h_{COND\ @\ p=125\ PSIG}$ stands for the heat of condensation of the steam at 125 PSIG. Finally, a representation of the overall modeled process is given in Annex 1.

2.2.8 Electric power requirement in sugar and bioethanol production

Electric needs of the plant have been introduced in the model from the study of the real data after being collected and selected from outliers. A linear regression has been performed in order to obtain the dependence between electric consumption of the sugar plant and milling rate. The number of data to produce the correlation was 141, and the data were daily collected from July 12th 2013 till November 30th 2013. With the output Y in kWh/day and the input X in ton/day, the correlation found was:

$$Y = 6.9174 * X + 104777 \left[\frac{kWh}{day}\right] \tag{2.71}$$

whose R^2 value is 0.756, which, according to the international standards about energy management (ISO 50001:2011) [9] is a sufficient indicator to establish that there is strong relationship between the studied parameters. Figure 2.15 shows the relationship between the daily milled cane and the electric energy consumption of the sugar plant.

Figure 2.15 Sugar plant electric consumption as a function of milling rate

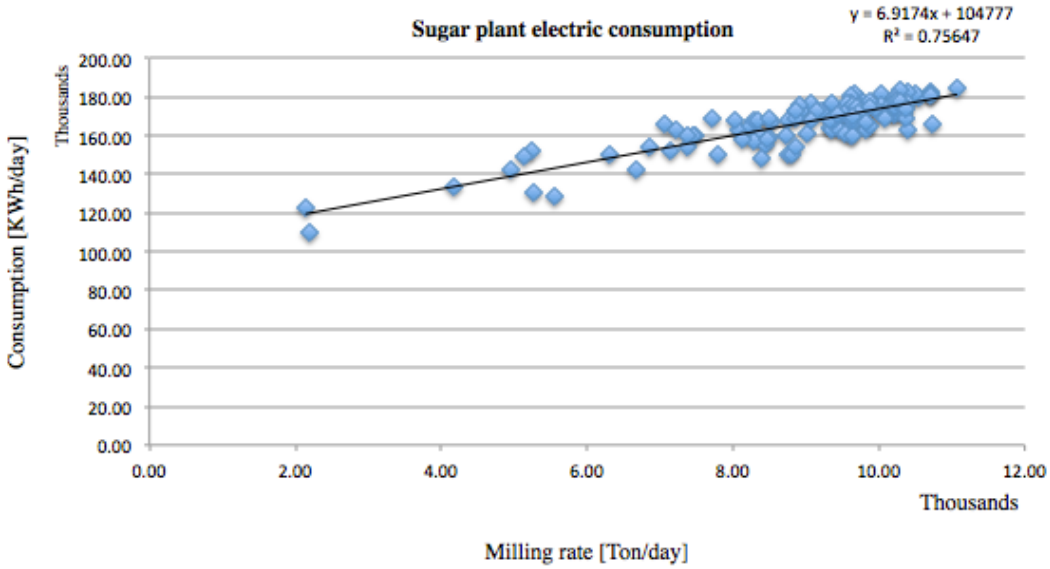

The study at each substation of the plant showed that, for the alcohol plant, there is not relationship between milling rate and electric consumption. The R^2 of the linear regression has a value of $6x10^{-4}$ and, moreover, the *Pearson's r* test of hypothesis on the correlation of these two variables fails: the value of the *r* is -0.025, to which a "*t value*" of -0.248 corresponds, which gives a "*p value*" higher than 0.05, which would be the minimum required to reject significantly the null hypothesis of lack of correlation. For this reason, it is reasonable to affirm that there is not any correlation, and so to model the electric consumption of the PAC (*Planta de Alcohol Carburante,* which means Fuel Alcohol Plant) constant was applied, equal to 50,360 kWh/day. Figure 2.16 shows the relationship between the daily milled cane and the electric energy consumption of the PAC.

Total electric energy consumption of Manuelita is the sum of the mill rate-depending part and of the constant one (PAC). Instead of kWh/day it can be expressed in function of the mill rate in Ton/h, getting in this way the energy consumption in kWh/h that corresponds, in value, to the instantaneous power in kW:

$$P_{el} = \frac{(6.9174 * mr + 104777 + 50360)}{24} \quad [kW] \tag{2.72}$$

Figure 2.16 PAC electric consumption as a function of milling rate

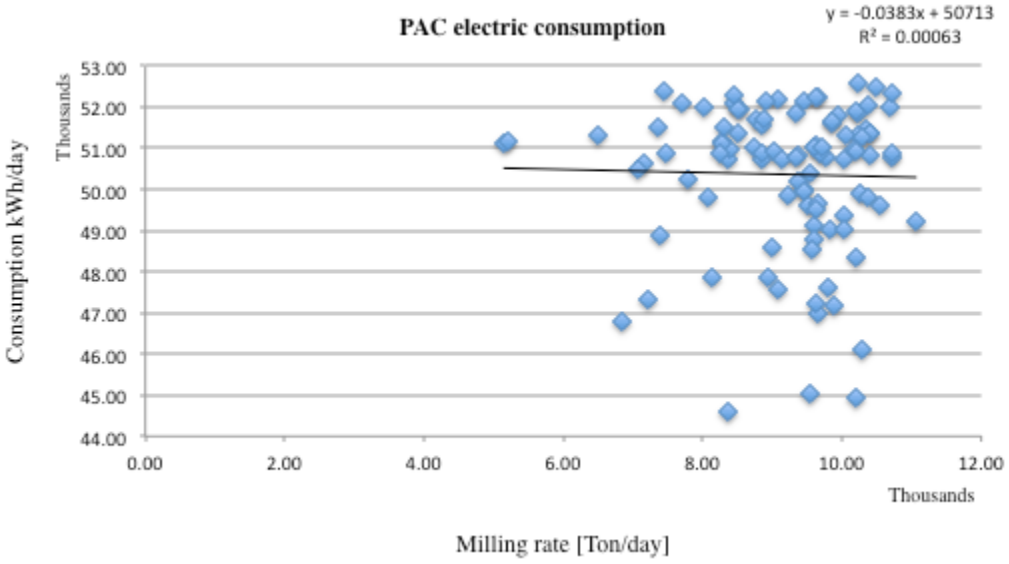

2.2.9 Process steam requirements in sugar and bioethanol production

The requirement of steam coming from the exhaust of turbines ($m_{VAP\text{-}VE}$) and from the head of 300 PSIG ($m_{VAP\text{-}300}$) of the sugar plant has been previously calculated and is expressed by Equations 2.73-2.74, where the term $m_{VAP\text{-}EVAP}$ stands for steam demand of the evaporators, $m_{VAP\text{-}H}$ for steam demand of heaters and $m_{VAP\text{-}D}$ for steam demand of drier. The steam demand of vacuum pans is not included in these needs because it is fully satisfied by Gases 1 and Gases 3.

$$m_{VAP-VE} = m_{VAP-EVAP} + m_{VAP-H} \quad \left[\frac{kg}{s}\right] \tag{2.73}$$

$$m_{VAP_{-300}} = m_{VAP-D} \quad \left[\frac{kg}{s}\right] \tag{2.74}$$

Once again, the statistic study on the PAC steam requirement shows that it is possible to assume that there is no correlation between steam demand of the PAC and milling rate.

The R^2 value of the regression is 0.008, the "*r*" of Pearson has a value of 0.094 and the corresponding "*t ratio*" is 1.43, corresponding to a "*p value*" between 0.1 and 0.05. This means that, being the "*t value*" higher than the critical at a 0.05 level, it is not possible to reject with strong statistic demonstration the null hypothesis; then the null hypothesis is considered true and no correlation is taken in account.

Because of this, PAC steam consumption is considered in the model as a constant with the value of 9.0148 kg/s ($7.79x10^5$ kg/day). 85% of this need is supplied by the head of 25 PSIG, while remaining 15% from the head of 300 PSIG. Figure 2.17 displays the relationship between the daily milled cane and the steam consumption of the PAC.

Figure 2.17 PAC steam consumption as a function of milling rate

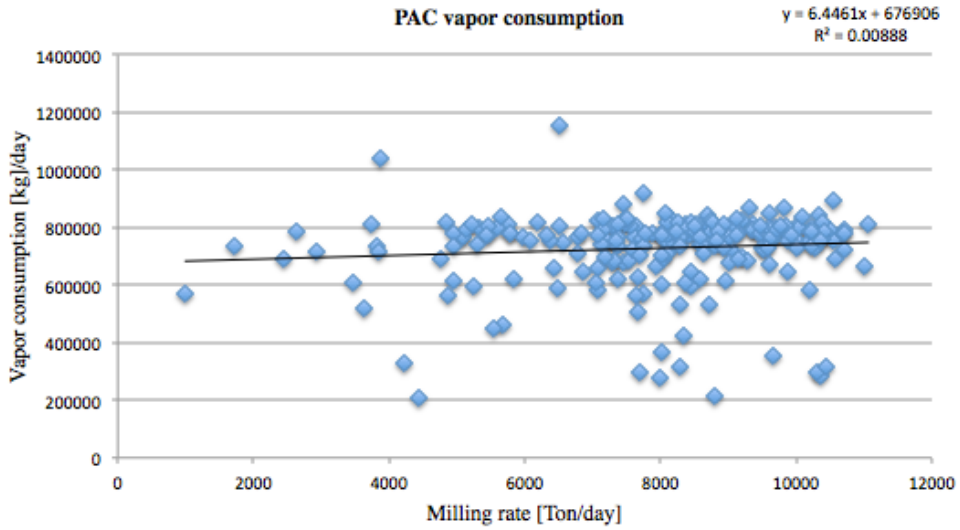

2.2.10 Cogeneration

Cogeneration scheme has been briefly explained in the previous chapter and it is illustrated in detail in Annex 3. The layout of the cogeneration cycle is quite complex, but it is of fundamental importance to have a clear idea of the logic that is governing the flow of the steam in order to later interpret the results about the steam demand, the efficiencies in function of the different parameters and all the characteristics of the plant itself. Figure 2.18 shows a simplified scheme of the cycle in a way that it is immediate to figure out the blocks that have been modeled. First of all let's remark that with this configuration only the steam required by the process is produced, since there is not possibility to produce a surplus of electric energy. All produced energy (electric and mechanical) is consumed inside the plant. So this is a limit on the amount of steam that can be expanded in the turbines. For this reason, the sugar and alcohol demands are the leading factors. For a determinate milling rate, heat requirement of these processes are fixed and, being the heat provided at a known pressure, steam mass flows are also known. This fact implies, with such scheme, to know the amount of steam required by the blocks called "PAC" and "Process".

Figure 2.18 Scheme of cogeneration cycle

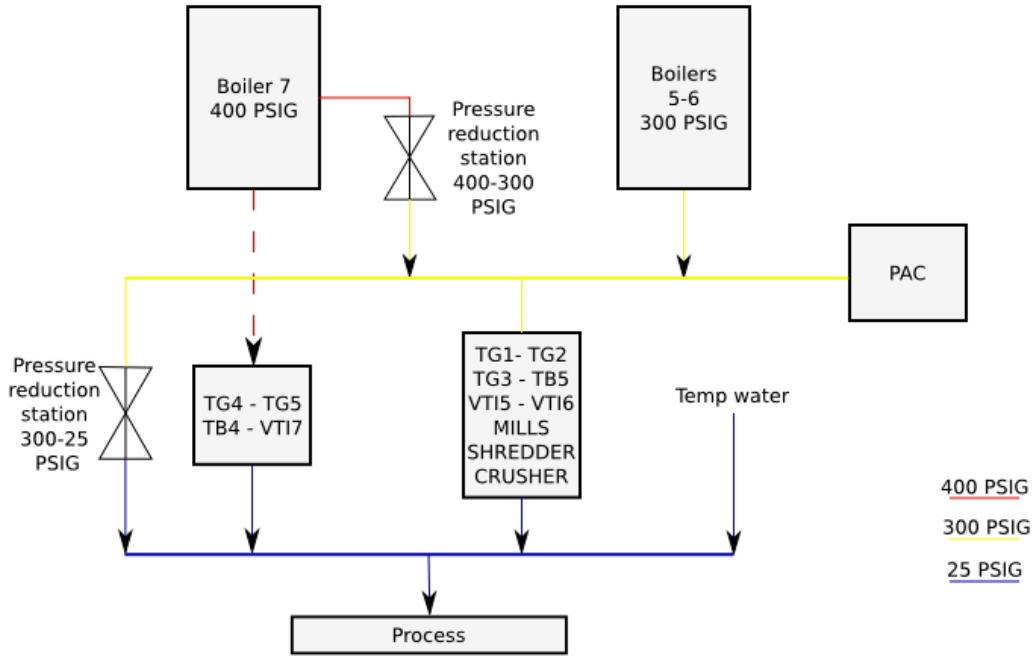

Moreover, the power requirements (and then the mass flows, by knowing the enthalpy difference between inlet and outlet of each machine) of the turbines are determined. The relationship between mills, shredder and crusher's powers and milling rate have already been provided, as well as the one for the electric energy production. For this reason, the steam mass flows of turbo-generators, mills' turbines, shredder's and crusher's ones are known. The turbines connected to turbo-pumps and the turbo-fans are related to the steam flowing to the boilers. They are modeled as constant at their nominal powers in order to not to increase too much the computational effort (they are strongly related to boilers steam production, so they would introduce a lot of recursive computation), but mainly because this assumption has a small effect on the overall steam balance. With these assumptions the two blocks of the scheme that represent the turbines can be modeled.

Given the power of the turbines, their characteristics, and the thermodynamic points at which they are working, steam mass flows are calculated with the following equations (2.79-2.81), where P_{BLD} stands for power at the blades of the turbine, P_{output} for power output of the turbine, w_{BLD} is the specific expansion work, h is the specific enthalpy of the steam, m_{VAP} the steam mass flow crossing the sections of the machine, $\eta_{B\text{-}S}$ is the mechanical efficiency (from blades to shaft):

$$P_{BLD} = \frac{P_{output}}{\eta_{B-S}} \quad [kW] \tag{2.75}$$

$$w_{BLD} = h_{in} - h_{out} \quad \left[\frac{kJ}{kg}\right] \tag{2.76}$$

$$m_{VAP} = \frac{P_{BLD}}{w_{BLD}} \quad \left[\frac{kg}{s}\right] \tag{2.77}$$

The tempering water block mass flow is obtained taking into account that the head of 25 PSIG is in saturated vapor condition. This implies recursive calculation because of the possible presence of laminated steam coming from the head of 300 PSIG. The following expressions were used to calculate the required mass flow of tempering water $m_{TW.}$

New variables were defined:

- Specific enthalpy of steam in the head of 25 PSIG h_{H25} [kJ/kg];
- Total steam mass flow at turbines' outlet $m_{VAP\text{-}T}$ [kg/s];
- Specific enthalpy of total steam mass flow at turbines' outlet $h_{out\ TURB}$ [kJ/kg];
- steam mass flow crossing the 300 to 25 bar redactors $m_{VAP\text{-}R300}$ [kg/s];
- Specific enthalpy of steam in the head of 300 PSIG h_{H300} [kJ/kg];
- Specific enthalpy of 25 PSIG saturated steam $h_{sat\ @25PSI}$ [kJ/kg];
- Specific enthalpy of tempering water h_W [kJ/kg];

$$h_{H_{25}} = \frac{m_{VAP-T} * h_{outTURB} + m_{VAP-R_{300}} * h_{H_{300}}}{m_{VAP-T} + m_{VAP-R_{300}}} \left[\frac{KJ}{Kg}\right] \tag{2.78}$$

$$m_{TW} = \left(m_{VAP-T} + m_{VAP-R_{300}}\right) * \frac{h_{H_{25}} - h_{SAT@25PSIG}}{h_{SAT@25PSIG} - h_W} \left[\frac{kg}{s}\right] \tag{2.79}$$

The blocks relative to the reduction stations are obtained by subtraction. The steam mass flowing through the reducer from 300 to 25 PSIG is different from zero if steam requirement of the head of 25 PSIG $m_{VAP\text{-}N25}$ is greater than the steam flowing through the blocks of the turbines.

$$m_{VAP-R_{300}} = m_{VAP-N_{25}} - m_{VAP-TURB} - m_{TW} \quad \left[\frac{kg}{s}\right] \tag{2.80}$$

The reduction in steam pressure from 400 to 300 PSIG ($m_{VAP\text{-}R400}$) is almost constant at different milling rates. Due to its higher efficiency, Boiler 7 is kept at full capacity (cap_{B7}), steam requirement of the head of 400 PSIG is almost constant too. Then, the steam flowing this reduction station is given by the subtraction of this head requirement ($m_{VAP\text{-}N400}$) from Boiler 7 capacity. The production on Boilers 5 and 6 ($m_{VAP\text{-}B56}$) is then covering the other part of 300

PSIG demand $m_{VAP\text{-}N300}$, which is given by the requirement of the 300 PSIG turbines ($m_{VAP\text{-}TURB300}$), the steam flowing through the reduction station, and by the PAC's requirement ($m_{VAP\text{-}PAC}$). Equations 2.81-2.83 provide steam mass balance at pressure reducer and at Boilers 5 and 6 while Equation 2.84 calculate the energy balance on the 300 PSIG head.

$$m_{VAP-R_{400}} = cap_{B7} - m_{VAP-N_{400}} \left[\frac{kg}{s}\right] \quad (2.81)$$

$$m_{VAP-N_{300}} = m_{VAP-TURB300} + m_{VAP-R_{300}} + m_{VAP-PAC} \left[\frac{kg}{s}\right] \quad (2.82)$$

$$m_{VAP-B56} = m_{VAP-N_{300}} - m_{VAP-R_{400}} \left[\frac{kg}{s}\right] \quad (2.83)$$

$$h_{H_{300}} = \frac{m_{VAP-B56} * h_{B56} + m_{VAP-R_{400}} * h_{B7}}{m_{VAP-N_{300}}} \left[\frac{kJ}{kg}\right] \quad (2.84)$$

The following parameters were assumed to describe the Rankine cycle:

- Temperature of Boiler 7 superheated vapour: T_{B7} = 410 °C;
- Pressure of Boiler 7 saturated vapour: P_{B7sat} = 470 PSIG (33.6 bar)
- Pressure of Boiler 7 superheated vapour: P_{B7SH} = 400 PSIG (28.6 bar);
- Boiler 7 efficiency: η_{B7} = 0.64 (from fuel to output of tempering);
- Temperature of Boilers 5 and 6: T_{B56} = 330 °C;
- Pressure of Boilers 5 and 6: P_{B56} = 300 PSIG (21.7 bar);
- Boilers 5 and 6 efficiency: η_{B56} = 0.58;
- Temperature after boiler 7 tempering water addition: $T_{B7\text{-}TEMP}$ = 370 °C
- Temperature loss from boilers 5 and 6 to 300 PSIG turbines: $\Delta T_{B56\text{-}turb}$ = 10/330 °C;
- Isentropic efficiency of the turbines: $\eta_{IS\text{-}turb}$ = 0.60;
- Isentropic efficiency of turbine for electric power generation 4 and 5: $\eta_{IS\text{-}TG45}$ = 0.68;
- Mechanical efficiency of the turbines (blades-shaft): $\eta_{B\text{-}S}$ = 0.98;
- Electric efficiency of the generators: η_{el} = 0.95;
- Turbine discharge pressure: p_{VE} = 25 PSIG (2.7 bar);
- Nominal power of Turbo-fan of boiler 7: P_{VTI7} = 615 kW;
- Nominal power of Turbo-fan of boiler 6: P_{VTI6} = 253 kW;
- Nominal power of Turbo-fan of boiler 5: P_{VTI5} = 201 kW;
- Nominal power of Turbo-generator 1: P_{TG1} = 1,250 kW;
- Nominal power of Turbo-generator 2: P_{TG2} = 1,250 kW;
- Nominal power of Turbo-generator 3: P_{TG3} = 2,500 kW;
- Nominal power of Turbo-generator 4: P_{TG4} = 3,760 kW;
- Nominal power of Turbo-generator 5: P_{TG5} = 8,510 kW.

Regarding the production of electric energy, turbo-generator 5 is the first that is used, till reaching 60% of its nominal value output power. If more energy is required, turbo-generator 4 starts, till reaching 50% of its nominal value output. Then, the other 3 turbos are switched on at full capacity, in the order turbo-generator 3, then 2 and, at last, 1.

The efficiency of the boiler is calculated to the nominal conditions, after the tempering water addition. So it is given by the ratio between the energy content of the steam mass flow leaving the boiler at 370 °C and the energy content of the inlet fuel. This definition does not really describe the boiler performance at different conditions, because it is affected by the selected value of the tempering. Anyway, it is possible to calculate the efficiency of the thermal exchange inside the boiler, where water is heated till being divided into two different streams of superheated (at 410 °C, 28.7 bar) and saturated vapor at 33.6 bar. The energy and mass balance of these two streams can be performed by knowing that their mixture will bring the steam to 370 °C at superheated condition.

For the sake of simplicity, it is supposed that, under different temperature condition, the boiler is run with the same excess of air. Therefore, it is reasonable to assume that the efficiency of the thermal exchange inside the boiler is constant. Such value has been calculated being 0.6574 (see following equations). Figure 2.19 depicts the streams in Boiler 7, where 33.6 bar saturated steam is firstly condensed and than mixed to 410 C° and 28.6 bar superheated steam.

Figure 2.19 Scheme of Boiler 7 and tempering water addition

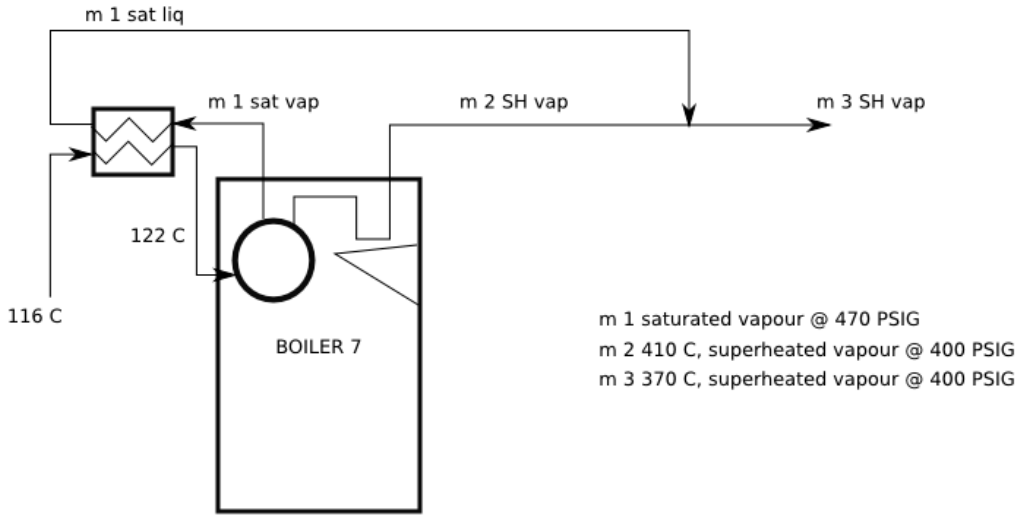

The procedure to calculate the boiler efficiency is given by the next equations, according to Figure 2.19:

- Q_{FUEL} represent fuel power input [kW];
- h_{in} stands for specific enthalpy of the stream of inlet feedwater [kJ/kg];
- Q_{in} is the heat power that the water is actually receving [kW];
- $h_{SAT\text{-}LIQ}$ is the specific enthalpy of saturated water at 470 PSIG pressure [kJ/kg];
- h_{SH} is the specific enthalpy of the steam at the outlet of the superheater [kJ/kg];
- η_{BOILER} is nominal boiler efficiency as previously defined;

$$Q_{FUEL} = m_3 * \frac{(h_3 - h_{in})}{\eta_{NOMINAL}} \ [kW] \quad (2.85)$$

$$m_1 = m_3 - m_2 \ \left[\frac{Kg}{s}\right] \quad (2.86)$$

$$Q_{in} = m_1 * \left(h_{SAT-LIQ} - h_{in}\right) + m_2 * \left(h_{SH} - h_{in}\right) \ [kW] \quad (2.87)$$

$$\eta_{BOILER} = \frac{Q_{in}}{Q_{FUEL}} \quad (2.88)$$

Knowing the inlet and outlet temperatures of feed water, the energy balance shows that more than 30% of the energy released by the condensing saturated steam is lost.

The indicators that have been selected to describe the performance of the cogeneration are the electric efficiency η_{el}, thermal efficiency η_{th}, mechanical efficiency η_{mech} and global efficiency of the plant η_g. New variables were then introduced:

- Fuel heat power input of Boiler 7 $Q_{FUEL\text{-}B7}$ and Boilers 5 and 6 $Q_{FUEL\text{-}B56}$ [kW];
- Steam mass flow produced by Boiler 7 $m_{VAP\text{-}B7}$ and Boilers 5 and 6 $m_{VAP\text{-}B56}$ [kg/s]
- Specific enthalpy difference of steam between outlet and inlet of Boiler 7 Δh_{B7} and of Boiler 5 and 6 Δh_{B56} [kJ/kg];
- Total heat fuel power input of the plant Q_{FUEL} [kW];
- Useful heat power used in the process of sugar and ethanol production Q_{US} [kW];
- Heat power used in juice heating (Q_J), effect one evaporation ($Q_{EVAP\text{-}EFF1}$), alcohol production (Q_{PAC}), sugar drying (Q_D) [kW];
- Total mechanical power used in sugar production process P_{mech} [kW];
- Mechanic power consumed by mills (P_{mills}), shredder ($P_{shredder}$) and crusher ($P_{crusher}$) [kW];

- Total electric power consumed by the plant P_{el} [kW];

(2.89) $$Q_{FUEL\_B7} = m_{VAP\_B7} * \Delta h_{B7} * \eta_{B7} \quad [kW]$$

(2.90) $$Q_{FUEL\_B56} = m_{VAP\_B56} * \Delta h_{B56} * \eta_{B56} \quad [kW]$$

(2.91) $$Q_{FUEL} = Q_{FUEL\_B7} + Q_{FUEL\_B56} \quad [kW]$$

(2.92) $$Q_{US} = Q_J + Q_{EVAP\_EFF1} + Q_{PAC} + Q_D \quad [kW]$$

(2.93) $$P_{mech} = P_{mills} + P_{shredder} + P_{crusher} \quad [kW]$$

(2.94) $$\eta_{el} = \frac{P_{el}}{Q_{FUEL}}$$

(2.95) $$\eta_{th} = \frac{Q_{US}}{Q_{FUEL}}$$

(2.96) $$\eta_{mech} = \frac{P_{mech}}{Q_{FUEL}}$$

(2.97) $$\eta_g = \eta_{el} + \eta_{th} + \eta_{mech}$$

2.3 References

[1] J. Toasa, *Colombia: A New Ethanol Producer on the Rise?* United States Department of Agriculture, WRS-0901, January 2009.
[2] P. Rein, *Cane sugar engineering*, 1st edition, Verlag Dr. Albert Bartens KG, Berlin, 2007.
[3] Manuelita S.A, Internal Report, 2013.
[4] International Association for the Properties of Water and Steam, *IAPWS Industrial Formulation 1997,* 1997.
[5] E. Hugot, *Handbook of cane sugar engineering*, 3rd edition, Elsevier, New York, 1986.
[6] Fivescail, http://www.fivesgroup.com, 2013.
[7] M. Asadi, *Beet Sugar Handbook*, Wiley Interscience, 2006.
[8] M. Mathlouthi, P. Reiser, *Sucrose properties and applications*, Champan & Hall, London, 1995.
[9] International Organization for Standardization, *ISO 50001:2011, Energy management systems – Requirements with guidance for use*, 2011.

3. Results and Discussion

3.1 Model Validation

Before to analyze the results of the simulation, the model has to be validated. Due to the lack of measurement of the majority of the flows in the process, two parameters have been selected to prove the consistency of the model, thanks to their reliability. The first is the sugar yield, called also commercial efficiency. This parameter is not time depending and is the ratio between the mass of final production of sugar and the initial sugar cane input mass. Figure 3.1 shows the comparison between the sugar yield slope predicted by the proposed model (0.0993) and the real data (0.0935) [ton/ton]. The real data are the average of the value of commercial efficiency of the last three years (0.0887, 0.0945, 0.0975). The difference between model and the real data can be assumed as "unknown sucrose losses" of the process, which of course in the model have not been taken into account, in order to maintain the material balances.

Figure 3.1 Sugar yield predicted by model

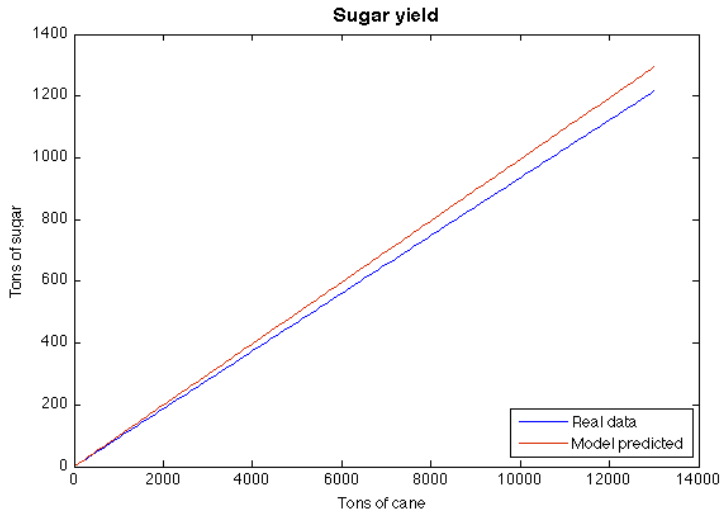

The second comparison between model outputs and real data is performed on the overall plant steam demand in function of the milling rate. This parameter considers all the steam demand of the plant since the steam is measured at the output of the boilers. It is the only trustable measurement among all steam streams. Figure 3.2 shows difference between model outputs and real data for steam plant demand. The normal steady-state operation of the plant is 417 ton/h, taking into account lost stop time. In the normal range of the plant operation, the model shows good accuracy, while a higher deviation occurs at low milling

rates. Such error is due to the sum of two factors. The first reason is that real data are measured on a daily base, so they take into account the lost production time, in which no cane is milled but boilers keep working, while the model does not. The second factor is the assumption of constant power absorbed by turbo-fans and turbo-pumps of the boilers. Such devices are modeled at nominal power. When the milling rate is low and heat demand decreases, these turbines work on a fraction of their nominal power and thus their steam consumption decreases.

The real curve of steam consumption was used as input for the optimization. The lost time was not predicted with the model but is fundamental to have a clear estimation of the cogeneration balance under working condition. The previous model was used to estimate the different steam streams in the production process, but not for cogeneration, where real data were available. Real steam consumption has to be expressed with an equation and the curve is converted to a heat power demand (Q_{need}). The reason is that steam demand is related to this operation condition, but changing temperatures or pressures of operation would imply to change steam requirement, not in heat requirement, which is only depending on milling rate. Equation 3.1 shows real process steam demand represented in Figure 3.2, and such regression has a 0.85 R^2 value. (*mr* stands for milling rate, in ton/h).

$$(3.1) \qquad m_{vap} = 20.32 * mr^{-0.453} * 1000 / (3600 * 2.205) \; [kg/s]$$

$$(3.2) \qquad Q_{need} = 234.86 * mr + 54546 \; [kW]$$

Figure 3.2 Total plant steam requirement as a function of milling rate

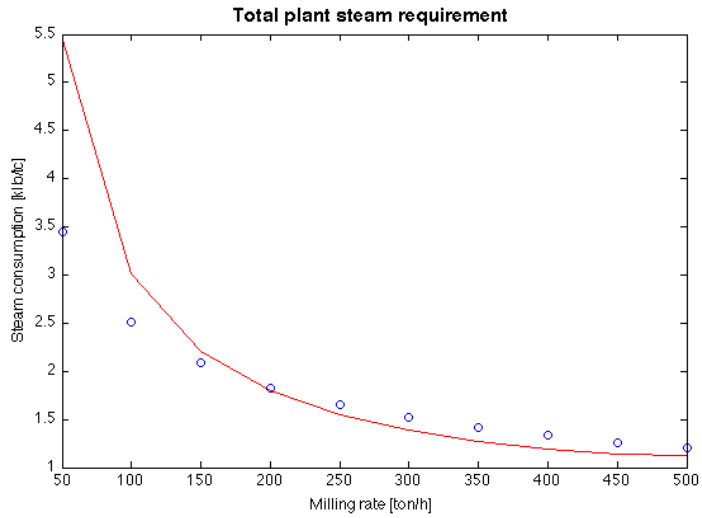

3.2 Milling rate dependence

The mass and energy balances (Figure 3.3) show that at 430 ton/h of milling rate (plant nominal condition), a fraction of total generated steam is flowing through the reduction stations ($m_{VAP\text{-}R400}$, $m_{VAP\text{-}R300}$). At these conditions, the computed global efficiency of the plant was 58.49%. Figure 3.3 shows the energy and mass balance of the plant, please notice the stream of 15.1 kg/s and the one of 0.3 kg/s flowing respectively through the 400 to 300 and 300 to 25 PSIG.

Figure 3.3 Mass and energy balance of cogeneration at 430 ton/h of cane

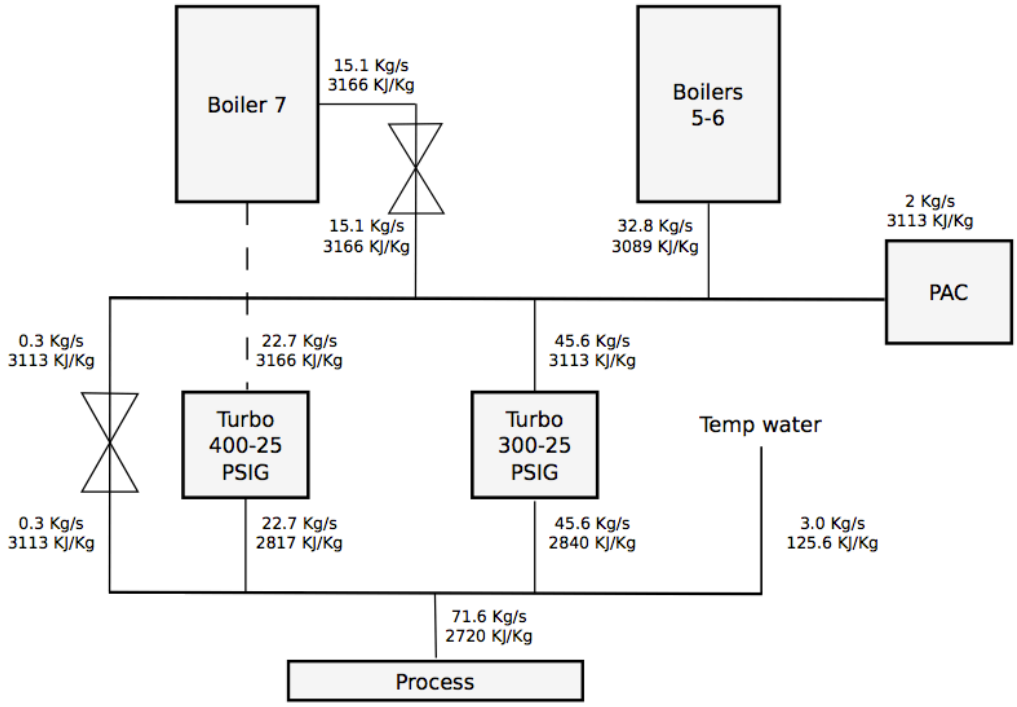

3.3 Exergy Losses

Through the results of the balances, it is possible to define the second principle efficiency (η_{II}) and the loss of exergy to the most critical steps. Second principle efficiency is similar to global efficiency but, in this case, useful heat power is multiplied by a factor in order to weight its value with mechanical and electrical power. Such factor is the Carnot efficiency, to multiply heat power by Carnot's efficiency means to estimate the maximum theoretical amount of mechanical power that could be extracted by this heat power if operated in a reversible machine between two constant temperatures, which are the temperature at which

the heat is available (in this case saturation temperature at 25 PSIG, 130 °C) and a reference cold reservoir at 25 °C. The process results to have a second principle efficiency of 19.62%. Equation 3.3 shows hot to calculate second principle efficiency, where P_{el} stand for electric power, P_{mech} for mechanical power, Q for useful heat power and Q_{FUEL} is the fuel energy input (in this case given by bagasse and coal).

$$\eta_{II} = \frac{\left[P_{el} + P_{mech} + \left(1 - \frac{298.15}{403.15}\right) * Q\right]}{Q_{FUEL}} \tag{3.3}$$

Exergy represents the amount of useful work that can be extracted by a system [1] and its definition takes into account the quality of the different forms of energy of the system and parameters to release this energy to the environment.

$$\varepsilon = \varepsilon_K + \varepsilon_P + \varepsilon_{PH} + \varepsilon_{CH} \quad \left[\frac{kJ}{kg}\right] \tag{3.4}$$

In the case of interest, specific chemical (ε_{CH}), potential (ε_P) and kinetic (ε_K) exergies were neglected [1] therefore exergy (ε) may be expressed as the only physical term (ε_{PH}):

$$\varepsilon = h - h_{REF} - T_{REF} * \left(s - s_{REF}\right) \left[\frac{kJ}{kg}\right] \tag{3.5}$$

where the subscript *ref* stands for reference, and *s* is the specific entropy. Each process is characterized by exergy losses (ε_{LOSS}). Introducing the term ε_{th} for the exergy related to the heat exchange, exergy balance in a steady state process is:

$$\varepsilon_{in} + \varepsilon_{th} = \varepsilon_{out} + P_{mech} + \varepsilon_{LOSS} \quad \left[\frac{kJ}{kG}\right] \tag{3.6}$$

In case of study, it is interesting to evaluate the exergy losses in processes like pressure reductions or temperature control with tempering water. The reason is that the pressure reductions are considered as isenthalpic (it means that the streams do not lose their enthalpy while crossing the pressure reducer), and in the balance of tempering water addition (Equations 2.82-2.83) the energy is conserved, but the exergy of these processes is not conserved and undergoes to big losses. Table 3.1 shows the exergy losses in such stages of the process.

Table 3.1 Exergy losses in steam pressure reduction and tempering water addition for a milling rate of 430 ton/h

Process	*Exergy loss [%]*
Boiler 7 tempering	3.6
400 to 300 PSIG reduction	3.2
300 to 25 PSIG reduction	26.4
25 PSIG head tempering	1.2

3.4 Renewable Efficiency

Here, let use define, *Renewable Efficiency*" of the plant as the amount of energy produced in a renewable way (with bagasse) respect to total energy required by the plant. Since it is known the bagasse to be the 31% of total cane weight, and its LHV is 7,984 kJ/kg [2] it is possible to calculate instantaneously bagasse flow (m_{BAG}), the yearly bagasse production ($m_{BAG\text{-}y}$), and then renewable efficiency, as shown in equations (3.7-3.11), by introducing the following variables:

- Year equivalent hours $HR_{eq\text{-}y}$ [h/year];
- Yearly milled cane $m_{C\text{-}y}$ [ton/year];
- Yearly available bagasse $m_{BAG\text{-}y}$ [ton/year];
- Milling rate mr [ton/h];
- Bagasse yearly available heat power $Q_{BAG\text{-}y}$ [kJ/year];
- Bagasse low heating value LHV_{BAG} [kJ/kg];

$$m_{BAG} = 0.31 * m_C \left[\frac{kg}{s}\right] \quad (3.7)$$

$$HR_{eq-y} = \frac{m_{C-y}}{mr} \left[\frac{h}{year}\right] \quad (3.8)$$

$$m_{BAG-y} = 0.31 * m_{C-y} * \frac{1000}{3600} \left[\frac{kg}{s}\right] \quad (3.9)$$

$$Q_{BAG-y} = m_{BAG-y} * LHV_{BAG} \left[\frac{kJ}{year}\right] \quad (3.10)$$

$$\eta_{REN} = Q_{FUEL} * \frac{HR_{eq-y}}{Q_{BAG-y}} \quad (3.11)$$

The calculation on the year balance provided a renewable efficiency of 97.6%. It means the plant is not energy self-sufficient, but some coal has to be bought, not only to guarantee stability of combustion in boiler chambers but also to satisfy the energy requirement of the plant. This value confirms that the current

configuration is far from the state-of-the-art technology, which is able to extract energy surplus from the raw bagasse (Table 1.3).

The plant efficiency can be expressed as a function of milling rate, Figures 3.4-3.6 show electric, mechanical and thermal efficiencies related to the milling rate. To understand the decreasing trend in Figure 3.4, it is necessary to mention that only the required energy is produced. It may be useful to analyze once again the real data about electric energy. The correlation is:

$$P_{el} = (6.9174 * mr + 104777 + 50360) \quad \left[\frac{kWh}{day}\right] \tag{3.12}$$

Following the instruction of the international standards [3], being the average consumption of electric energy of 216,937 kWh/day, it results that 71.5% of electric consumption is not related to production. This value is obtained from the expression of the linear regression (Equation 2.109) "$y = a*x + b$". The term b, standing for the intercept with the vertical axes, is divided by the daily average electric power consumption (166,578 kWh) and such ratio represents the amount of consumption that is not related to production. This implies that the electric energy requirement increases really slightly with milling rate, while mechanical and heat power increase much faster. The demand of heat and mechanical power requires a strong increase in energy input from fuel. The increase in energy input due to increase in milling rate, correspond to a low increase in electric energy production, so electric efficiency is penalized.

Figure 3.4 Electric efficiency as a function of milling rate

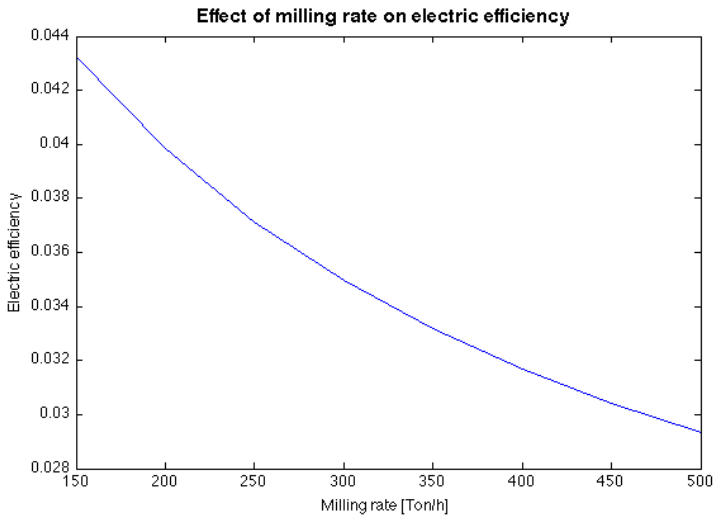

As shown in Figure 3.5, the mechanical efficiency increases because mechanical

power requirement increases with the milling rate. At null milling rate its value is zero because no mechanic energy is produced, while steam has to be produced in order to fulfill electric and heat fix requirements (not related to production and then required at null milling rate also).

Figure 3.6 shows that thermal efficiency decreases while milling rate increases. The reason for this is found at the 300 to 25 PSIG steam reduction. Figure 3.7 shows that the steam mass flow, which undergoes to this pressure reduction, increases with milling rate. While increasing milling rate, heat demand of the process is such that the steam flowing through the turbines (and covering mechanic and electric needs) is not able to cover it, and then additional steam has to be processed through the 300 to 25 PSIG steam reduction station to guarantee the correct amount of steam to the process. This implies an increasing loss of exergy that, as shown in Table 2.4, represents a weak point of the process. Additionally, the increase of steam mass flow coming from the reduction raises the specific enthalpy of the 25 PSIG head. This head has to be kept in saturated steam. Then more tempering water has to be introduced into the head, causing other exergy loss.

Figure 3.5 Mechanical efficiency as a function of milling rate

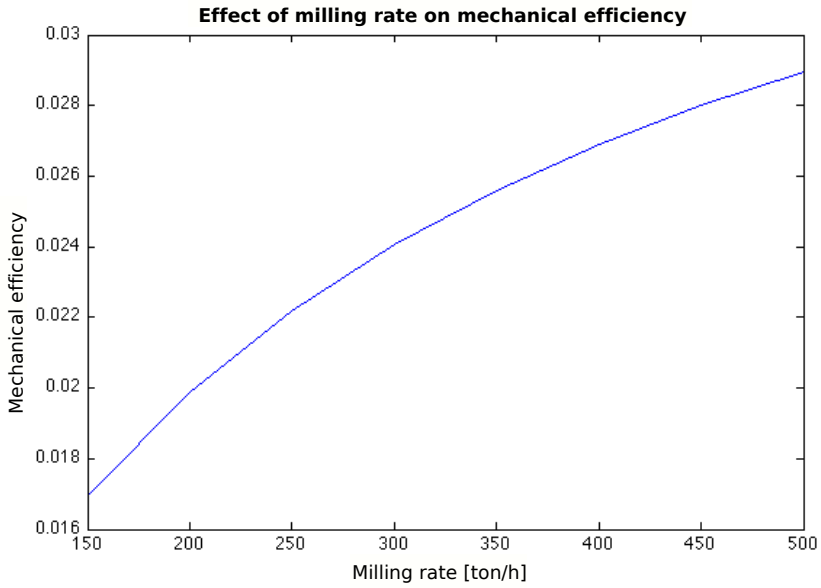

Figure 3.6 Thermal efficiency as a function of milling rate

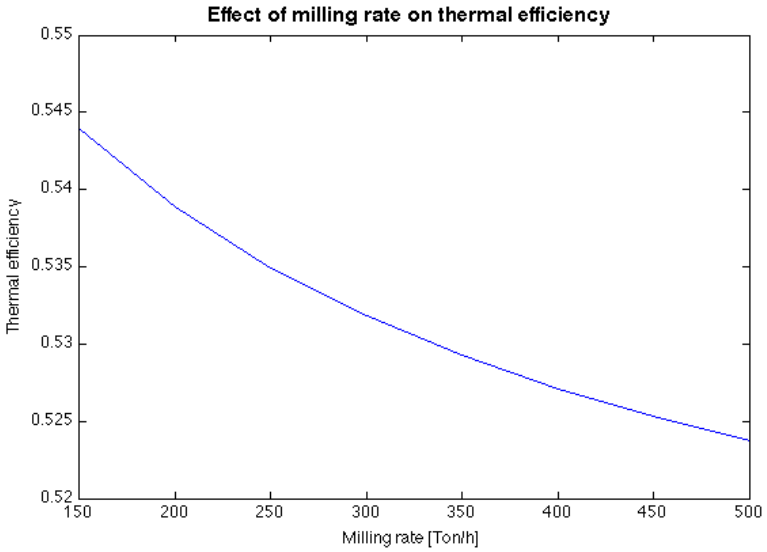

Figure 3.7 Steam mass flow through the 300 to 25 PSIG reduction station

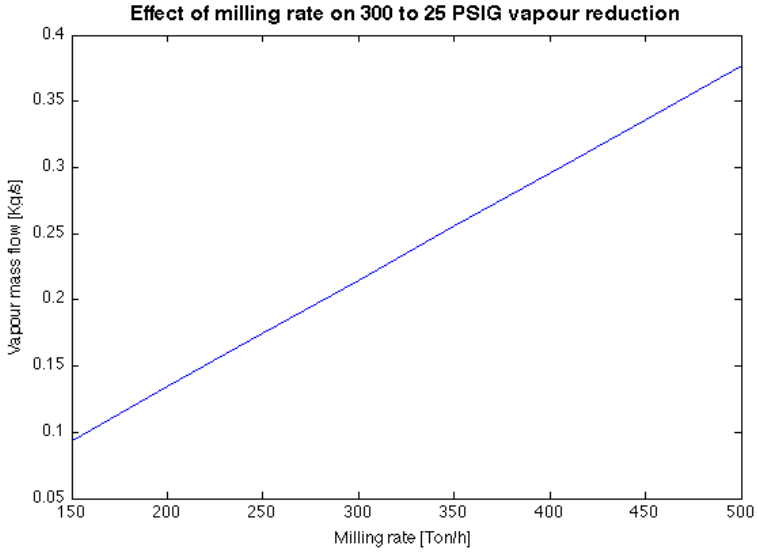

Global efficiency is given by the sum of mechanical, electric and thermal efficiencies. Since the thermal is the governing efficiency, then the global efficiency decreases while milling rate increases, as shown in Figure 3.8.

Figure 3.8 Global efficiency as a function of milling rate

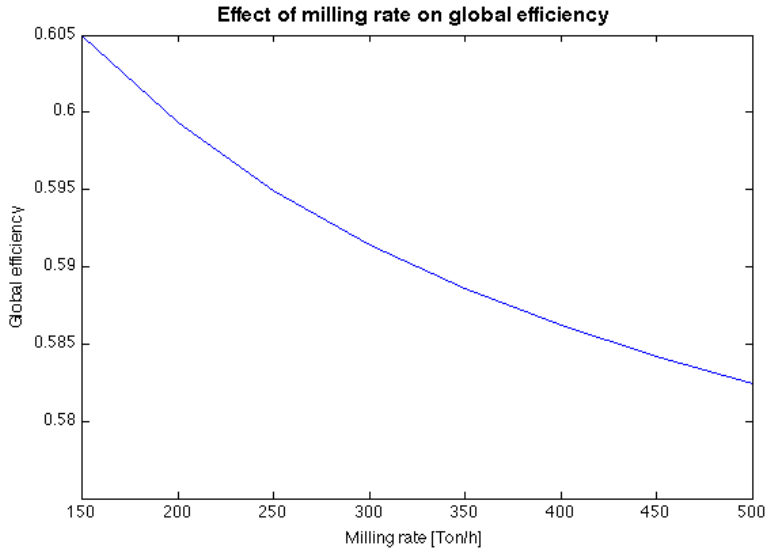

The selected logic for the modeling of the cogeneration implies that the steam mass flow reduced from 400 to 300 PSIG is constant respect to the milling rate. Since the main part of electric power required is not related to production, even at very low or high milling rate the turbo-generators 4 and 5 produce the same power because they are asked to work at a fraction of their nominal power. Moreover, as previously defined, turbo-pump and turbo-fan of Boiler 7 are modeled as constants. Boiler 7 is working at constant full capacity at each milling rate, the steam mass flow required by the 400 PSIG turbines is constant and then the mas flow through the 400 to 300 PSIG steam reduction stations results constant because found with material balance at the boiler.

3.5 Sensitivity Analysis

Sensitivity analysis involves investigation of the effect of selected design variables on considered objective functions. In this case, the objective function was the global efficiency of the plant η_g and the selected variables are pressures and temperatures of boilers and tempering. The analysis is performed on nominal plant operation (milling rate equal to 430 ton/h). When a variable effect is studied all the others are not moved from their nominal values.

3.5.1 Sensitivity analysis on pressure of boilers

Figure 3.9 shows the effect of Boiler 7 outlet pressure on the global efficiency. An optimum is detected and its presence is explained by energy and mass

balances (Table 3.2). When pressure of the Boiler 7 rises, the specific enthalpy of steam decreases. Enthalpy of the 300 PSIG head decreases too. Inlet condition of the turbines connected to this head changes. Consequently the output of the turbines changes because they operate between a lower enthalpy drop. They require a low increase in mass flow.

A stronger effect is given by the reduction of inlet enthalpy in the turbines of 400 PSIG, which are forced now to operate across a higher enthalpy difference, requiring then less steam mass flow. For this reason steam mass flow reduced from 400 to 300 PSIG increases, because the Boiler 7 is producing at a constant nominal rate. 400 PSIG steam has lower specific enthalpy than 300 PSIG one and this is the reason of the reduction of 300 PSIG head specific enthalpy decreases. The reduction of this mass flow is stronger than the increase of 300 PSIG turbines demand. The head of 25 PSIG reduces its specific enthalpy because all turbines' outlet have lowered: the sum of all these events gives an increase in the steam mass flow that has to cross the 300 to 25 PSIG reduction station (Figure 3.10) and this translates into a decreased efficiency.

If pressure is reduced from nominal one, the behavior of the system is opposite. 400 PSIG turbines require higher steam mass flows. Steam mass flow, whose pressure is reduced from 400 to 300 PSIG, is lower but has higher enthalpy. Thus the enthalpy of 300 PSIG increases, forcing 300 PSIG turbines to operate on a lower enthalpy drop. These turbines require higher mass flow to fulfill the power demand of the process and because of this no steam flows through the 300 to 25 PSIG reduction station (Figures 3.10-3.11).

Figure 3.9 Effect of Boiler 7 pressure on global efficiency

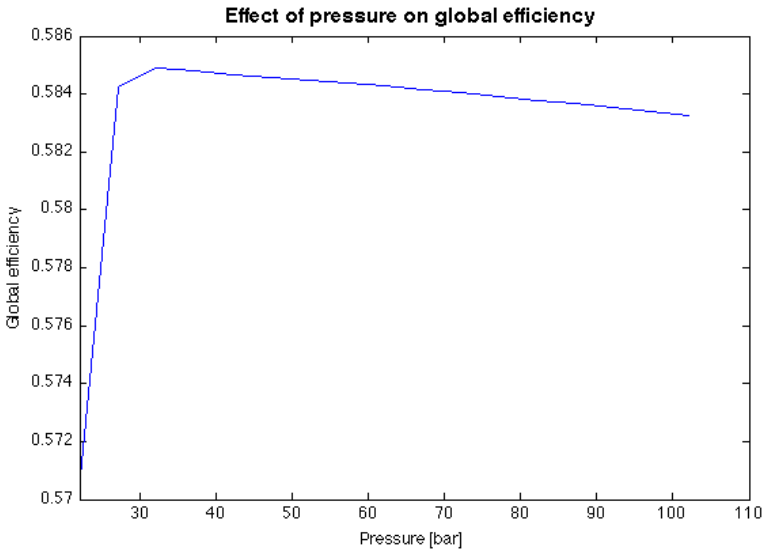

Figure 3.10 Effect of Boiler 7 pressure on steam mass flow through 300 to 25 PSIG reduction station.

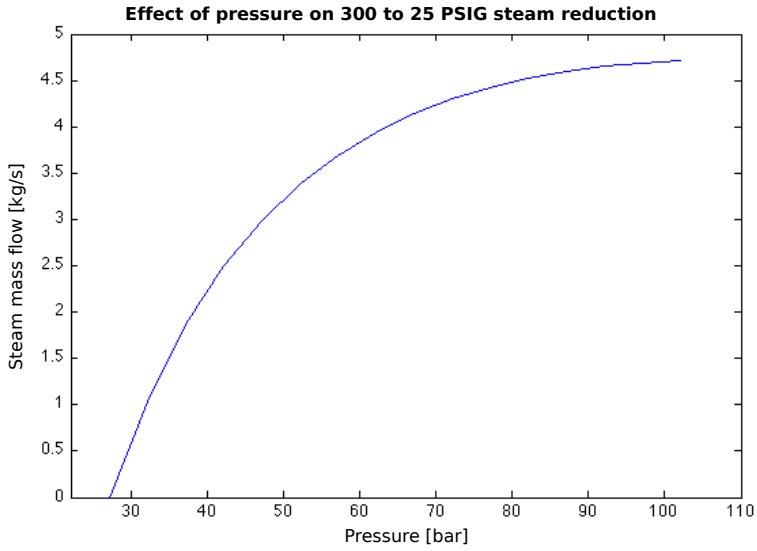

Figure 3.11 Enlargement of effect of Boiler 7 pressure on steam mass flow through 300 to 25 PSIG reduction station

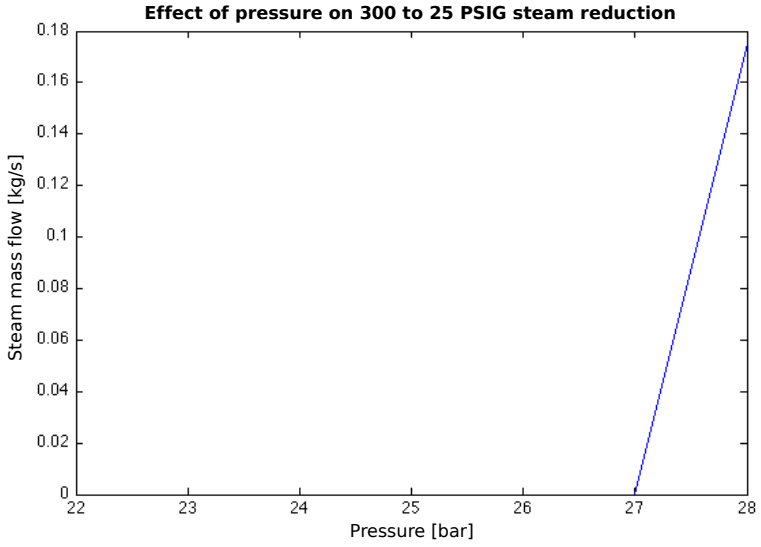

The range at which the pressure of Boilers 5 and 6 can move is lower than the range of Boiler 7 because the logic of the current process forces the maximum value to be lower than Boiler 7 one. At very low pressures, it appears that the global efficiency increases with pressure, till reaching 20 bar (Figure 3.12),

when pressure reduction of steam starts in order to supply heat power requirements of the process (Figure 3.13). From this point ahead, even if slowly, the trend starts decreasing.

In practice, it would be impossible to manage the pressure at very low values because the enthalpy drop would of the expansion be so low that the necessary steam mass flow to cover power need would be more than the boilers capacity. Analyzing the thermodynamic aspect of the increase of Boiler 5 and 6 pressures (for eligible values close to the nominal condition) while keeping the temperature constant implies a decrease of specific enthalpy of 300 PSIG head. Enthalpy of turbines outlet decreases also and the result is an increase of enthalpy drop in the expansion, with a consequent decrease of steam mass flow through 300 PSIG turbines. Consequently, the steam flow crossing the 300 to 25 PSIG reduction station increases, and the efficiency decreases (Please, refer to Table 2.5).

The decrease in Boilers 5 and 6 pressure has the opposite effect in the global efficiency. The necessity to reduce steam through the station is avoided and global efficiency assumes a positive trend with pressure, as common behavior for Rankine cycles.

Figure 3.12 Effect of Boilers 5 and 6 pressure on global efficiency

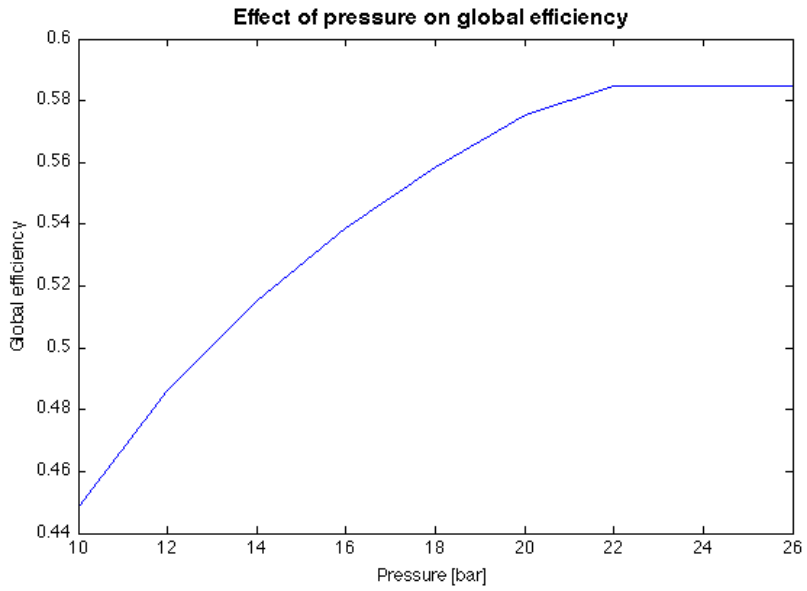

Figure 3.13 Effect of Boilers 5 and 6 pressure on steam mass flow through 300 to 25 PSIG reduction station

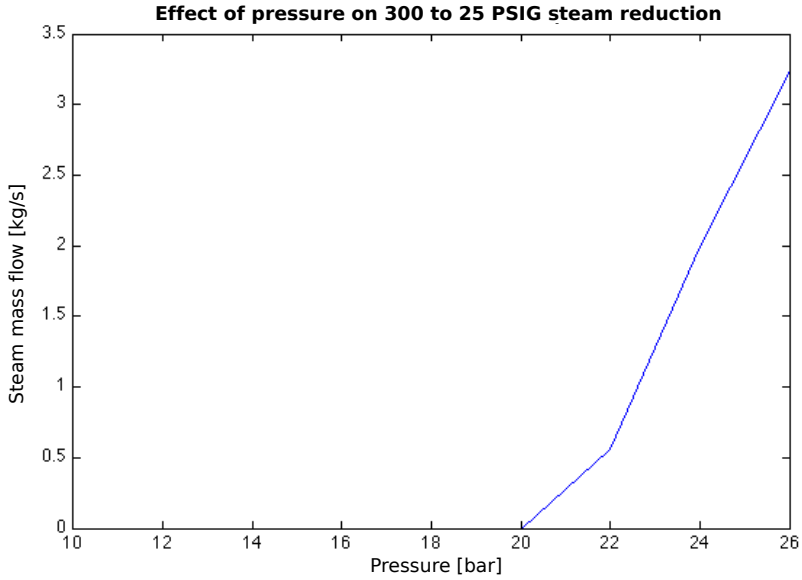

3.5.2 Sensitivity analysis on the temperatures of boilers

Figure 3.14 shows a negative trend of global efficiency with the increase of inlet temperature of Boiler 7 with a fixed tempering temperature. The rise of boiler internal temperature implies the mix of a high temperature steam with a lower temperature (saturated condition) water. The higher the temperature difference and the stronger is the effect on efficiency because more saturated steam has to be condensed, losing an important energy content. Temperature inside the boiler does not affect the steam reductions, because this variable involves just the thermal exchange inside the boiler, but boiler's output conditions are controlled by the temperature at tempering output and are then fixed.

Figure 3.15 shows the decreasing trend of global efficiency with temperature of Boilers 5 and 6. If the temperature rises, enthalpy of steam increases, the change of operation point leads to an increase of enthalpy difference across the expansion. Thus steam mass flow required by 300 PSIG turbines decreases and steam mass flow through 300 to 25 PSIG reduction station increases to fulfill the requirement of the process (Figure 3.16). If temperature is reduced from the nominal one no steam pressure reduction is necessary and the global efficiency has a positive increasing trend with temperature.

Figure 3.14 Effect of Boiler 7 temperature on global efficiency

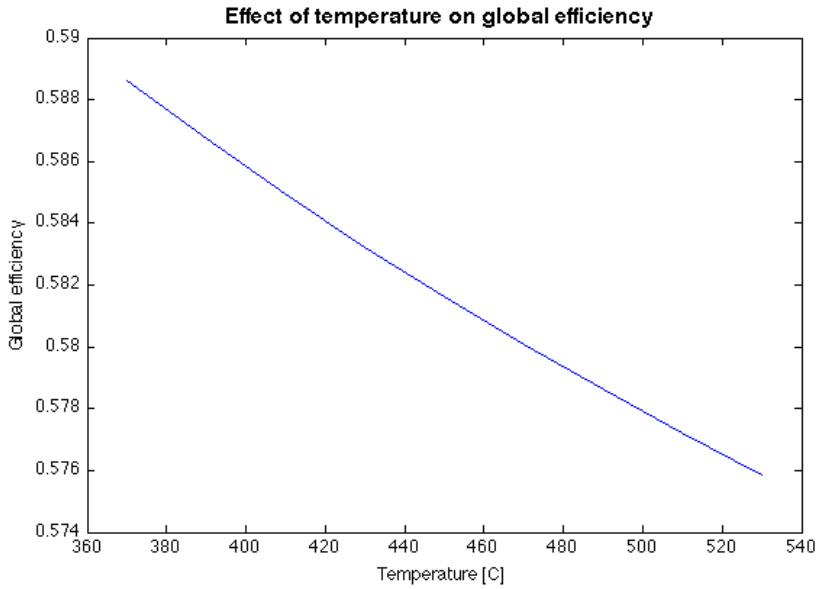

Figure 3.15 Effect of Boilers 5 and 6 temperature on global efficiency

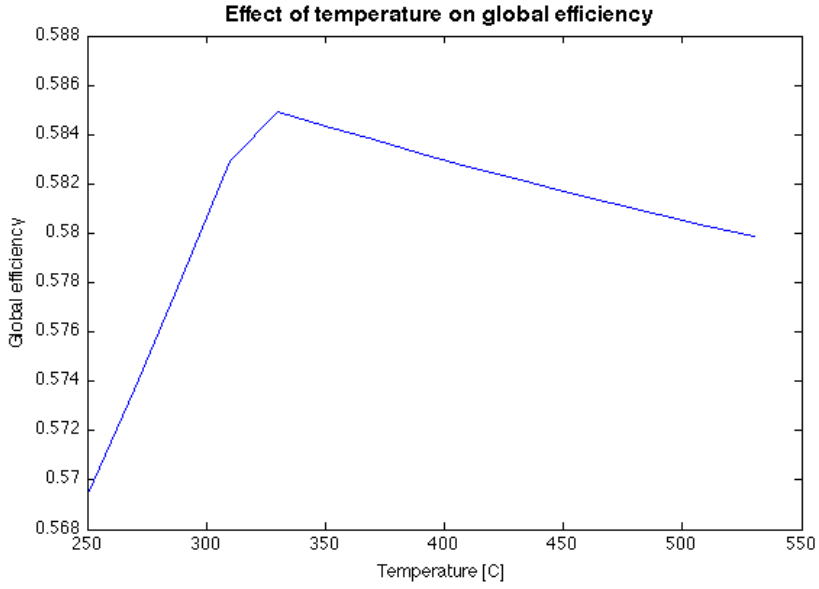

Figure 3.16 Effect of Boilers 5 and 6 temperature on steam mass flow through 300 to 25 PSIG reduction station

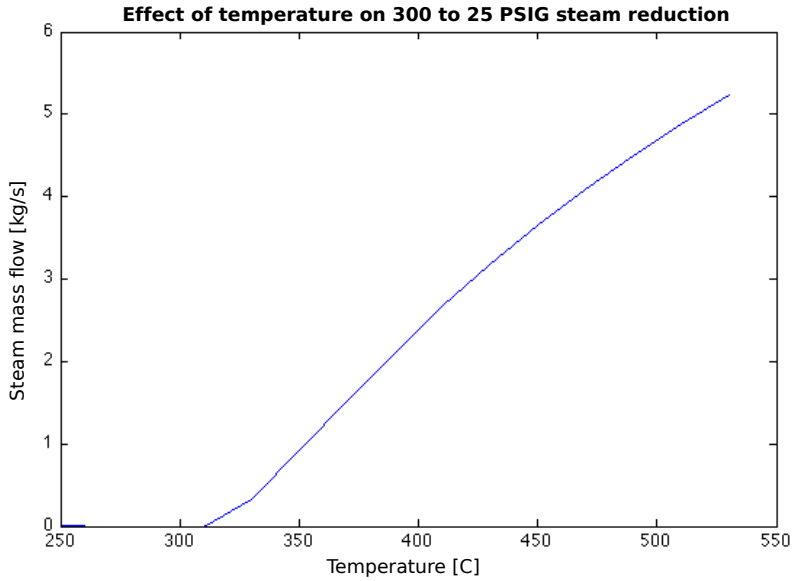

Tempering temperature of Boiler 7 has a positive impact on global efficiency (Figure 3.17). Its range is upper limited by boiler internal temperature (410 °C). The tempering is aimed to protect the turbines from thermal stresses by controlling the temperature of steam but represents a considerable loss of energy and exergy. Losses decrease if tempering temperature is close to the boiler internal temperature, and are null if they are equal. The trend of efficiency reflects this behavior.

Table 3.2 shows material and energy balances of the process at different conditions, computed with the exposed model in order to understand the exposed sensitivity analysis. Equations 3.13-3.14 show the mass balance at the 300 PSIG head and the energy balance at the 25 PSIG head. Please refer to Figure 3.18 for nomenclature.

$$G = H + L \quad \left[\frac{kg}{s}\right] \tag{3.13}$$

$$r = \frac{L * p + M * q + O * k}{L + M + O} \quad \left[\frac{kJ}{kg}\right] \tag{3.14}$$

Figure 3.17 Effect of Boiler 7 tempering temperature on global efficiency

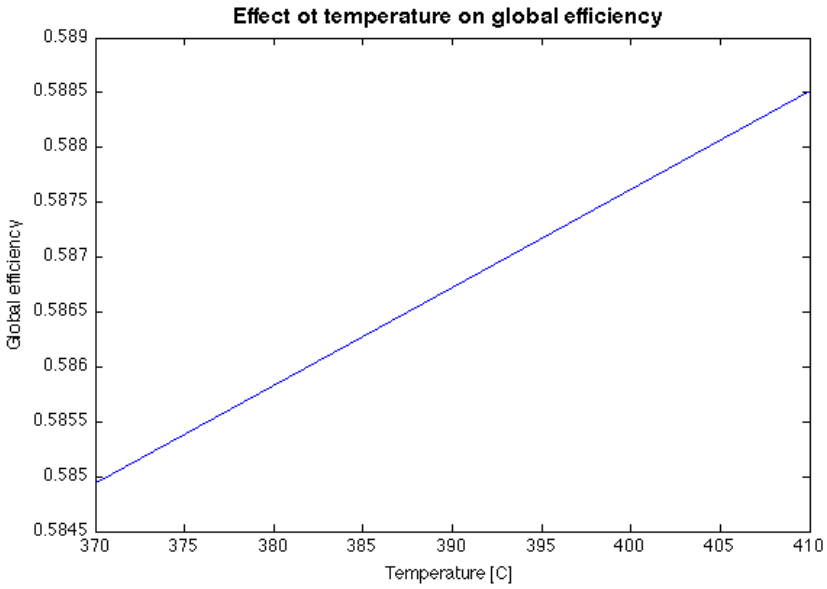

Figure 3.18 Nomenclature of streams and properties analyzed in Table 3.2

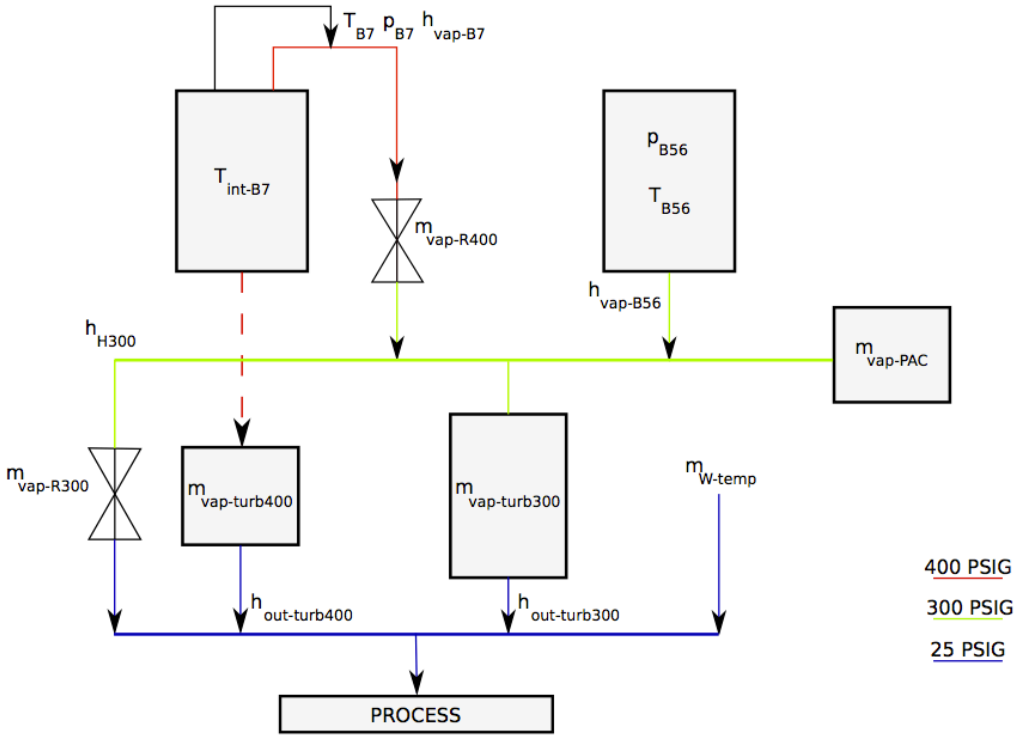

Table 3.2 Mass and energy balances at different process conditions

430 ton/h	***Nominal***	*P boil 7* ↑	*T inlet turb 400* ↑	*P boil 5-6* ↑	*T boil 5-6* ↑	*T boil 7* ↑
P boiler 7 outlet [bar] p_{B7}	28.6	40	28.6	28.6	28.6	28.6
Internal T boiler 7 [°C] $T_{int\text{-}B7}$	410	410	410	410	410	440
P boilers 5-6 [bar] p_{B56}	21.7	21.7	21.7	26	21.7	21.7
T boilers 5-6 [°C] T_{B56}	330	330	330	330	400	330
T boiler 7 tempering [°C] T_{B7}	370	370	400	370	370	370
m_{vap} *boilers 5-6 [kg/s]* $m_{vap\text{-}B56}$	32.8	33.1	31.9	33	31.2	32.8
m_{vap} *boiler 7 [kg/s]* m_{vapB7}	37.8	37.8	37.8	37.8	37.8	37.8
m_{vap} *rid 400-300 [kg/s]* $m_{vap\text{-}R400}$	15.1	16.9	16.2	15.1	15.1	15.1
h tempering out [kJ/kg] h_{vapB7}	3166	3143	3234	3166	3166	3166
h boilers 5-6 out [kJ/kg] h_{vapB56}	3089	3089	3089	3078	3245	3899

h head 300 [kJ/kg] h_{H300}	3113	3107	3138	3106	3219	3113
m_{vap} *turbo 400 [kg/s]* $m_{vap\text{-}turb400}$	22.7	20.8	21.6	22.7	22.7	22.7
m_{vap} *turbo 300 [kg/s]* $m_{vap\text{-}turb300}$	45.6	45.8	44.7	42.8	42	45.6
m_{vap} *PAC [kg/s]* $m_{vap\text{-}PAC}$	2	2	2	2.1	1.9	2
m_{vap} *rid 300-25 [kg/s]* $m_{vap\text{-}R300}$	0.32	2.3	1.4	3.2	2.4	0.32
h out turbo 400 [kJ/kg] $h_{out\text{-}turb400}$	2817	2761	2868	2817	2817	2817
h out turbo 300 [kJ/kg] $h_{out\text{-}turb300}$	2842	2838	2862	2817	2925	2842
h flow to head 25 [kJ/kg]	2836	2823	2870	2830	2899	2835
m_{water} *temp head 25 [kg/s]* $h_{W\text{-}temp}$	3	2.7	3.8	2.9	4.5	3
η electric	0.0312	0.0311	0.0313	0.0311	0.031	0.031
η mechanical	0.0278	0.0278	0.0279	0.0278	0.0277	0.0277
η thermal	0.526	0.5258	0.5284	0.5258	0.5242	0.5237
η global	0.585	0.5847	0.5876	0.5847	0.5829	0.5824
Q process need [kW]	155540	155540	155540	155540	155540	155540
Q model calculated [kW]	155590	155590	155590	155590	155590	155590

3.6 Numerical optimization

The optimization of Rankine cycles has been widely studied, for different processes and with different targets. For example, Dincer [4] performed a thermodynamic analysis and optimization of reheat steam power plants while Emam and Dincer performed an exergy and exergoeconomic optimization of the organic cycle for geothermal applications [5]. Likewise, the theme has been investigated for what concerns sugar plants also, including different aspects of the process. Dias and others optimized second generation ethanol production by optimizing first generation process [6], while other authors focused on the split of bagasse among the different needs of the second generation process plant to obtain the economic optimum [7].

The optimization of the global efficiency was carried out with an algorithm based on the "Pattern Search" method, which is appropriate to solve optimization problems with non-smooth objective functions, because it is not related to derivatives calculations [8]. The method is feasible for problems of the form:

$$\min f_x \text{ such that } \begin{cases} c(x) \le 0 \\ ceq(x) = 0 \\ A * x \le b \\ Aeq * x = beq \\ lb \le x \le ub \end{cases} \tag{3.15}$$

where x is a vector of variables, if the problem is multi-dimensional, and the constraints may be linear or non linear inequalities and equalities, and upper and lower bounds.
In the case of this study, $f(x)$ is the global efficiency of the plant η_g (Equation 2.97), and x is a vector of five variables: pressure and temperature of boiler 7 outlet (p_{B7}, T_{b7}), pressure and temperature of boilers 5 and 6 (p_{B56}, T_{B56}) and temperature of boiler 7 tempering (T_{TB7}). According to Matlab format, the variables and the optimization are coded as follows (Equations 3.16-3.17):

(3.16)
```
X(1) = pB7
X(2) = TB7
X(3) = pB56
X(4) = TB56
X(5) = TTB7
```

(3.17)
```
[Xps, Fps] = patternsearch(ObjectiveFunction, X0, A,
b, Aeq, beq,  LB, UB, NONLCON, options);
```

where *Xps* stands for the vector of the variables, *Fps* is the result of the optimization, *X0* is the starting point, *NONLCON* represents the nonlinear constraints and the other terms are referred to Equations 3.23-3.25. The objective function, accepting the variables in the vector *X*, has the form of Equation 3.18.

(3.18)
```
function [ n_global_plant ] = ObjectiveFunction( X )
```

The pattern search algorithm computes a sequence of points that get closer to the optimal point. At each step, the algorithm searches a set of points, called mesh, around the current point (computed at previous step). The mesh is formed by adding the current point to a scalar multiple of fixed set of vectors called pattern. If the algorithm finds out a point in the mesh that improves the objective function at current point (successful poll), the new point becomes the current point at the next step of the algorithm. If the poll is unsuccessful, the algorithm build a new smaller mesh around the same current point and starts again to compute the values of the objective function for this mesh [9]. Figures 3.19-3.20 shows how the new mesh is built if the minimum of first mesh grid is found in a generic point (case *a*) or in the central point of mesh (case *b*).

Figure 3.19 New Pattern Search mesh building if the minimum of the first mesh is the central point

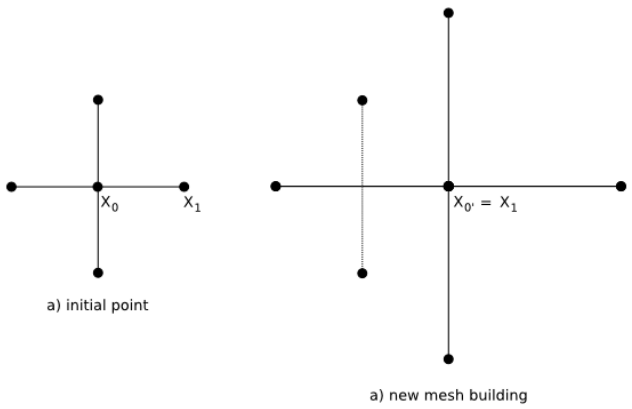

Figure 3.20 New Pattern Search mesh building if the minimum of the first mesh is a generic point

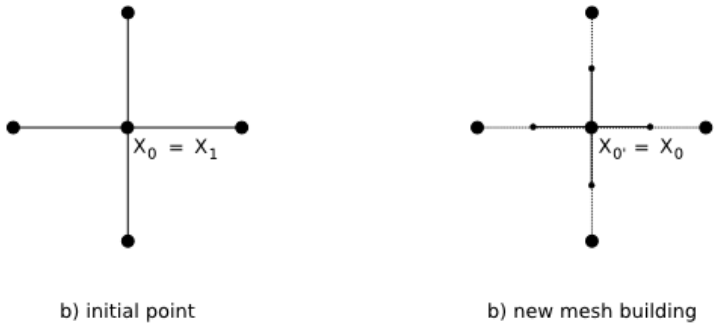

Unluckily, just like other optimization algorithms, the pattern search cannot recognize local minima so the starting point influences the result. By properly choosing the starting point (analyzing the sensitivity analysis) and repeating the optimization beginning at difference points it is possible to find an optimum which has good probabilities to be the global. As a first check, the optimization was performed by giving lower and upper bounds of the variables imposed by technological limits (shown at Table 3.3), to verify if the plant is operating in the theoretical optimum. All the optimizations are performed at the nominal milling rate of 430 ton/h.

Table 3.3 Range of the variables for the theoretical optimization

Variable	*Minimum value*	*Maximum value*
Pressure boiler 7	21.7 bar	125 bar
Pressure boilers 5 and 6	2.8 bar	125 bar
Temperature boiler 7	216 °C	540 °C
Temperature boilers 5 and 6	132 °C	540 °C
Boiler 7 tempering temperature output	216 °C	540 °C

Linear and non-linear constraints were given to variables and to other parameters that characterize the Rankine cycle. Temperature of the tempering has to be lower than the one inside the boiler, outlet temperature of the turbines has to be higher than saturation temperature at 25 PSIG (and this value is added with 5 °C for a safety margin). Moreover it has to be considered that the maximum steam production capacity of Boilers 5 and 6 is of 38 kg/s.

$$T_{TB7} < T_{B7} \quad [°C] \tag{3.19}$$

$$p_{B7} > p_{B56} \quad [bar] \tag{3.20}$$

$$T_{out_{TURB}} > 135 \quad [°C] \tag{3.21}$$

$$m_{B56} < 38 \quad \left[\frac{kg}{s}\right] \tag{3.22}$$

In Matlab language coding the linear constraints, upper and lower bounds according to Equation 3.17, have the form:

```
A=[0 -1 0 0 +1; -1 0 1 0 0]
```
(3.23)

```
b=[0;0]
```
(2.121)

```
LB=[21.7 216 2.8 132 216]
```
(3.24)

```
UB=[125 540 125 540 540]
```
(3.25)

Non linear constraint are computed in a separated Matlab function and, in Matlab programming language, are expressed by the following code lines:

```
- ToutTurb  + 135
```
(3.26)

```
- mB56 + 38
```
(3.27)

Moreover, all the fluxes were imposed to be greater or equal to zero, the following expressions 3.28-3.32 represent the Matlab code of this constraint:

```
- mvapTURB300
```
(3.28)

```
- mvapTURB400
```
(3.29)

```
- mvapR400
```
(3.30)

```
- mvapR300
```
(3.31)

```
- mTW
```
(3.32)

The current operating point was selected as starting point *X0* of the pattern search. It was chosen because the sensitivity analysis suggested that the current operating conditions are close to the possible optimal operating point. In Matlab, it was coded as follows:

```
X0=[28.6 410 21.7 330 370]
```
(3.33)

The optimization was run on a *MacBook Pro* machine, with a 2.7 GHz *Intel Core i7* processor, with a 4 GB, 1333 MHz *DDR3* Ram memory. The results were obtained in 7 hours and showed that a small increase in the global efficiency is possible. This optimal condition can be obtained by lowering the pressures of the boilers, leaving the same temperature of Boilers 5 and 6, decreasing of a couple of degrees Boiler 7 temperature and increasing tempering output one till reaching the same value of inlet boiler temperature. A comparison between actual and optimum case is given in Table 3.4, while the mass and energy balances (Figure 3.21) shows that the optimum is obtained in correspondence of a mass flow of steam reduced from 300 to 25 PSIG equal to zero. The small order of magnitude of the possible increase in global efficiency is once again due to the scheme of the steam of the plant, which wouldn't allow to fully exploiting a more enthalpy charged steam stream. The only variable that significantly should change is the one of tempering, as shown by the sensitivity analysis, the closer this temperature to the one internal in the boiler, the best for the efficiency.

Table 3.4 Comparison between numerical optimal condition and real operation

430 Ton/h	*P boiler 7 [bar]*	*T boiler 7 [°C]*	*P boilers 5,6 [bar]*	*T boilers 5,6 [°C]*	*T outlet tempering boiler 7 [°C]*	*Global efficiency*
Actual case	28.6	410	21.7	330	370	0.5849
Optimal case	28.1	406	19.8	330	406	0.5884

With these values of input variable a second principle efficiency of 19.74% is obtained (no exergy losses for 300 PSIG reduction are now present), while the renewable efficiency grows till 98.15%. A money saving can be associated to the increase in global efficiency, because bagasse has a small market where its value is 22.4 €/ton (56,000 COP/ton), so it could be sold instead of burnt. Equation 3.34-3.38 show the procedure to obtain the year saving. The following variables and nomenclature are required:

- Subscript *y* indicates that the variable, previously introduced, is considered on a year base;
- Subscript *OPT* indicates that the variable, previously introduced, is considered with its optimal value;
- Subscript *SV* indicates the saving of the previously introduced variable;
- The term *saving* stands for the possible money saving, expressed in [€];
- Bagasse cost *c* [€/ton].

The potential saving for a milling rate of 430 ton/h were calculated in 107,800 €/year (269,500,000 COP/year).

Figure 3.21 Mass and energy balance of theoretical optimum of cogeneration at 430 ton/h of cane

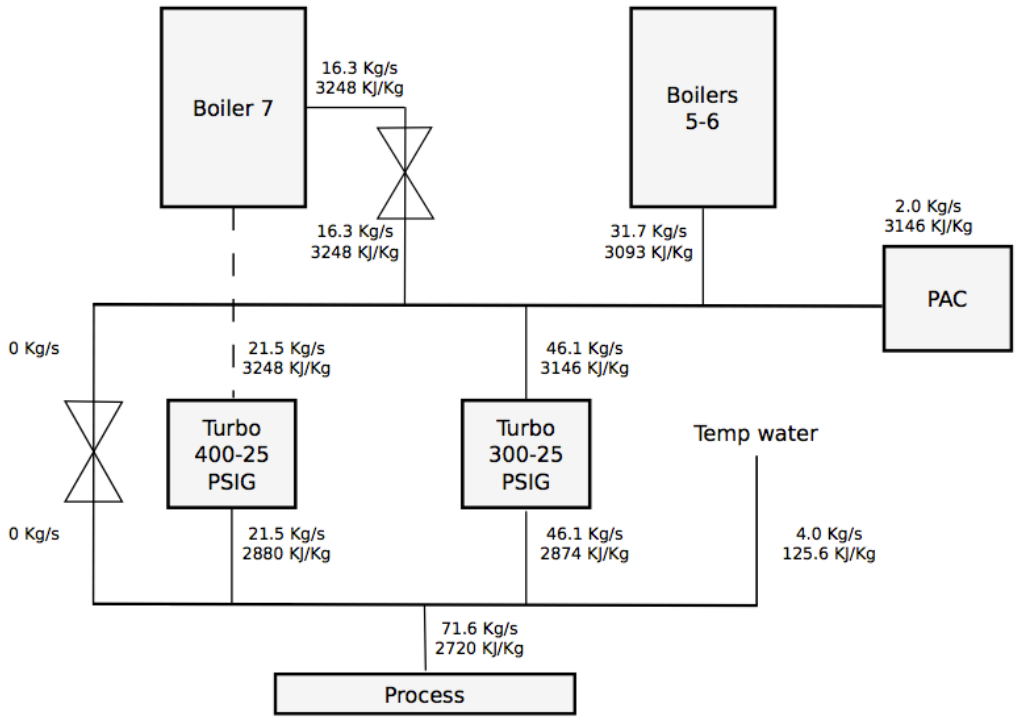

$$Q_{FUEL\_y} = Q_{FUEL} * HR_{eq\_y} \left[\frac{kWh}{year}\right] \quad (3.34)$$

$$Q_{FUEL\_OPT\_y} = \eta_g * \frac{Q_{FUEL\_y}}{\eta_{g\_OPT}} \left[\frac{kWh}{year}\right] \quad (3.35)$$

$$Q_{FUEL\_SV\_y} = Q_{FUEL\_y} - Q_{FUEL\_OPT\_y} \left[\frac{kWh}{year}\right] \quad (3.36)$$

$$m_{BAG\_SV\_y} = Q_{FUEL\_SV\_y} * \frac{3600}{LHV_{BAG}} \left[\frac{kg}{year}\right] \quad (3.37)$$

$$saving_y = m_{BAG\_SV\_y} * \frac{c}{1000} \left[\frac{€}{year}\right] \quad (3.38)$$

From a practical point of view, it is impossible to run the plant in these conditions, because all the machines and equipment are designed with specific nominal values of temperatures and pressures. Changing these parameters can badly affect their performances and also cause them damages or breakages. In particular, it is not allowed to change pressures at inlet of turbines, because the blades would not resist to higher forces. Tempering output temperature can not be equal to the one inside the boiler because it would lose its function to prevent variations in boiler's temperature to affect the turbines: for these reasons it is chosen to insert in the constraint a minimum gap of 10 °C.

$$T_{B7} > T_{TB7} + 10 \quad [°C] \tag{3.39}$$

Turbo-generators 4 and 5 accept a possible change in their inlet temperature of 5 °C, the turbo of the head of 300 PSIG can accept higher changes, because they are smaller and already operating at different temperatures, depending on the mill rate (that affect the enthalpy of the head of 300 PSIG). The variables are then reduced to the only temperatures. Their bounds are given in Table 3.5 and the following equations describe the vector of variables, the constraints and the initial point, which was once again selected as the current operating point, in Matlab programming language.

(3.40)
```
X(1) = TB7
X(2) = TB56
X(3) = TTB7
```

(3.41)
```
X0=[410 330 370]
```

(3.42)
```
A=[-1 0 1]
```

(3.43)
```
b=[-10]
```

(3.44)
```
LB=[365 310 365]
```

(3.45)
```
UB=[540 350 375]
```

(3.46)
```
- ToutTurb  + 135
```

(3.47)
```
- mB56 + 38
```

(3.48)
```
- mvapTURB300
```

(3.49)
```
- mvapTURB400
```

(3.50)
```
- mvapR400
```

(3.51) - mvapR300

(3.52) - mTW

Table 3.5 Range of the variables for the optimization with real bounds

Variable	*Minimum value [°C]*	*Maximum value [°C]*
Temperature boiler 7	365 °C	540 °C
Temperature boilers 5 and 6	320 °C	340 °C
Boiler 7 tempering Temperature output	365 °C	375 °C

The algorithm converged in 5 hours once again to an optimum that corresponds to a point of operation in which no 300 to 25 PSIG reduction is present (Figure 2.40) and where the temperature difference for the tempering of Boiler 7 is reduced to the minimum allowed value; the results are shown in Table 3.6.

Table 3.6 Current and optimal case comparison considering real bounds

430 Ton/h	*P boiler 7 [bar]*	*T boiler 7 [°C]*	*P boilers 5,6 [bar]*	*T boilers 5,6 [°C]*	*T outlet tempering boiler 7 [°C]*	*Global efficiency*
Actual case	28.6	410	21.7	330	370	0.5849
Optimal case	28.6	380	21.7	320	370	0.5880

The results of the optimization show that the plant is already operating very close to its optimum condition. It is possible to reach a second principle efficiency of 19.72% and a renewable efficiency of 98.08%; from economic point of view this correspond to a saving of 95,513 €/year (238,782,500 COP/year).

Figure 3.22 Mass and energy balance of optimum of cogeneration at 430 ton/h of cane

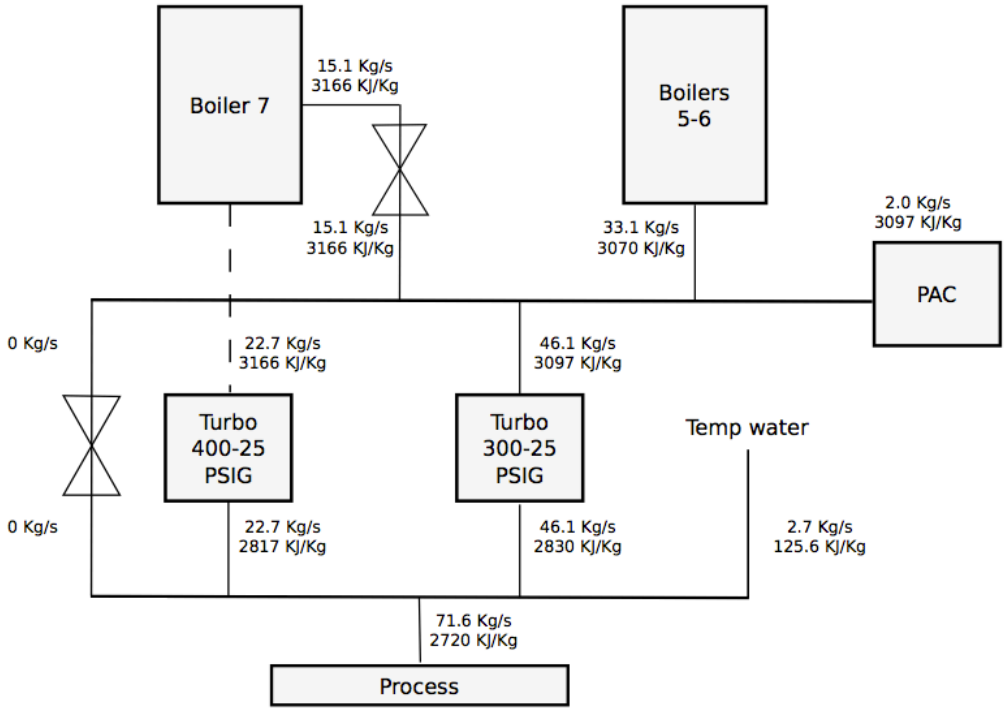

3.7 References

[1] D. Paz, C. J. Cardenas, *Evaluación exergética de propuestas de disminución de consumo de vapor en usinas azucareras*, Revista Industrial y Agrícola de Tucumán Tomo 82 (1-2) (2005), pp 1- 8; 2005.
[2] Manuelita S.A., *Internal Report*, 2013.
[3] International Organization for Standardization, *ISO 50001:2011, Energy management systems – Requirements with guidance for use*, 2011.
[4] I. Dincer, H. Al-Muslim, *Thermodynamic analysis of reheat cycle steam power plants,* International Journal of Energy Research 25, pp 727-739, 2001.
[5] R. S. El-Emam, I. Dincer, *Exergy and exergoeconomic analyses optimization of geothermal organic Rankine cycle,* Applied Thermal Engineering, vol. 59, 2013.
[6] M. O. S. Dias, T. L Junqueira, C. D. F. Jesus, C. E. V. Rossell, R. Maciel Filho, A. Bonomi, *Improving second generation ethanol production though optimization of first generation production process from sugarcane,* Energy 43, pp. 246-252, 2012.
[7] F. F. Furlan, C. B. Borba Costa, G. de Castro Fonseca, R. de Pelegrini Soares, A. Resende Secchi, A. J. Goncales da Cruz, R. de Campos Giordano, *Assessing the production of first and second generation bioethanol from sugarcane through the integration of global optimization and process detailed modeling,* Computers and Chemical Engineering 43, pp. 1-9, 2012.
[8] R. Hooke, T.A. Jeeves, *"Direct search" solution of numerical and statistical problems,* Journal of the Association for Computing Machinery (ACM), vol.8, pp 212-229, 1961.
[9] The MathWorks Inc, *Genetic Algorithm and Direct Search Toolbox for Use with Matlab User's Guide,*
http://www.mathworks.com/help/releases/R13sp2/pdf_doc/gads/gads_tb.pdf, 2004.

4. Future Prospective and Repowering

4.1 Introduction

Sugar plants worldwide are evolving and moving towards two different directions: the rise of pressure and temperature of boilers of the Rankine cycles or the switch to BIGCC systems (Biogas Integrated Gasification Combined Cycle [1-3]. What is common for both the strategies is the substitution of steam driven equipment with electric ones. The production of electric energy with bigger turbines allows a better energy conversion and a simplification of the steam scheme of the plants. The possibility to upgrade and repower the plant is taken into account for Ingenio Manuelita. Starting from the idea to convert the machines into electric ones by substituting the steam moved machines with electric motors, and to produce an electric energy surplus to be sold to the grid, different solutions are analyzed in this chapter. The cogeneration is studied in case of two different phases of sugar process steam reduction and two new possible layouts for the repowering are evaluated.

4.2 Electric machines

Nowadays the two milling tandems of Ingenio Manuelita are steam driven. Six mills, moved by three turbines, provide Tandem 1. Tandem 2 has six mills too, each one equipped by a own steam turbine. The first step in the purchase of the complete substitution of the steam driven machines into electric driven ones is the shutdown of Tandem 1 and the installation of electric motors to the mills of Tandem 2. The electric motors have to work (at the beginning) in help to the existing turbines in order to supply all the energy required.

Converging all the cane into Tandem 2, at a milling rate of 430 ton/h, by estimating an increase of tandem's power need from 17 to 17.5 HP/t.f.h-mill (because of strong increase in the amount of cane which has to be processed) the model predicts a mechanic power demand of 5.5 MW (see Chapter 2). Being the installed power of the turbines 4.5 MW (6,000 HP), the electric motors will have to supply the remaining 1 MW. The most efficient turbo-generator of the plant is the number 5, operating between 400 and 25 PSIG. This machine is now used for the production of 5 electric MW but, having a nominal capacity of 8.5 MW, and can be easily charged of the power demand of 1.05 MW (considering a 95% of electric efficiency) of the mills. The result of this switch has a negative impact on the efficiency of the plant. Figure 4.1 shows the energy and material balance of the cycle, where it is possible to notice that, for the additional electric

power requirement, more steam flows into the block of 400 PSIG turbines and less through the 300 PSIG ones (the turbines of Tandem 1 are now switched off). The steam coming from the outlet of the big turbo-generators has a lower specific enthalpy value, so the energy required by sugar and alcohol processes has to be supplied by a small increase in the mass flow of the pressure reduced steam.

This loss of efficiency may represent a cost. Following the procedure explained in Chapter 3, the value of this cost is estimated into 23,120 €/year (57,800,000 COP/year). A comparison between actual and the new configuration is given in Table 4.1, while Table 4.2 shows how the power of the mills is split between electric motors and turbines.

Figure 4.1 Material and energy balance for a milling rate of 430 ton/h with electrification of the Tandem 2

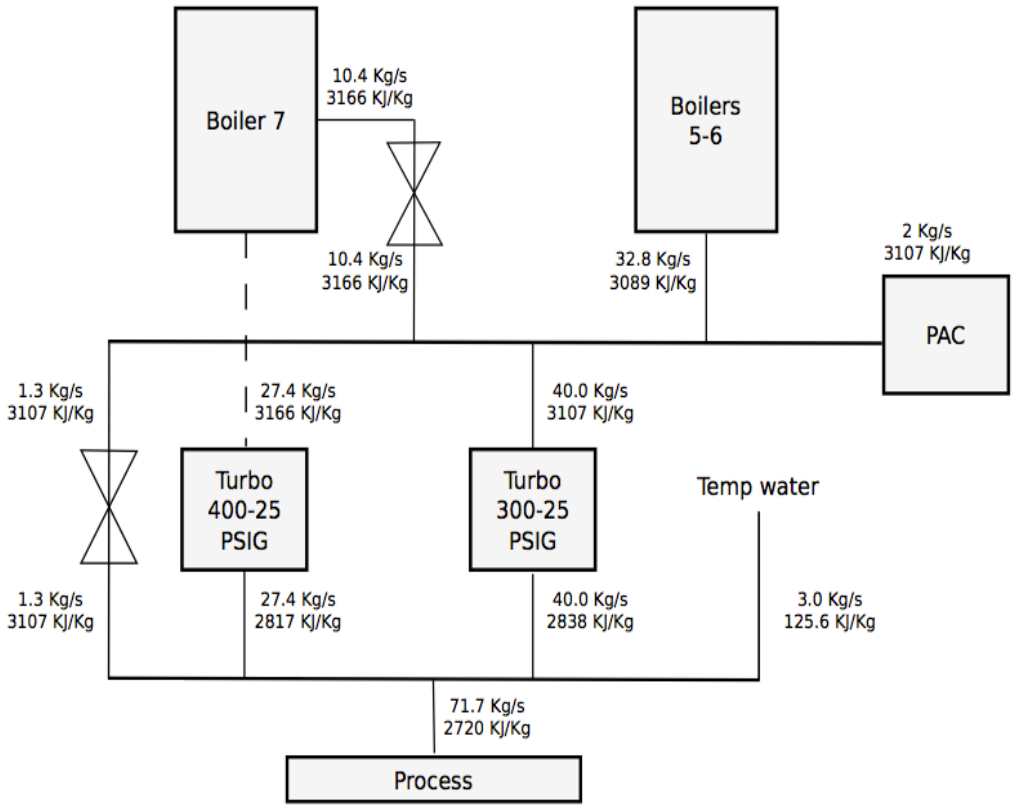

Table 4.1 Comparison between parameters of current situation vs configuration with electrified Tandem 2 for milling rate of 430 ton/h

430 ton/h	*m vap rid 300-25 PSIG [kg/s]*	η_{el}	η_{mech}	η_{therm}	η_{glob}
Steam Driven	0.39	0.0312	0.0278	0.5260	0.5849
Electric Driven	1.3	0.0319	0.0266	0.5257	0.5842

Table 4.2 Tandem 2 power requirement split

Mill	*Mill power [kW]*	*Steam turbine power [kW]*	*Electric motor power [kW]*
Mill 1	1,143	750	393
Mill 2	970	750	220
Mill 3	867	750	117
Mill 4	833	750	83
Mill 5	833	750	83
Mill 6	833	750	83
Total	5,480	4,500	979

It is clear that in such a complex system, it is meaningless to consider separately the cogeneration and the production processes, because any improvement on the cogeneration has to be related with a reduction of process steam demand. Decreasing the heat power required by the process and installing electric machines will allow having surplus steam for electric power production.

4.3 Process steam reduction: Phase 1

It is estimated [4] that at the end of 2014 the process steam demand, at a milling rate of 430 ton/h, will be reduced of 36.7 kg per ton of cane. According to this estimation, 4.4 kg/s of steam are saved, corresponding to 11.3 thermal MW. This will be possible thanks to the addition of new heat exchangers in sugar process, which will have the aim to heat the juice at low temperature and will be feed with steam coming from the evaporators. In this case, it is not useful to compare global efficiency (now 57.62%) with the current one (58.49%), because, decreasing heat power demand, the global efficiency would also decrease. A comparison may be done on second principle efficiency, which gives a fair weight to heat power respect to mechanic and electric ones. Figure

4.2 shows that steam demand of sugar and alcohol production are less than the one required by the turbines for the electric and mechanical power generation (please notice the values of the flow streams crossing the blocks corresponding to the turbines and the one related to the sugar process). Because of this there is an amount of steam, which has to be released to atmosphere after the expansion. The efficiency is strongly affected because this mass flow does not contribute in heat useful effect. For sure this is not the best efficiency solution, in fact its second principle efficiency is just 19.00%.

Figure 4.2 Material and energy balance for a milling rate of 430 ton/h with process steam reduction

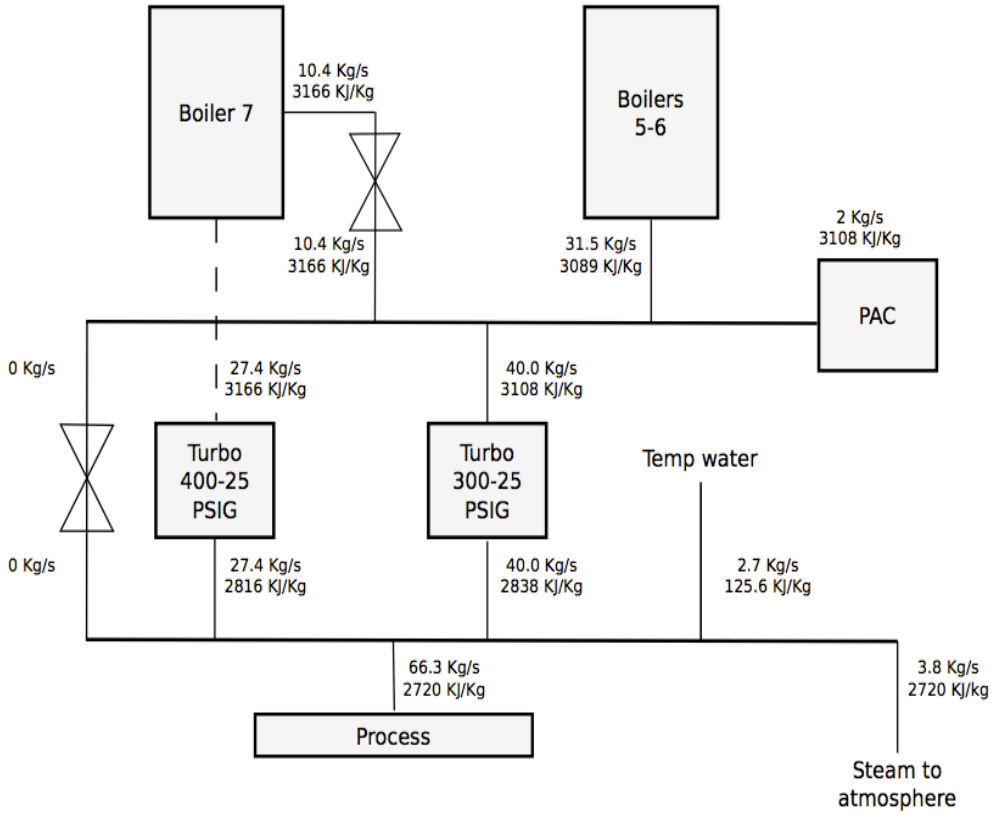

In this case, it becomes interesting to fully switch the steam driven machines into electric moved ones, to reduce the amount of steam need. With the actual equipment, a bottleneck is found in the electric power generation capacity. The electric power capacity still available in turbo-generators 5 and 4 is of 3.5 MW (respect to the previous case, where mills electric motors are already providing 979 kW), while, in these proposed fully electrified conditions, the requirement

of the mills is still 4.5 additional MW. Table 4.3 shows in details the power requirement of the mills in this situation.

Table 4.3 Tandem 2 power requirement split with maximum electric share

Mill	*Mill power [kW]*	*Steam turbine power [kW]*	*Electric motor power [kW]*
Mill 1	1,143	0	1,143
Mill 2	970	0	970
Mill 3	867	0	867
Mill 4	833	0	833
Mill 5	833	329	504
Mill 6	833	750	83
Total	5,479	1,079	4,400

With this configuration (material and energy balances in Figure 4.3) global efficiency grows (but stays anyway lower than the actual value). If we consider the second principle efficiency (that gives a weight to heat power, in order to be able to compare it with mechanic and electric) a 2% increase is noticed. It means that there is an overall better use of the fuel. Moreover, with this configuration, the plant reaches 101% value of "renewable efficiency" (the procedure to calculate this parameter is explained in Chapter 2), which means that its energy requirement is fully covered by biomass and that, produced biomass is even more than the required one. Still there is a release of steam at 25 PSIG to the atmosphere. With such an improvement in the production process, the cogeneration becomes the "weak" part of the process. Once again, the importance to develop in strictly relation all the aspects of the process is remarked. Table 4.4 shows the comparison between performance parameters of actual and Phase 1 completed layouts.

Table 4.4 Comparison between performance parameters of current and phase 1 completed layout

430 ton/h	η_{el}	η_{mech}	η_{therm}	η_{glob}	η_{II}
Steam driven	0.0312	0.0278	0.5260	0.5849	0.1962
Electric driven	0.0489	0.0135	0.5139	0.5762	0.2117

Figure 4.3 Material and energy balance for a milling rate of 430 ton/h with full exploitation of turbo-generators 4 and 5

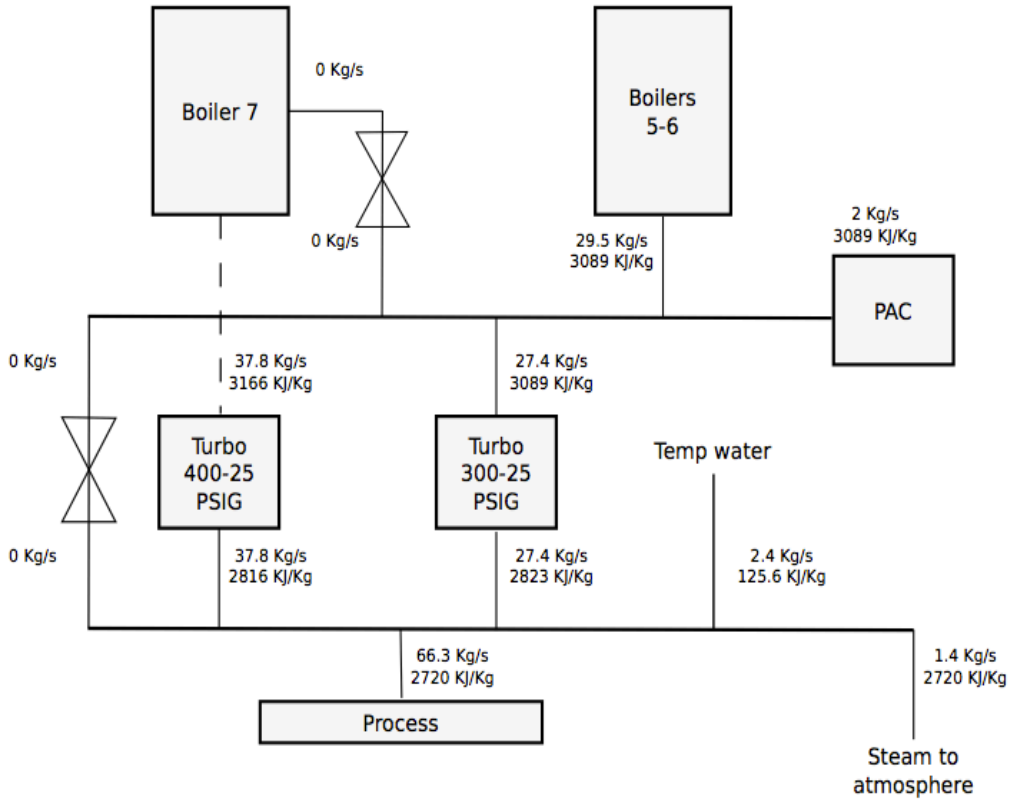

4.4 Process steam reduction: Phase 2

4.4.1 The concept

The ambitious goal for the future is to further decrease the steam demand of sugar and alcohol production till reach, for a milling rate of 430 Ton/h, an heat power demand of just 103.8 MW, corresponding to a saturated steam mass flow of 47.8 kg/s at 2.72 bar of pressure. It means a decrease of 33% respect to current process. Studies [4] affirm that this target may be obtained with a better use of the steam extracted by the production of sugar. A better use of the gases of the evaporators, the use of the steam coming from the flash tank, the use of Gases 4 and Gases 5, which are now condensed, can be purchased. Moreover, it is estimated [4] that all the heat requirement of alcohol production could be extracted from the sugar process also. With such a scenario, to repower

completely the plant becomes a priority. Therefore, a new Rankine cycle, with new boilers and new pressure levels has to be designed.

The objective is to optimize the maximum production of surplus electric energy, which implies the optimization of economic revenues. The system is studied in order to have a fully sustainable process. Based on all and only the available energy from bagasse, the process energy requirement has to be satisfied while searching for the configuration that allows a higher electric energy production. While global efficiency may decrease, higher second principle efficiency will be obtained. The idea, in order to not to conduct big investment, is to turn off only old Boilers 5 and 6 and to substitute all the turbines with electric motors. A new big state of the art boiler should be installed supporting a cogenerative Rankine cycle with a condensing steam turbine provided by a bleeding to feed the process.

It is well known that the electric efficiency of a Rankine cycle increases with the pressure and temperature of the turbine inlet, and this is valid also in case of design of an ideal cycle with extraction of steam to feed heat demands. This is shown in Figure 4.4 where the electric efficiency of an ideal Rankine cycle of a typical sugar plant has been evaluated in function of pressure and temperature at turbine's inlet.

Figure 4.4 Electric efficiency of an ideal, typical cogenerative Rankine cycle of a sugar plant. Adapted from [5]

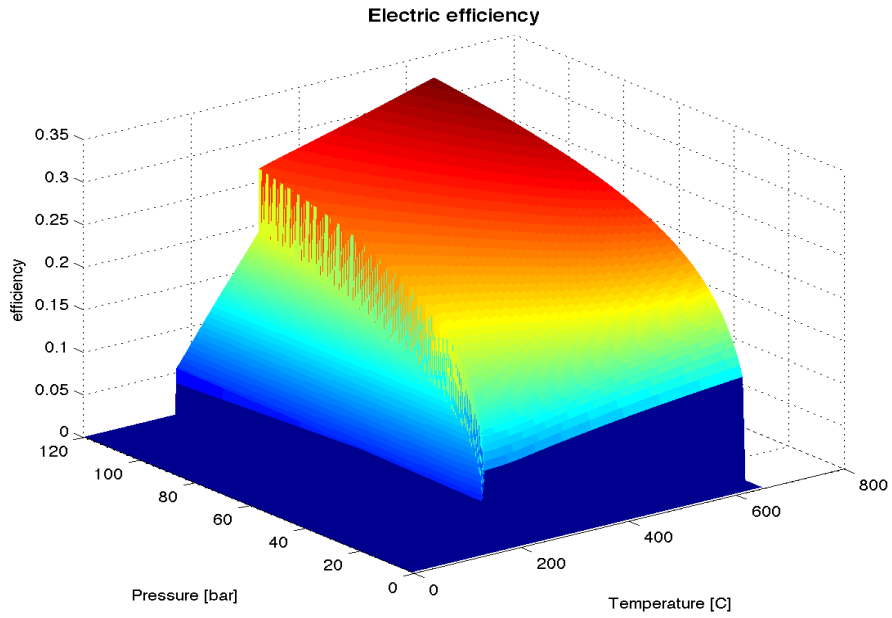

Unluckily, in real cases, once fixed bleeding pressure and temperature (25 PSIG, 5 °C superheated condition), this is not true anymore. Rising too much the boiler pressure would imply to expand steam with a worse isentropic efficiency, and this would badly affect the overall efficiency. On the contrary, it is impossible to rise too much the temperature because isentropic efficiency cannot be higher than one (1) from a theoretical thermodynamic point of view, and is much lower in real machines. Moreover, not all the combinations of pressure and temperature can be chosen because commercially available boilers for bagasse, or for combination of coal and bagasse, offer just a few nominal working points and ranges, from which may represent a risk to move. Table 4.5 offers an overview of the nominal conditions of suitable selected boilers for a sugar plant. The state of the art guarantees efficiencies of 68% [4].

Table 4.5 Operating parameters of commercially available boilers produced by Indian manufacturers as Thermax, Isgec and Whalchandngar [4]

Pressure [bar]	*Temperature [°C]*
42.2	480
45.1	440
64.7	485
65.7	495
65.7	520
66.7	510
66.7	515
85.3	515
86.3	510
86.3	515
86.3	540
87.3	515
104	540
106.9	540
107.9	540
108.9	540
108.9	540

4.4.2 Repowering - Option 1

The first repowering option is the simplest one: beside the Boiler 7 scheme, a new superheated Rankine cycle is set up, with extraction at 25 PSIG, pressure regeneration, and a as low as possible condensing pressure. Figure 4.5 shows the

new cogeneration layout of the plant, while Figure 4.6 focuses just on the new cycle. The starting point, taking into account that one of the targets is the process sustainability, is the calculation of available fuel heat power. Being interested in the optimization for a milling rate of 430 ton/h, and considering constant in the future the amount of processed cane in one year, the result is that the plant can work for the same equivalent hours per year (5,982) and the instantaneous availability of fuel energy is 295 MW. This value is obtained by multiplying bagasse LHV times the instantaneous bagasse production, according to the procedures explained in model description in Chapter 2.

The capacity of the new boiler depends on its pressure and temperature, which determine the amount of steam that can be produced with available fuel heat power and the amount, which is required to satisfy the heat demand of the process. The logic of the new scheme is to fully exploit the heat capacity of the fuel, by satisfying the energy requirement of the plant, and by producing a surplus of electric energy. Boiler 7 will be now able to produce less steam, because it will be connected only to the turbo-generators 4 and 5, whose power is limited to 12 MW, obtained with a mass flow of 36.6 kg/s, which is able to cover the 80% of process heat demand. Anyway, being the new boiler and cycle characterized by higher efficiency, it is chosen to operate Boiler 7 at minimum (50% of nominal capacity) to exploit the better performances of the new devices. In these conditions, boiler 7 will be processing 19 kg/s and covering the 41% of heat process demand.

The T-s diagram of this cycle (Figure 4.6) immediately remarks what can be a limit of this new cycle. Once fixed the bleeding at 25 PSIG to be slightly supersaturated, in order not to have condensation in the head before sugar process, point number 3 is given in the chart. A strong limit on the increase of pressure and temperature of the boiler is introduced because the thermodynamic limit of the isentropic efficiency which has to be lower than 1. From graphical point of view, the isentropic efficiency is represented by the slope of the expansion line (point 1 – point 4) and it cannot be too steep (according to the physical and technical limits on such efficiency).

Considering not to change the characteristics of the bottoming cycle of 400 PSIG, the variables to be studied in order to optimize the objective function are pressure and temperature of the new cycle (to be chosen between commercial boilers), pressure of regeneration, steam mass flow of regeneration ($m_{vap\ reg}$,) that influences inlet temperature of boiler). Minimum capacity of the boiler ($m_{vap\ boiler}$) will be determined for each couple of pressure and temperature, while condensing pressure has been chosen to be 0.1 bar, being the water available at around 30 °C and considering a condenser split temperature of 15 °C.

Figure 4.5 Layout of repowering Option 1

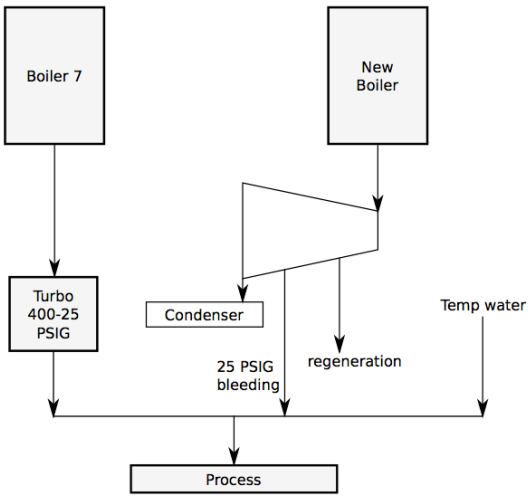

Figure 4.6 T-s diagram of repowering Option 1. Point 1: Turbine inlet; Point 2: Regeneration bleeding; Point 3: Process bleeding; Point 4: Turbine outlet; Point 5: Condenser outlet; Point 6: Process condensed water; Point 7: Addition of regeneration vapor; Point 8: Pump and boiler's inlet

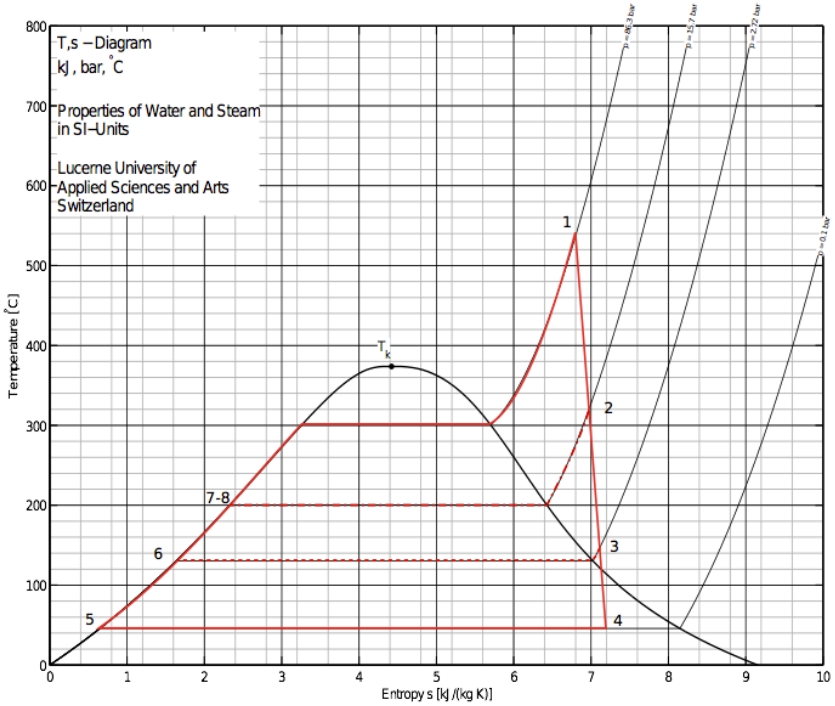

Figure 4.7 Layout of new high pressure cycle, repowering Option 1

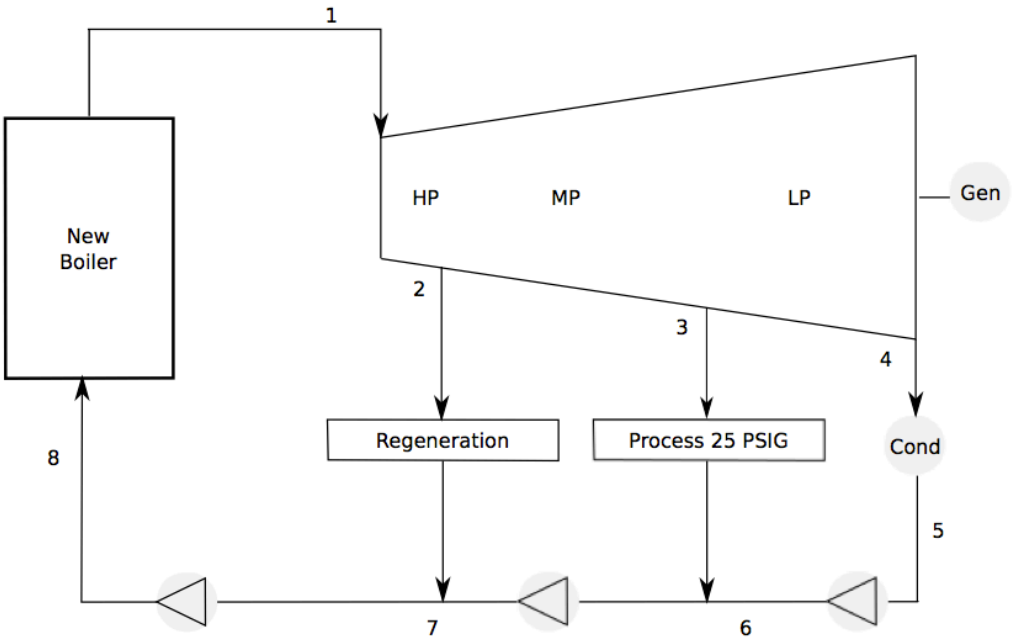

The model is very similar to the current case, with the difference that the turbine is characterized by different mass flows in high ($\boldsymbol{m_{vap\ HP}}$), medium ($m_{vap\ MP}$) and low ($m_{vap\ LP}$) pressures:

$$(4.1) \quad m_{vap\ HP} = m_{vap\ boiler} \ [kg/s]$$

$$(4.2) \quad m_{vap\ MP} = m_{vap\ HP} - m_{vap\ reg} \ [kg/s]$$

$$(4.3) \quad m_{vap\ LP} = m_{vap\ MP} - m_{vap\ TOP\ process} \ [Kg/s]$$

Steam mass flow coming from high pressure cycle and going to the process ($m_{vap\ TOP\ process}$) is obtained by the definition of the share of process heat of the cycle and by maintaining the head of 25 PSIG under saturated vapor condition. The term q_{top} represents the share of total process heat power demand $Q_{process}$ covered by the new cycle. The amount of process heat power satisfied by the new cycle is then called $Q_{TOP\ process}$. The term q_{BOT} stands for the share of the low pressure cycle. As mentioned before, it is set to 41% in order to keep the Boiler 7 working at its minimum technical capacity and to exploit as much as possible the new boiler. The subtitle *temp* for the tempering water flow, and h_3 is the specific enthalpy of bled steam:

$$(4.4) \quad q_{BOT} = 0.41$$

$$(4.5) \quad q_{TOP} = 1 - q_{BOT}$$

$$(4.6) \quad Q_{TOP\ process} = Q_{process} * q_{TOP} \ [kW]$$

$$(4.7) \quad m_{vap\ process} = m_{vap\ TOP\ process} + m_{vap\ temp} \ [kg/s]$$

$$(4.8) \quad m_{vap\ TOP\ process} = (Q_{TOP\ process} * h_{vap\ sat@25PSIG} - m_{vap\ temp} * h_{temp}) / h_3 \ [kg/s]$$

The objective function is given by the electric energy surplus that can be obtained by each ton of bagasse. Being $P_{el\ surplus}$ the total plant electric power surplus, the energy index E_{index} is expressed in Equation 4.9:

$$(4.9) \quad E_{index} = P_{el\ surplus} * 1000 / (m_{BAG} * 3600) \ [kWh/ton_{BAG}]$$

The sensitivity analysis is separately conducted on each variable, while keeping constant the values of the others. Reference values of the variables for the analysis are given in Table 4.6.

Table 4.6 Reference values of the variables for sensitivity analysis

Variable	Boiler pressure [bar]	Boiler temperature [°C]	Regeneration pressure [bar]	m steam regeneration [kg/s]
Value	66.7	510	40	2

Sensitivity analysis on boiler pressure in Figure 4.8 shows the negative trend assumed by the energy surplus when the pressure rises. The reason of this is found in what was previously remarked to be a strong constraint of the model. Forcing the temperature at 25 PSIG (2.72 bar) bleeding to be of 135 °C (5 °C of super saturation), the effect of rising the pressure implies a change in the slope of the expansion on the T-s diagram. From a thermodynamic point of view, it means a decrease in the isentropic efficiency of the turbine. The available enthalpy drop between inlet and outlet of the turbine is less exploited and a decrease in efficiency and work output occurs.

Figure 4.9 represents the sensitivity analysis on the boiler temperature. Energy surplus behaves in the opposite way than with pressure. It increases with temperature because the rise of temperature implies a higher isentropic efficiency in the expansion, and then higher work output and cycle efficiency. For both of these variables, not all the values are possible, because the isentropic efficiency of the expansion has to assume reasonable values (<0.9), so

temperature cannot freely rise till material limits as well as pressure cannot decrease too much.

Figure 4.8 Effect of new cycle boiler's pressure on energy surplus index

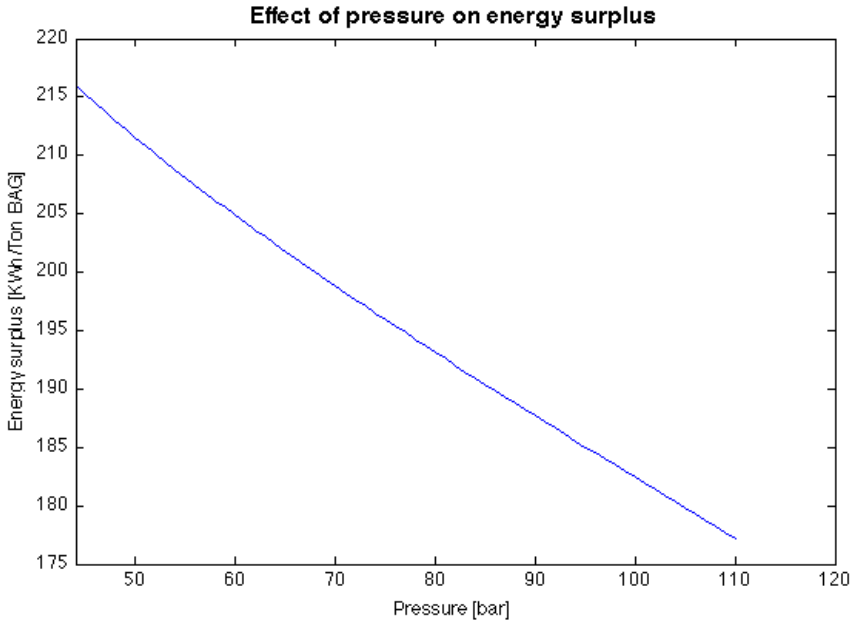

Figure 4.9 Effect of new cycle boiler's temperature on energy surplus index

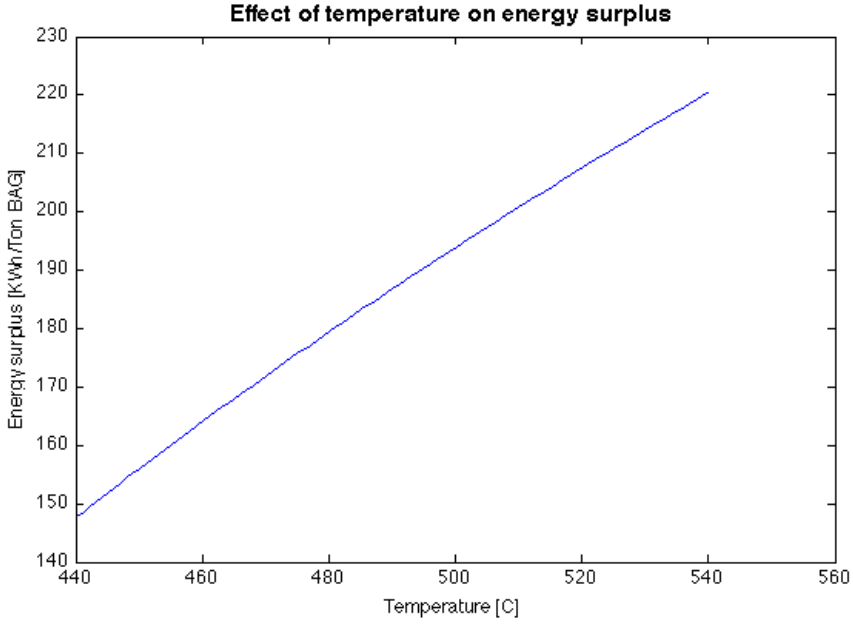

For given reference variables, sensitivity analysis on regeneration shows a decrease with its pressure (Figure 4.10) and an increase of objective function (surplus electric energy) with regeneration mass flow (Figure 4.11). This behavior may seem abnormal but it is related to the different point of view from which the problem is studied. In this case steam mass flow of the cycle is not fixed, while fuel input is given. In this case, increase the mass flow of regeneration increases the efficiency, which means –given fuel input- to raise the steam produced by the boiler. It corresponds to an increase in power output also. Moreover, given a steam mass flow for regeneration, it will be much more effective if bled at a pressure that guarantees to rise feed water temperature close to saturation one. A trade off has to be found then for regeneration pressure because, at higher pressure, feed water can income more heat and rise more its temperature, but work output will decrease, badly effecting the objective function.

Figure 4.10 Effect of regeneration pressure on energy surplus index

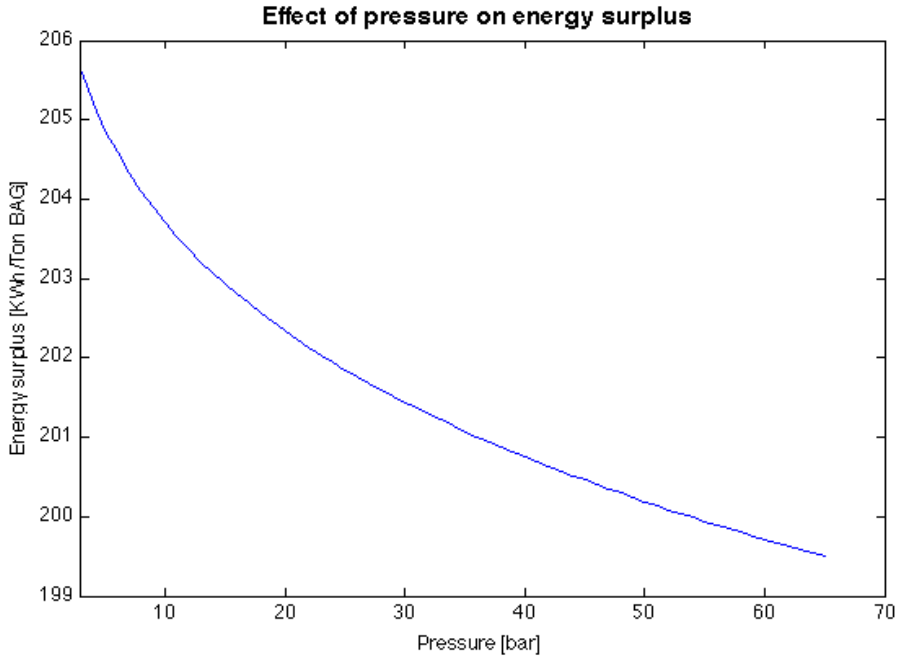

Figure 4.11 Effect of regeneration mass flow on energy surplus index

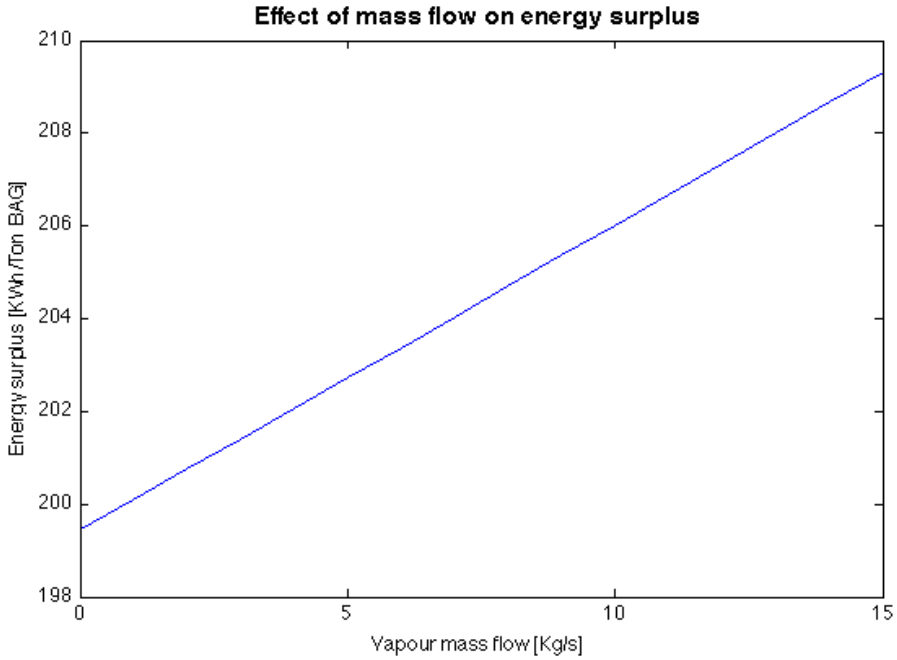

The optimization has to take into account several limits, on both topping and bottoming cycles. In particular, temperature of feed water after the mix with regeneration steam T_7, has to be lower than saturation temperature, and a security margin of 3 °C is chosen. The steam fraction x_4 at the end of the expansion has to be higher then 0.87 to avoid an excessive condensation inside the turbine. These limits are expressed in Equations (4.10-4.16). The subscripts are referred to the point in the thermodynamic cycle shown in Figure 4.6 and 4.7

$$(4.10)\quad 0 < q_{BOT} < 0.8$$

$$(4.11)\quad p_3 < p_{reg} < p_1 \quad [bar]$$

$$(4.12)\quad T_7 < Ts_{at\ @\ p\ 7} - 3 \quad [°C]$$

$$(4.13)\quad x_4 > 0.87 \quad [kg/kg]$$

$$(4.14)\quad \eta_{is} < 0.9$$

$$(4.15)\quad m_{vap\ MP} > 0 \quad [kg/s]$$

$$(4.16)\quad m_{vap\ LP} > 0 \quad [kg/s]$$

For each possible pressure and temperature combinations of the boilers, pressure and mass flow of regeneration are optimized, verifying to satisfy all the technical and thermodynamic constraints. The results are shown in Table 4.7, and Figure 4.12 represents the energy and material balances of the optimal case. The difference in the cash flow respect to current situation has to be evaluated. The cash flow represents the sum of all the revenues and costs that the process implies. The new revenues are given by selling electric energy and by savings related to the coal that is not bought anymore. Some coal may be bought to guarantee flame stabilities in the boilers, but would be in this case exchanged on LHV basis, so it would not affect the cash flow. The saving related to the coal is mostly related to the decrease of process steam demand, thus it is not considered into account in this work. It is estimated that Manuelita S.A. could potentially sell electric energy at a price of 0.048 €/kWh (February 2013) [4]. The optima for each possible pair of pressure and temperature are shown in Table 4.7. In such table are reported also the minimum new boiler capacity, and the power required by the new turbine, which are necessary data to design the new devices.

The best result are given by the boiler with 86.3 bar of pressure and 540 °C of temperature, with boiler inlet temperature of 199 °C obtained with a regeneration bleeding of 9.1 kg/s at 15.6 bar of pressure. This configuration would then give a year cash flow of 8,665,500 €/year (21,663,750,000 COP/year).

Table 4.7 Results of optimization for repowering Option 1

Boiler P [bar]	Boiler T [°C]	Boiler capacity [kg/s]	Boiler inlet T [°C]	P regeneration [bar]	m vap regeneration [kg/s]	P turbine top [MW]	η isentropic expansion	P surplus [MW]	η plant	Surplus [kWh/ton]
42.2	480						>0.9			
45.1	440	57.4	176	9.8	7.9	37.2	0.871	23.9	0.2371	179.2
64.7	485	56.7	187	12.5	8.6	39.9	0.863	26.5	0.2459	198.7
65.7	495	56.4	189	12.8	8.6	40.8	0.8772	27.4	0.2489	205.4
65.7	520						>0.9			
66.7	510	55.9	192	13.7	8.7	42.2	0.9000	28.7	0.2534	215.4
66.7	515						>0.9			
85.3	515	56.5	196	14.8	9.2	41.5	0.8468	27.9	0.2507	209.4
86.3	510	57.1	199	15.8	9.6	41.0	0.8350	27.4	0.2489	205.3
86.3	515	56.8	199	15.8	9.5	41.5	0.8440	27.8	0.2505	208.9
86.3	540	55.5	199	15.7	9.1	43.8	0.8858	30.2	0.2584	226.4
87.3	515	57.1	202	16.7	9.8	41.4	0.8411	27.8	0.2503	208.5
104	540	56.8	208	19.0	10.2	42.9	0.8415	29.2	0.2551	219.0
106.9	540	57.1	210	19.7	10.4	42.8	0.8350	29.0	0.2545	217.8
107.9	540	56.9	208	18.8	10.2	42.8	0.8328	29.0	0.2544	217.4
108.9	540	56.9	208	18.8	10.2	42.7	0.8306	28.9	0.2542	217.0

Figure 4.12 Material and energy balance of first option optimal repowering for a milling rate of 430 ton/h

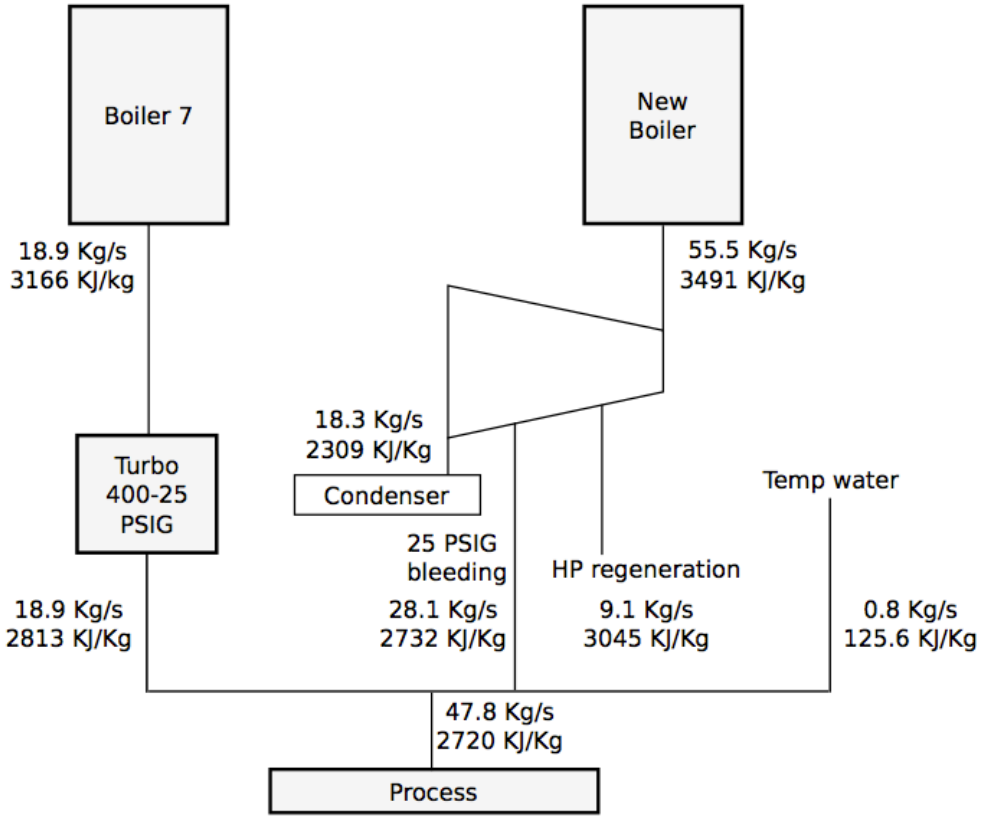

The choice to keep Boiler 7 at minimum production capacity may be considered wise also from another point of view. The design of new boiler and cycle with these constraints implies the capability of this cycle to satisfy the steam process demand alone. Once having the economic possibility and willing to further improve the power generation of the plant, it would be possible to substitute the actual 28 bar cycle and boiler with a higher pressure one. This ultimate cycle would not be related to the process (fully fed by other boiler and turbines), and could exploit in the highest efficient way the available bagasse energy. For these reasons it may be considered to divide the expansion of this first repowering option between two different turbines: a backpressure one, whose nominal capacity has to be equal to the total process demand, and a condensing one. Figure 4.13 focuses on the new boiler and expansion scheme, which would be coupled to the current cycle fed by Boiler 7. The backpressure turbine would, in this first configuration, expand an amount of steam equal to its nominal capacity. At its outlet, the steam would be divided between the process and the condensing turbine. The condensing turbine would process all the other steam

generated by the boiler and would receive at 25 PSIG part of the steam coming from the backpressure turbine. Once setting up the cycle that would substitute 400 PSIG current one, the condensing turbine would be switched off. The backpressure turbine would send all the steam to the process and all the remaining fuel power would be processed by the ultimate cycle.

Figure 4.13 New cycle's expansion scheme

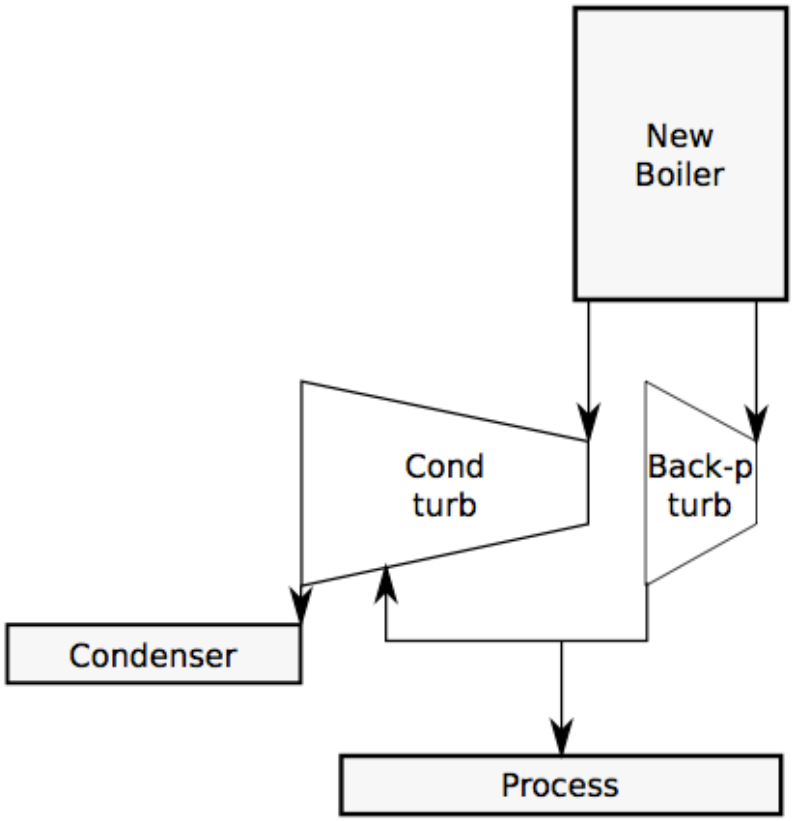

4.4.3 Repowering - Option 2

The second repowering option is similar to the first one but has a slightly more complex new cycle, which is provided of reheating at middle pressure. The logic is identical to first option. The available fuel power is fixed, the plant is designed in a way that, in steady state conditions, all the produced bagasse is burnt in the boilers and old Boiler 7 is run at minimum capacity (50% of nominal one). Figures 4.14 and 4.15 show the layout of repowering Option 2 and the equipment required by this configuration.

Figure 4.14 Layout of repowering Option 2

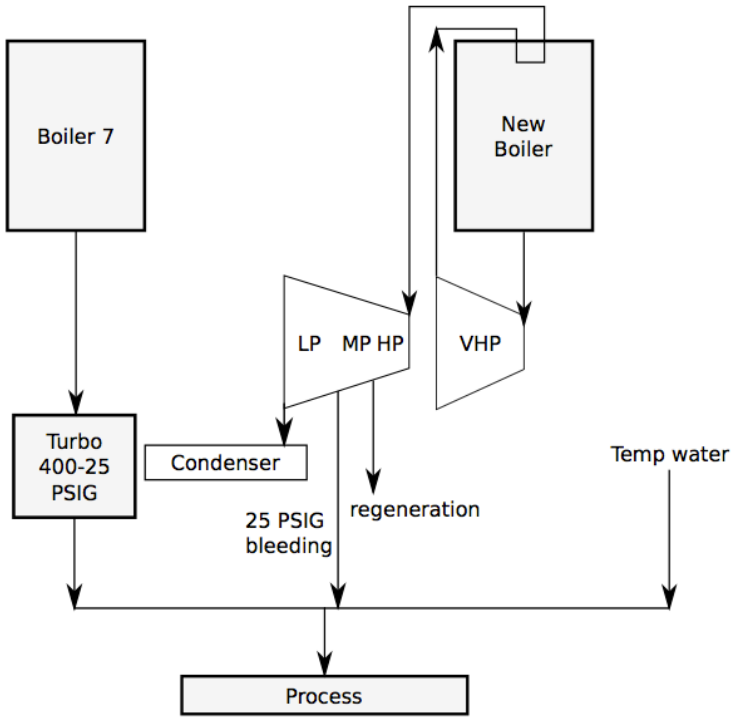

Figure 4.15 Layout of new high-pressure cycle, repowering Option 2

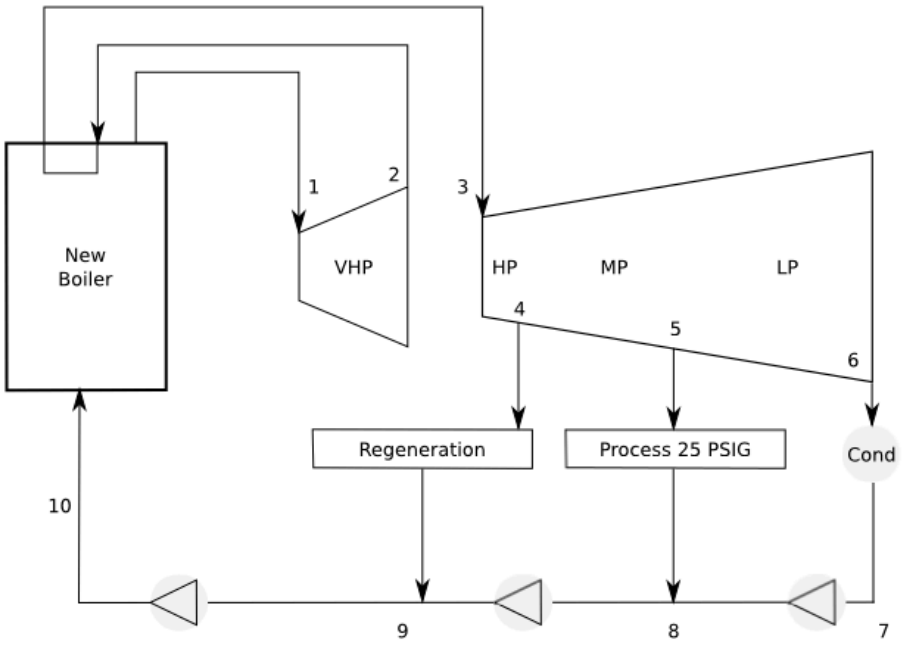

The expansion is divided into two blocks of turbines. For the first block an isentropic efficiency of 88% is assumed, while the one of the second turbine is a variable, left free to float till a maximum value of 90%. In this case, turbine outlet temperature is not fixed, but it is a parameter computed by the model, considering as constraint that it has to be at least 5 °C superheated. Just like Option 1, it would be wise to divide the block HP-MP-LP into two different turbines (a backpressure and a condensing), to permit to run the equipment in design conditions once further upgraded the plant.

The variables characterizing the systems are then 6: pressure and temperature of the boiler (to be chosen among the commercial available devices), isentropic efficiency of second turbine, pressure of reheating and pressure and steam mass flow of regeneration. For the sensitivity analysis, boiler pressure and temperature are assigned the optimum value of previous case, reheating pressure is set to 45 bar, regeneration at 16 bar with 2 kg/s of bled steam and the isentropic efficiency of the second part of expansion is fixed at 80%. The choice of these values may influence the results of the sensitivity analysis, so they are chosen far from their upper and lower limits. Once fixed all other variables, and considering that fuel power input is given, pressure of the boiler has a positive influence on the energy surplus, as shown in Figure 4.16, because, on a T-s diagram, it corresponds to increasing the area under the thermodynamic cycle by turning away the lines of the heating.

Figure 4.16 Effect of new cycle boiler's pressure on energy surplus index

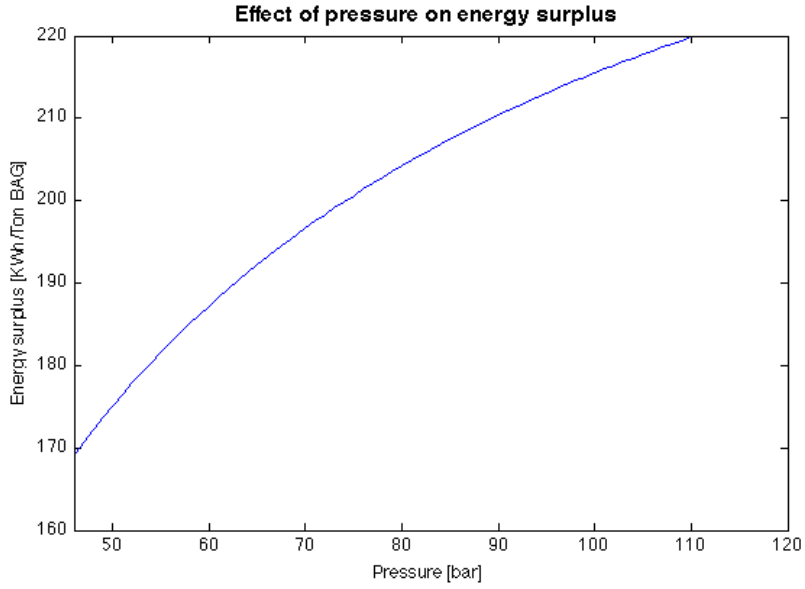

Although the increase of pressure implies a reduction of the steam mass flow, the increase of specific work of expansion is stronger, as shown in Figure 4.17.

Figure 4.17 Effect of boiler's pressure on specific expansion work-to-steam mass flow ratio

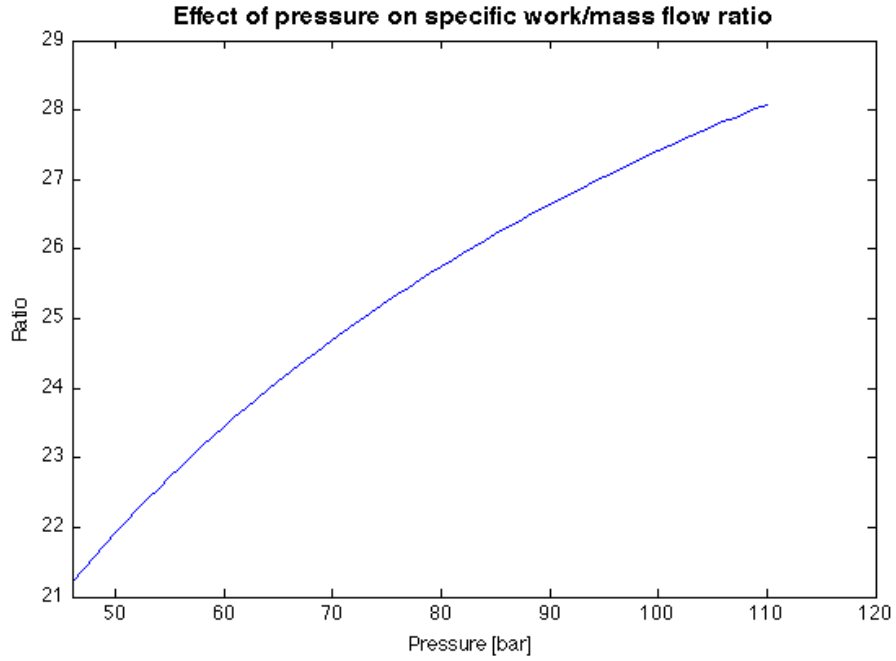

Temperature of the boiler, pressure and vapour mass flow of regeneration, have identical behaviour to first repowering option, so will not be further analyzed. Figure 4.18 displays the sensitivity analysis on reheating in the possible range of values (given the slope of expansion). Observe the presence of an optimum of the energy surplus index which is given by the tradeoff between the opposite trends of steam mass flow and specific work (Figure 4.19).

The effect of isentropic efficiency is clearly positive on electric energy surplus because it implies a better use of the available enthalpy difference between turbine inlet and outlet. Figure 4.20 shows the sensitivity analysis on the isentropic efficiency of the expansion of new cycle.

Figure 4.18 Effect of reheating pressure on energy surplus index

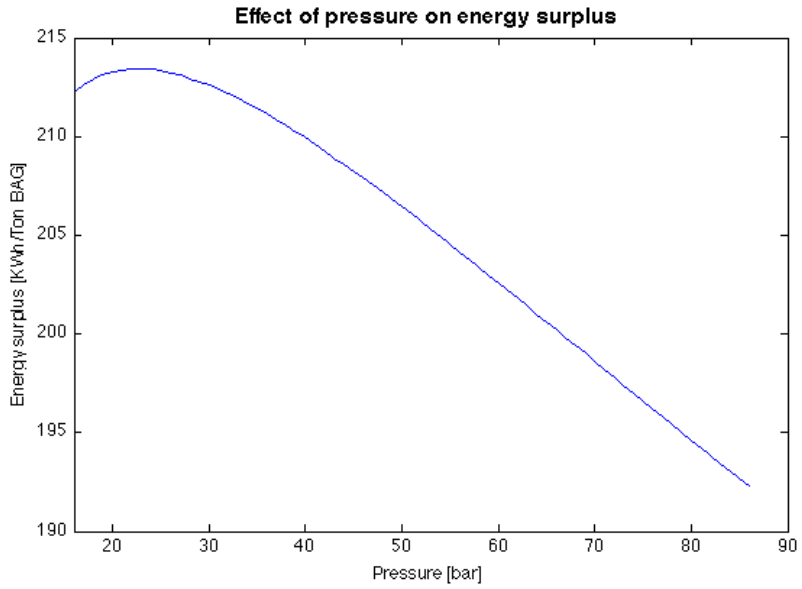

Figure 4.19 Effect of reheating pressure on specific expansion work and on steam mass flow

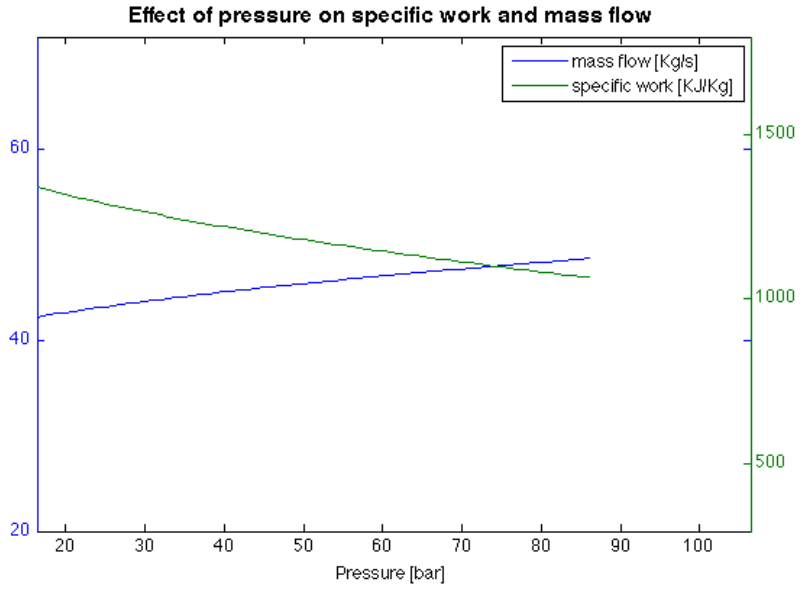

Figure 4.20 Effect of second expansion's isentropic efficiency on energy surplus index

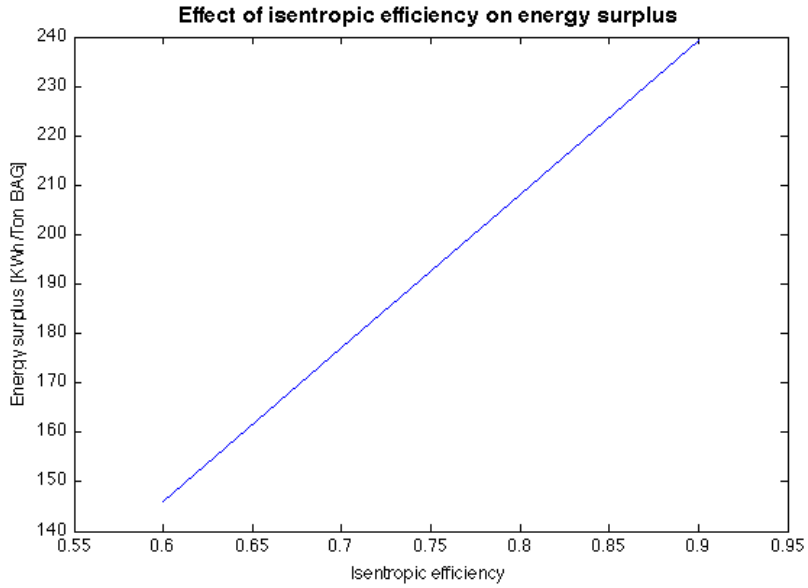

The optimization of the second layout has the same range and similar constraints of previous proposal, with the only addition of a linear constraint forcing reheating pressure to be higher than regeneration one. Subscripts related to thermodynamic cycle are related to T-s diagram of Figure 4.21.

$$\eta_{is} < 0.9 \quad (4.17)$$

$$m_{vap\ MP} > 0 \ [Kg/s] \quad (4.18)$$

$$m_{vap\ LP} > 0 \ [Kg/s] \quad (4.19)$$

$$T_9 < Ts_{at\ @\ p\ 9} - 3 \ [°C] \quad (4.20)$$

$$x_6 > 0.87 \ [Kg/Kg] \quad (4.21)$$

$$T_5 > T_{Sat@p5} + 5 \ [°C] \quad (4.22)$$

$$p_2 > p_4 \ [bar] \quad (4.23)$$

Figure 4.21 T-s diagram of repowering Option 2. Point 1: VHP turbine inlet; Point 2: VHP turbine outlet; Point 3: Reheating outlet; Point 4: Regeneration bleeding; Point 5: Process bleeding; Point 6: LP turbine outlet; Point 7: Condenser outlet; Point 8: Process condensed water; Point 9: Addition of regeneration vapor; Point 10: Pump and boiler's inlet

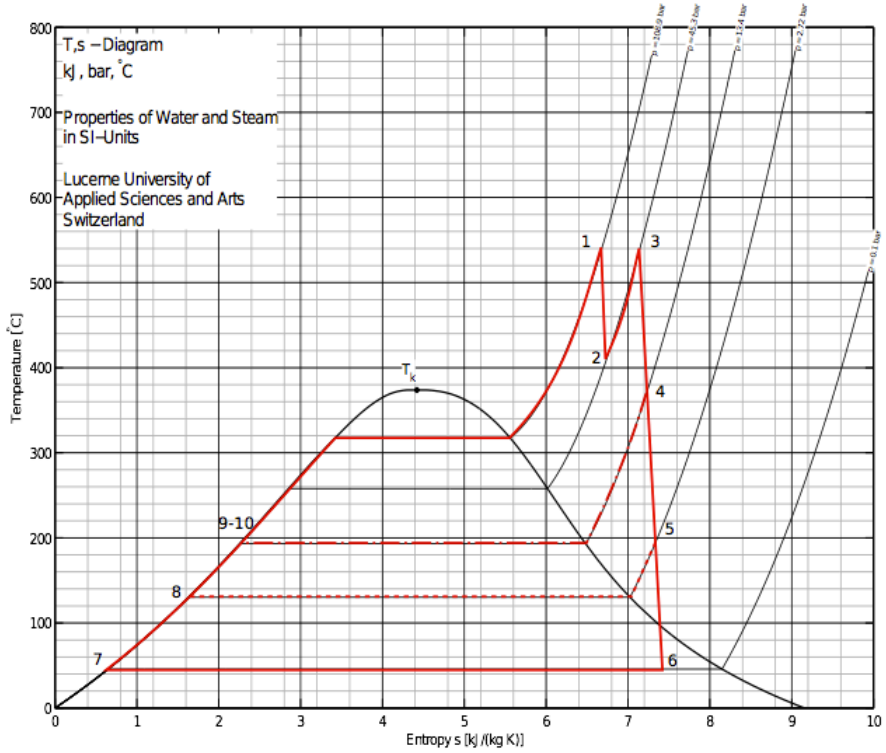

Optimization results are shown in Table 4.8. The higher the couple boiler pressure and temperature and the better results can be obtained. Maximum energy surplus index is obtained with a boiler of 108.9 bar and 540 °C, which could give 251.9 kWh per each ton of bagasse. The optimal configuration is obtained with reheating pressure of 43.8 bar, regeneration bleeding of 8 kg/s at 15.3 bar. Optimal material and energy balance of this optimum are represented in Figure 4.22. In this case, not being any point of the expansion fixed, the optimization follows the typical behavior of Rankine cycles, which can reach the highest performances with the highest possible pressure and temperature at expansion inlet. The cash flow related to the sell of optimal energy surplus is 9,639,600 €/year (24,099,000,000 COP/year) and is greater than Repowering Option 1.

Table 4.8 Results of optimization for repowering Option 2

Boiler P [bar]	Boiler T [°C]	Boiler capacity [kg/s]	Boiler inlet T [°C]	p. reheat [bar]	p. reg. [bar]	m vap. regeneration [kg/s]	P turbine top. [MW]	η is HP-MP-LP	P surplus [MW]	η_{el} plant	Surplus [kWh/tonne]
42.2	480	49.8	183	14.3	10.7	6.3	39.3	0.9	26.0	0.2443	195.3
45.1	440	51.9	163	22.2	6.3	5.7	39.2	0.9	25.9	0.2439	194.3
64.7	485	52.1	181	35.2	11.5	6.9	42.3	0.9	28.9	0.2540	216.8
65.7	495	49.3	159	30.8	5.4	5.0	42.8	0.9	29.4	0.2557	220.3
65.7	520	46.6	192	20.2	12.7	6.6	43.2	0.9	29.8	0.2571	223.6
66.7	510	49.8	176	30.9	8.4	6.1	43.3	0.9	29.9	0.2574	224.3
66.7	515	50.0	192	26.8	12.9	7.0	43.3	0.9	29.9	0.2575	224.5
85.3	515	49.0	179	32.1	10.2	6.1	44.9	0.9	31.4	0.2625	235.6
86.3	510	51.9	202	38.6	16.3	8.2	44.9	0.9	31.4	0.2625	235.1
86.3	515	50.9	190	40.5	11.8	7.3	45.1	0.9	31.6	0.2631	236.9
86.3	540	47.5	177	30.6	12.0	5.5	45.3	0.9	31.7	0.2637	238.1
87.3	515	52.3	221	32.9	22.1	9.3	45.0	0.9	31.5	0.2627	236.1
104.0	540	51.3	218	41.7	21.5	8.9	46.8	0.9	33.1	0.2683	248.5
106.9	540	52.6	226	47.8	24.3	9.8	46.9	0.9	33.2	0.2687	249.5
107.9	540	49.3	192	42.1	12.3	7.0	47.1	0.9	33.5	0.2695	251.2
108.9	540	50.3	204	43.8	15.3	8.0	47.3	0.9	33.6	0.2699	251.9

Figure 4.22 Material and energy balance of second option optimal repowering for a milling rate of 430 ton/h

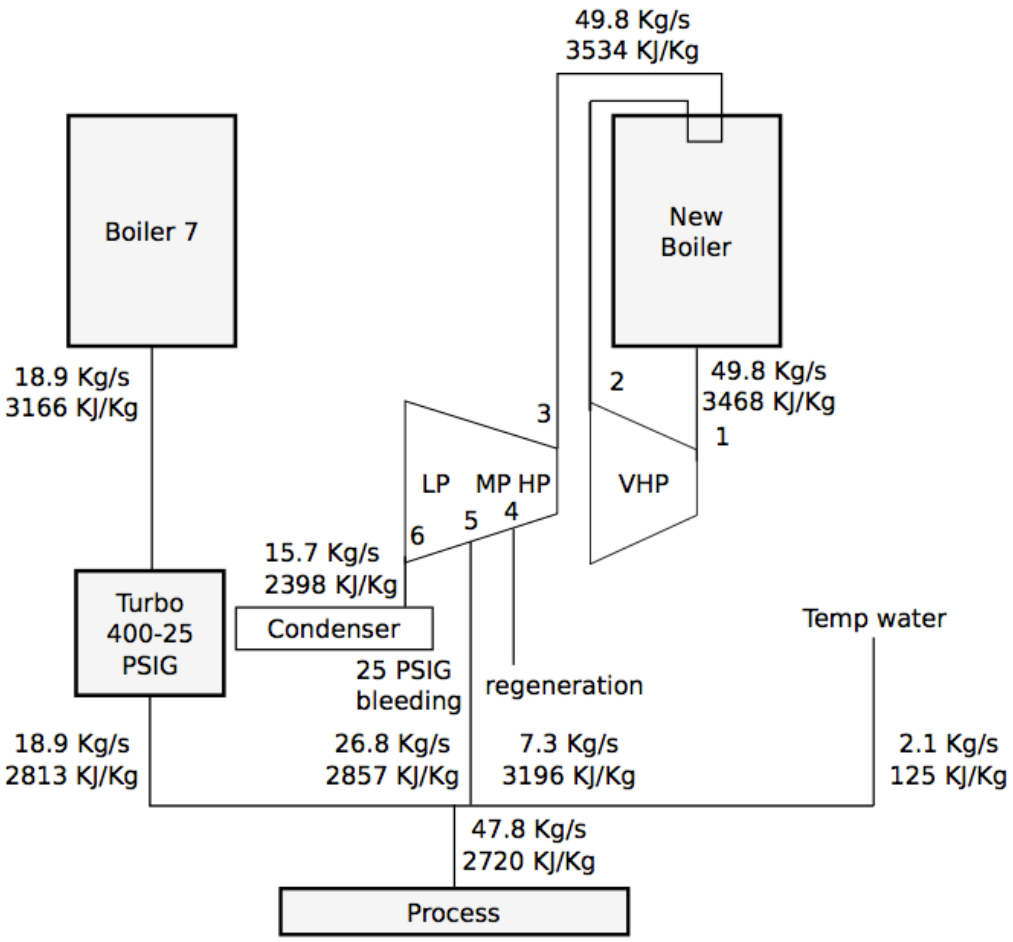

4.5 Economic analysis

4.5.1 Fixed capital cost

The two (2) different options, previously analyzed, are now studied to evaluate the feasibility of the investment and to compare their results. Being the new configuration proposal a very first step of design process, a fifth class cost estimation is carried out aimed to establishing the order of magnitude of the investment [6]. Total fixed capital cost is the sum of direct and indirect costs. Direct costs include purchased equipment, purchased equipment installation, instrumentation and controls, piping and electrical (installed), buildings, yard improvements, service facilities and land. Indirect costs include engineering and supervision, construction expenses, contractor's fee and contingency [7]. The

equipment to be bought is: a boiler, turbine, generator, condenser and electric motors for the mills, pumps and fans. To estimate the investment of purchased equipment, the procedure consists into two steps, based on the knowledge of the cost of a similar device to the one to be bought [7,8].

The first step is aimed to obtain the cost of a new device by relating its size or capacity to the known one with an exponential rule. Given the cost and size of the known machine ($Cost_0$ and $Size_0$), and the value of exponential factor (N), new cost's ($Cost_1$) formula reads as follows:

$$(4.24)\quad Cost_1=Cost_0*(Size_1/Size_0)^N$$

The value of the exponent N depends on the type of equipment but it is in general comprised between 0.3 and unity. If the value for particular devices is not specified, as a general rule, a value of 0.6 is considered. The obtained cost is then scaled on the dimension of new equipment, but it is still related to the year in which reference price is considered. The second step updates this value to current year by the use of indexes based on the inflation rate. In this work CEPCI (Chemical Engineering Plant Cost Index) indexes were used, updated to 2013. Being now $Cost_1$ and $Index_1$ the reference ones, $Index_2$ the current inflation index and $Cost_2$ the updated cost value, final purchased equipment cost is given by Equation 4.25.

$$(4.25)\quad Cost_2=Cost_1*(Index_2/Index_1)$$

Selected reference sizes for new equipment cost evaluation were consulted in a literature [8], with the only exception of the boiler. Literature [8] indicates the capacity (ton/h of produced vapour) as a reference unit, but the presence of a reheating (which implies another passage of steam in the boiler, but just in its super-heater part) complicates the usage of this reference. For this reason, the fuel power input is selected. For what concerns the condenser, it has been sized with the LMTD (Log Mean Temperature Difference) method [9]. Although not suitable for very precise calculation of a condenser, because based on a linear heat exchange hypothesis, it is acceptable in this case as a first approximation. Cooling water flow rate m_w of 600 l/s and global heat exchange coefficient U equal to 2550 W/m^{2}K [10] are considered. LMTD is a logarithmic average of the temperature difference between hot and cold fluid in the exchanger and is used to determine the temperature driving force in the system. Naming ΔT_1 the temperature difference between the fluids at hot fluid inlet side of the condenser, and ΔT_2 the difference at its outlet (Figure 4.23), LMTD is defined as shown in the following equation.

$$(4.26)\quad LMTD = \frac{\Delta T1 - \Delta T2}{\log\left(\frac{\Delta T1}{\Delta T2}\right)} \quad [°C]$$

Figure 4.23 Scheme of temperature difference in the condenser

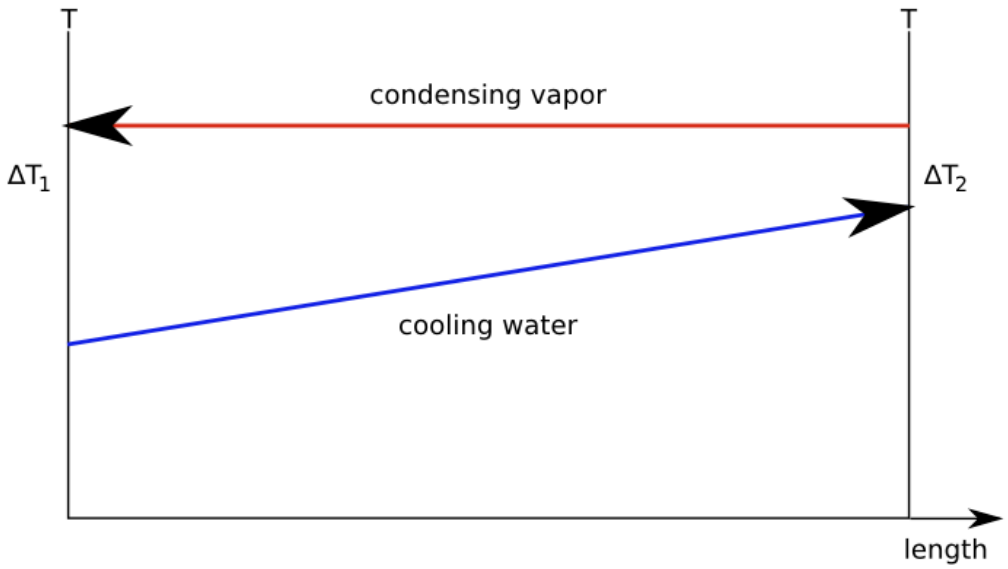

Being the condenser heat power Q, the required area of the exchanger, in m^2 is obtained by relation 4.27:

$$(4.27)\quad Q = m_w * U * LMTD \quad [W]$$

Table 4.9 collects the cost estimation for each of the new devices. The references have been taken from Manuelita S.A. budgeting [4] and Euro value was taken in February 2014. Total purchased equipment of Option 1 costs 18.91 million Euro (47,275 million COP), while Option 2 is estimated in 18.92 million Euro (47,300 million COP).

Table 4.9 Purchased equipment cost evaluation

Equipment	*Ref Year*	*Ref Cost [€]*	*Ref Size*	*Exp. factor*	*Inflation coefficient*	*Size option 1*	*Cost Option 1 [€]*	*Size option2*	*Cost Option 2 [€]*
Boiler	2012	12942900	228190 [kW fuel]	0.6	0.9660	215.59 [MW fuel]	120834417.3	215.59 [MW fuel]	120834417.3
Turbine + generator	2012	3507211.2	25 [MW]	0.3	0.9660	44.0 [MW]	4014143.1	47.5 [MW]	4107382.4
Condenser	2013	151840	1000 [m^2]	0.53	1.0000	3715 [m^2]	304413.8	2014 [m^2]	220058.3
Pump 1 motor	2012	66417.6	900 [kW]	0.8	0.9660	6 [kW]	1165.2	5.5 [kW]	1086.8
Pump 2 motor	2012	66417.6	900 [kW]	0.8	0.9660	78.5 [KW]	9115.1	199.2 [kW]	19199.8
Pump 3 motor	2012	66417.6	900 [kW]	0.8	0.9660	516.9 [kW]	41171.0	621 [kW]	47680.4
Tandem motors	2012	2467775.2			0.9660		2383870.9		2383870.9
Fan Boiler 7 motor	2012	66417.6	900 [kW]	0.8	0.9660	217 [kW]	20560.5	217 [kW]	20560.5
Fan new Boiler motor	2012	66417.6	900 [kW]	0.8	0.9660	775 [kW]	56925.6	775 [kW]	56925.6
Total							18914782.0		18940182.0

Peters and Timmerhaus [7] estimate that the cost of purchased equipment represents 15-40% of total fixed capital cost. Considering 27.5% as an average value, it results that the investment for Option 1 is 68.78 million Euro (171,953 billion COP) and 68.87 million Euro for Option 2 (172,183 billion COP).

4.5.2 Investment analysis

To evaluate the feasibility of the investment some concepts are introduced:

- PV (Present Value), also known as present discounted value, is a future amount of money that has been discounted in order to reflect its current value, as if it existed today. The discount rate "*i*" represents the interest rate and the presence of this term implies that a given cash flow has a higher value in the present than in a future year horizon "*Y*". For this study the discount rate is considered with a 3.5% value [11].

$$(4.28)\ PV = Cash\ flow_Y/(1+i)^Y \quad [€]$$

- NPV (Net Present Value) of a time horizon is the sum of the present values of each year of the series.
- PBT (Pay Back Time) is the time required to recoup the funds expended in the investment.
- IRR (Internal Rate of Return) is the discount rate that makes null the NPV at the selected horizon.

Table 4.10 and 4.11 shows the expected results for the investment in the 20-year horizon.

Table 4.10 PV calculation for Option 1

Year	*Cashflow Option 1 [€/year]*	*Present Value Option 1 [€/year]*	*Cumulative Present Value Option 1 [€]*
0	-68781027.42	-68781027	-68781027
1	8665500	8372464	-60408564
2	8665500	8089337	-52319227
3	8665500	7815785	-44503442
4	8665500	7551483	-36951960
5	8665500	7296118	-29655841
6	8665500	7049390	-22606451
7	8665500	6811005	-15795447
8	8665500	6580681	-9214766
9	8665500	6358146	-2856620

10	8665500	6143136	3286516
11	8665500	5935397	9221913
12	8665500	5734683	14956596
13	8665500	5540757	20497353
14	8665500	5353388	25850741
15	8665500	5172356	31023097
16	8665500	4997445	36020542
17	8665500	4828449	40848991
18	8665500	4665168	45514160
19	8665500	4507409	50021569
20	8665500	4354985	54376553

Table 4.11 PV calculation for Option 2

Year	*Cashflow Option 2 [€/year]*	*Present Value Option 2 [€/year]*	*Cumulative Present Value Option 2 [€]*
0	-68873388.98	-68873389	-68873389
1	9639600	9313623	-59559766
2	9639600	8998670	-50561096
3	9639600	8694367	-41866729
4	9639600	8400354	-33466375
5	9639600	8116285	-25350090
6	9639600	7841821	-17508269
7	9639600	7576638	-9931631
8	9639600	7320424	-2611207
9	9639600	7072873	4461666
10	9639600	6833694	11295360
11	9639600	6602603	17897962
12	9639600	6379326	24277289
13	9639600	6163600	30440889
14	9639600	5955169	36396058
15	9639600	5753787	42149845
16	9639600	5559214	47709059
17	9639600	5371222	53080281
18	9639600	5189586	58269867
19	9639600	5014093	63283960
20	9639600	4844534	68128494

Both the options present a NPV higher than zero at the selected horizon. Option 1 predicts 54.38 million Euro (135,941 million COP) 20 year-NPV, while

Option 2 gives 68.13 million Euro (170,321 million COP). This result means that, with given discount rate, the investment is feasible. The PBT is 10 years for first option and 9 years for the second option. Half of the horizon time will be required to return the investment, while the positive cash flows of the other half will represent profits for the company. With the same horizon, the two IRRs result to be 11.0% and 12.7%. If the company has actually access to lower interest capital than the IRR the investment will be profitable, otherwise it will not.

Table 4.12 compares the most important data and indexes related to the optima solution of Option 1 and Option 2.

Table 4.12 Option 1 optimum vs Option 2 optima

	Option 1	*Option 2*
Investment [€]	18914782	18940182
Plant surplus energy index [kWh/ton$_{BAG}$]	226.4	251.9
Electric energy sell revenue [€/year]	8665500	9639600
20 years NPV [€]	54376553	68128494
PBT [year]	10	9
IRR [%]	11.0	12.7

4.6 References

[1] D. Khatiwada, J. Seabra, S. Silveira, A. Walter, *Power generation from sugarcane biomass - A complementary option to hydroelectricity in Nepal and Brazil*, Energy 48 (2012), pp 241-254.
[2] Coordination BNDES and CGEE, *Sugarcane-based bioethanol, Energy for sustainable development,* Rio de Janeiro, http://www.sugarcanebioethanol.org/en/download/ bioetanol.pdf; 2008.
[3] L. F. Pellegrini, S. de Oliveira Jùnior, J. C. Burbano, *Supercritical steam cycles and biomass integrated gasification combined cycles for sugarcane mills*, Energy 35 (2010). pp 1172–1180.
[4] [Manuelita S.A, Internal Report, 2013.
[5] S. C. Kamate, P. B. Gangavati, *Exergy analysis of cogeneration power plants in sugar industries*, Applied Thermal Engineering 29 (2009) pp 1187–1194.
[6] L. R. Dysert, *Sharpen Your Cost Estimating Skills*, Cost Engineering, Vol. 45, No.6, AACE International , Morgantown, WV, 2003.
[7] M. Peters, K. D. Timmerhaus, *Plant design and economics for chemical engineers*, Third Ed, Mc Graw Hill, New York, 1980.
[8] A. Kayode Coker, *Ludwig's Applied Process Design for Chemical and Petrochemical Plants,* Vol. 1, Fourth Ed, Elsevier, 2007.
[9] H&C Heat Transfer Solution, www.hcheattransfer.com/coefficients.html, 2014.
[10] Y. A. Cengel, A. J. Ghajar, *Heat and Mass Transfer: Fundamentals & Applications,* 4th Ed, Mc Graw Hill, 2011.
[11] UK Government, *The Green Book Appraisal and Evaluation in Central Government,* pp. 26, 97, London, 2011, https://www.gov.uk/government/uploads/system/uploads/attachment_data/file/220541/green_book_complete.pdf.

Conclusions and Further Developments

The model for the mass and energy balances presented in this Thesis turned out to have a good accuracy in the typical operating range of the plant. The analysis on the current configuration showed some critical points from the point of view of the energy efficiency, corresponding to the addition of tempering water in the Boiler 7 and to the reduction of steam pressure. The strongest negative effect is given by the flow of steam through the 300 to 25 PSIG reduction station, which is necessary when the steam demand of the turbines to guarantee the mechanical and electric power is less than the 25 PSIG saturated steam required by the sugar and ethanol production process. The model outlined that the process of Ingenio Manuelita is far from the State of the Art. While many sugar mills are able to extract an energy surplus from the combustion of bagasse, Ingenio Manuelita can cover only 97.6% of its own energy needs and has to buy coal to satisfy all the demand. Nevertheless, due to the way in which the plant was designed, the sensitivity analysis on the main variables and the numerical optimization confirmed that the boilers are already working close to their optimal conditions.

Considering the next evolutions of the sugar process, which will permit to reduce the steam consumption, the model predicted a possible improvement in second principle efficiency from current 19.6% to 21.2%, thanks to the switch from steam driven machines to electric ones. This electrification of the machines can be only partial because there is a bottleneck in the available electric power generation capacity. Moreover, the need to develop in parallel the reduction of process steam and the cogeneration, in order to avoid the lamination of steam or its release to the atmosphere.

The results of the first steam reduction phase outpointed the need to design a new cogenerative cycle to be coupled with the second and strong steam reduction phase. Substituting the old Boilers 5 and 6 with a new one, two different Rankine cycles were proposed to satisfy the electric and thermal energy requirement of Ingenio Manuelita, and to produce an electric energy surplus. The first proposal was a normal condensing with extraction Rankine cycle, while the second proposal was a reheating Rankine cycle. The optimal first configuration allows the whole plant to reach 25.8% second principle efficiency. Better results in terms of efficiency and energy surplus may be obtained with the reheating cycle, whose second principle efficiency is 27.0%. Such new configurations could would require an investment whose Internal Rate of Return is 11.0% and 12.7% respectively.

Further developments of this work should consider the analysis of a new boiler and Rankine cycle to substitute current Boiler 7 and to join the repowering configuration here depicted. Following the proposal of Chapter 4, such new cycle would be decoupled from cogeneration and its layout should be designed in order to reach the highest electric energy generation performances. A supercritical Rankine cycle should be taken into account.

Other studies on the plant of Ingenio Manuelita should consider the direct substitution of all the boilers. This repowering would allow having a completely renewed State of the Art plant. The investment would be higher than the options showed in this work but it would guarantee better efficiencies and better energy surplus. An economic analysis should be carried on in order to compare this solution with the partial repowering presented.

A more advanced research considering the switch from the Rankine cycle layout to the Biomass Integrated Gasification Combined Cycle layout should be also carefully analysed.

Annex 1 Scheme of the production process of Ingenio Manuelita

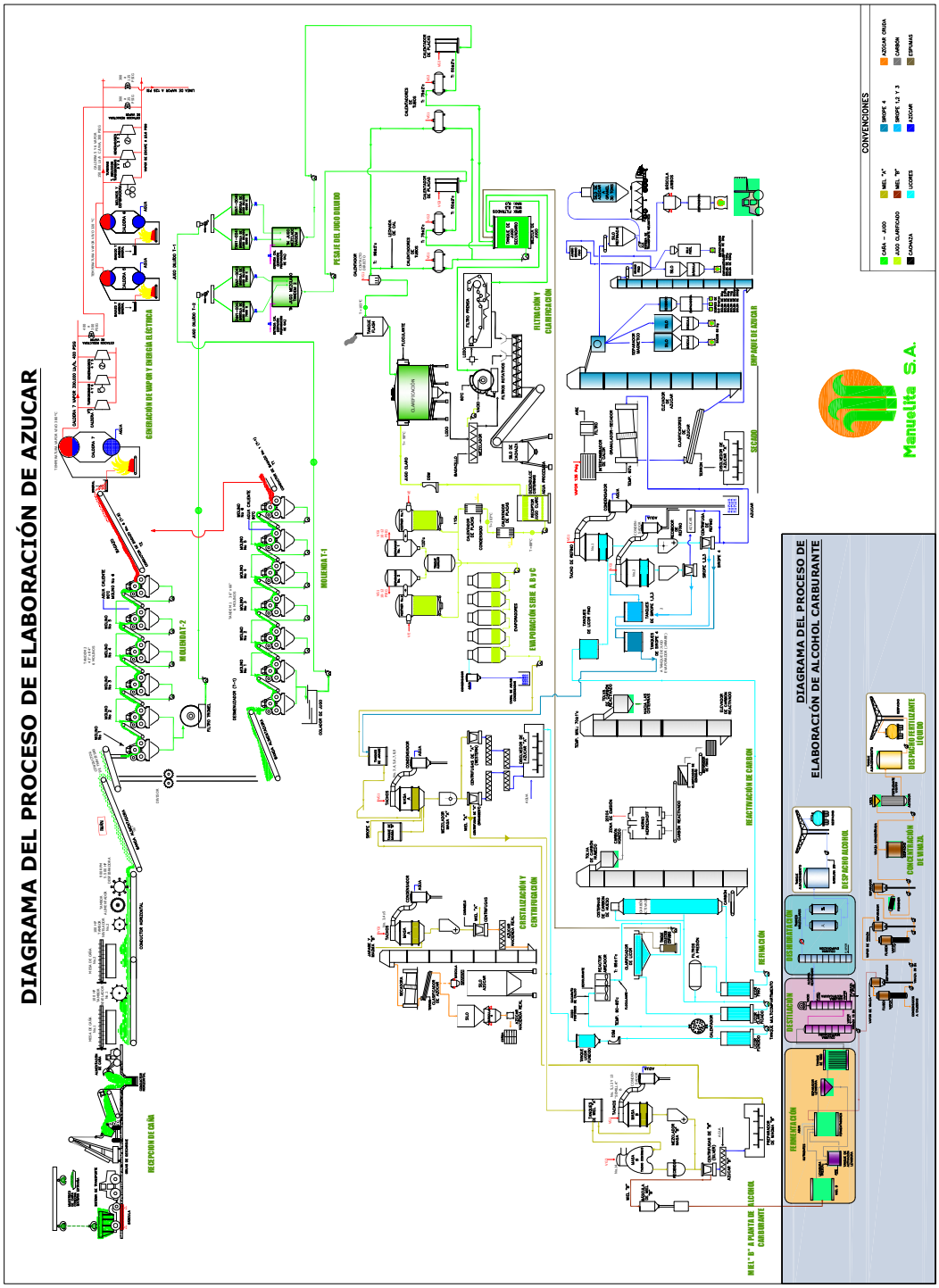

Annex 2 Pictures of the plant and of sugar production

View of Cauca Valley from the plant

Sugarcane truck

Cane receiving area

Milling Tandem 1

Sugarcane bagasse

“Cachaza” sludge

Multi-effect evaporator

Vacuum Pans

Centrifuges

Chimneys of the boilers. Boiler 7 (highest chimney) is provided by electro-filter

View of the PAC

Annex 3 Scheme of the cogeneration of Ingenio Manuelita

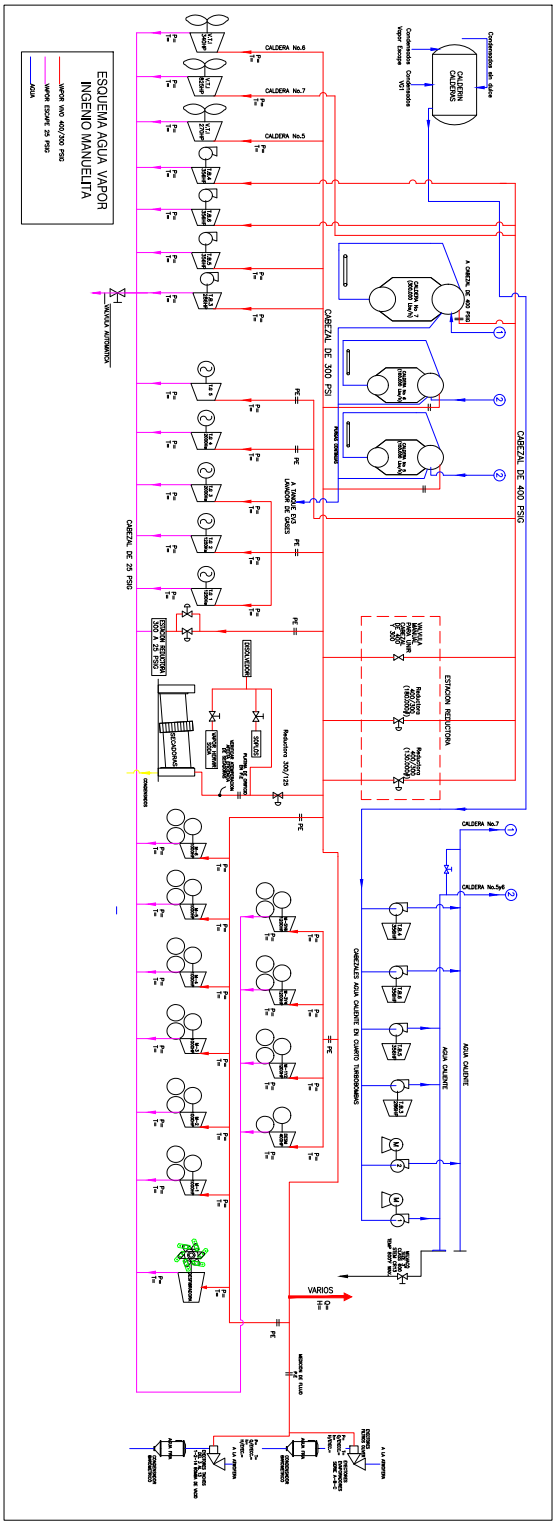

Nomenclature

SYMBOLS and ACRONYMS

B = Brix degrees [°Bx]
BPR = Boiling Point Rise
D = diameter [m]
HR = hours
IRR = Internal rate of return [%]
$KS_{\%}$ = solubility in percentage [% kg/kg]
KS_{pure} = solubility of pure solution [kg/kg]
KS_{impure} = solubility of impure solution [kg/kg]
LHV = low heating value [kJ/kg]
NPV = Net Present Value [€]
NSW = non sucrose to water ratio [kg/kg]
P = power [kW]
PBT = Payback time [years]
PV = present value [€]
Q = heat power [kW]
T = temperature [°C]
TF = total force on mill [ton]
LP = low pressure
$LMTD$ = log mean temperature difference
MP = medium pressure
H = humidity [kg/kg]
HP = high pressure
U = global heat exchange coefficient [W/m^{2}K]
VHP = very high pressure
YCC = year cash flow [€/year]
ΔT = temperature difference [°C]
Δh = enthalpy difference [kJ/kg]

c = cost of bagasse unit [€/ton]
cp =specific heat at constant pressure [kJ/kgK]
cap = capacity [kg/s]
e = extraction
h = specific enthalpy [kJ/kg]
k = constant
m = mass flow rate [kg/s]
mr = milling rate [kg/s]
n = rotational speed [rpm]
p = pressure [bar]
q = share of process heat
r = removal
s = specific entropy [kJ/kgK]
st = saturation coefficient [%]
v = vacuum [cmHg]
w = specific work [kJ/kg]
x = fraction
ε_k = kinetic specific exergy [kJ/kg]
ε_P = potential specific exergy [kJ/kg]
ε_{PH} = phisic specific exergy [kJ/kg]
ε_{CH} = chemical specific exergy [kJ/kg]
ε_{LOSS} = loss specific exergy [kJ/kg]
Φ = sucrose purity
η = efficiency

SUBSCRIPTS

AIR = air
AJ = alkalized juice
$A\text{-}MS$ = A massecuite
$A\text{-}SG$ = A sugar
$B7$ = Boiler 7
$B56$ = Boiler 5 and 6
BAG = bagasse
BL = bagacillo
BLD = blades
$B\text{-}M$ = B magma
$B\text{-}S$ = blade to shaft
BOT = bottoming
C = cane

CJ = clarified juice
CNJ = concentrated juice
CNT = centrifuged
COND = condensation
CR = clarifier of refining
CRS = crystals
D = drier
DJ = diluted juice
EFF = effect of the evaporator
EVAP = evaporation
EX = exhaust
F = foam
FJ = filtered juice
FL = flocculating
H = heaters
H25 = head of 25 PSIG
H300 = head of 300 PSIG
HP = high pressure
II = second principle
INS = insoluble
J = juice
L = liquor
LIQ = liquid
LP = low pressure
MILL = milling
ML = molasses
MP = medium pressure
MS = massecuite
OPT = optimal
P = pans
PAC = alcohol plant
RS = reducing sugars
REF = reference
REN = renewable
S = sludge
SAT = saturation
SC = sucrose
SG = sugar
SH = superheater
SL = other soluble
SOL = total soluble
SR = syrup
SV = saving
T = temperature
TB = turbo-pump
TG = turbo-generator
TI = tank input
TO = tank output
TOP = topping
TURB = turbines
TW = tempering water
US = useful
VAP = steam
VAP-B56 = steam of Boilers 5 and 6
VAP-300 = steam at 300 PSIG
VAP-400 = steam at 400 PSIG
VAP-N25 = steam need at 25 PSIG
VAP-N300 = steam need at 300 PSIG
VAP-N400 = steam need at 400 PSIG
VAP-R300 = steam reduced from 300 to 25 PSIG
VAP-R400 = steam reduced from 400 to 300 PSIG
VAP-T = steam of turbines
VE = turbine exhaust steam
VG1 = Gases 1
VG2 = Gases 2
VG2-3 = Gases 2 to Effect 3
VG2-ST = Gases 2 to the shell and tube heater
VG3 = Gases 3
VG4 = Gases 4
VG4-5 = Gases 4 to Effect 5
VTI = turbo-fan
W = water

el = electric
eq = equivalent
g = global
in = inlet
int = internal
is = isentropic

mech = mechanical
out = outlet
reg = regeneration
th = thermal
turb = turbine
y = year